



Posttranscriptional regulation of the microRNA-17-92a cluster

Dissertation

zur Erlangung des Doktorgrades der Naturwissenschaften
vorgelegt beim Fachbereich Biowissenschaften (FB15) der
Goethe Universität in Frankfurt am Main

von Eva-Marie Heinrich

aus Mainz

Frankfurt 2013

vom Fachbereich der Biowissenschaften der
Johann Wolfgang Goethe Universität angenommen.

Dekan: Prof. Dr. A. Starzinski-Powitz

Gutachter: Prof. Dr. S. Dimmeler

Prof. Dr. B. Suess

Datum der Disputation:

Abbreviations

6-PFK	6-Phosphofructokinase
ACE	Angiotensin to Angiotensinogen converting enzyme
ADAR	Adenosine deaminase acting on RNA
Ago2	Argonaute protein 2
A-to-I	Adenosine to Inosine editing
A-to-G	Adenosine to Guanosine substitution
APS	Ammonium persulfate
ATP	Adenosine triphosphate
BMP	bone morphogenic protein
bp	basepair(s)
BRCA	Breast cancer
c. elegans	caenorhabditis elegans
cDNA	complementary DNA
ciR	circular RNA
Ct	cycle threshold
ctrl.	Control
DEAD box	Asparagin Glutamine Alanin Asparagin motif box
DFO	Deferoxamin
DNA	desoxyribonucleic acid
Dnd1	Dead end 1
dsRNA	double stranded RNA
DTT	Dithiothreitol
e.g.	(lat.)exempli gratia – for example
EBM	endothelial basal medium

ECs	endothelial cells
EHD	Eps15 (epidermal growth factor receptor substrate 15) homology domain containing protein
eIF4A2	eukaryotic initiation factor 4A2
EMSA	electric mobility shift assay
ER	endoplasmatic reticulum
g	gravitational constant ($6.67 \cdot 10^{-11} \text{ N (m/kg)}^2$)
GTP	guanosine triphosphate
HDL	high density lipoprotein
HEK	human embryonic kidney
HIF-1 α	Hypoxia inducible factor 1 α
hnRNP A1	heterogeneous nuclear ribonucleoprotein A1
HPCs	hematopoietic progenitor cells
HRP	horse radish peroxidase
hrs	hours
HUVEC	human umbilical vein endothelial cell
IgG	Immunoglobulin G
IRE-1 α	Inositol requiring enzyme 1 α
kDa	kilo Dalton
Klf2	Krüppel like factor2
KSRP	KH-type splicing regulatory protein
lncRNA	long non-coding RNAs
LTQ	linear trap quadropole
MALAT1	metastasis associated lung adenocarcinoma transcript 1
MEF	mouse embryonic fibroblast
mESCs	mouse embryonic stem cells
miR	microRNA

mRNA	messenger RNA
ncRNA	non-coding RNA
nM	nano molar (nano mol per 1 liter)
nm	nano meter
NPM1	Nucleophosmin 1
nt	nucleotide(s)
NTA	nanoparticle tracking analysis
PBS	phosphate buffered saline
PCDP4	programmed cell death protein 4
piRNA	piwi-interacting RNA
pre-miR	precursor microRNA
pri-miR	primary microRNA
PRPF8	pre-mRNA processing factor 8
PTEN	Phosphate and Tensin homologue
PVDF	Polyvinylidene fluoride
qRT-PCR	quantitative real time polymerase chain reaction
RE	response element
RIP	RNA immunoprecipitation
RISC	RNA-induced silencing complex
RNA	ribonucleic acid
RPLP0	60S acidic ribosomal phosphoprotein P0
rRNA	ribosomal RNA
scaRNA	small cajal body specific RNA
SDS-PAGE	Sodium dodecyl sulfate polyacrylamide gel electrophoresis
SEM	standard error of the mean
siCo	siRNA control

siRNA	small interfering RNA
SMAD	small (body size) drosophila protein
SMC	smooth muscle cell
SND1	Staphylococcal nuclease domain containing protein 1
snoRNA	small nucleolar RNA
snRNA	small nuclear RNA
snoRNA	small nucleolar RNA
Spred1	Sprouty related domain containing protein 1
ssRNA	single stranded RNA
TCA	Trichloroacetic acid
TEMED	N,N,N,N-tetramethylethyldiamin
TDP-43	TAR DNA binding protein 43
TGF β	transforming growth factor beta
TRBP	HIV transactivating response RNA binding protein
tRNA	transfer RNA
T-Tubules	transverse tubules
TUT4	terminal uridylyltransferase 4
UTR	untranslated region
v	volt
VEGF	vascular endothelial growth factor
VEGFR2	vascular endothelial growth factor receptor 2
VSMCs	vascular smooth muscle cells
w	washing fraction

Content

I.	Introduction.....	1
I.1.	Non-coding RNAs.....	1
I.2.	microRNAs (miRs).....	2
I.2.1.	Discovery of miRs	2
I.2.2.	Canonical biogenesis of miRs	3
I.2.3.	RNA interference of miRs and siRNAs	5
I.2.4.	Regulation of miRs.....	7
I.2.4.1.	Regulation of the processing of miRs.....	7
I.2.4.1.1.	Positive regulators of miR processing	8
I.2.4.1.1.a.	DEAD box helicases p68 and p72.....	8
I.2.4.1.1.b.	SMADs.....	8
I.2.4.1.1.c.	P53.....	9
I.2.4.1.1.d.	BRCA1	9
I.2.4.1.1.e.	KSRP	10
I.2.4.1.1.f.	hnRNP A1.....	10
I.2.4.1.1.g.	Autoregulation	11
I.2.4.1.1.h.	TDP-43	11
I.2.4.1.2.	Negative regulators of the processing of miRs.....	13
I.2.4.1.2.a.	TUT4.....	13
I.2.4.1.2.b.	IRE1 α	13
I.2.4.1.2.c.	ADARs.....	14
I.2.4.1.2.d.	Hormones	14
I.2.4.2.	Regulation of mature miRs.....	17
I.2.5.	MiRs in endothelial cells.....	18
I.2.5.1.	miR-126	19
I.2.5.2.	The miR-17-92a cluster	21
I.2.5.2.1.	Functions of the miR-17-92a cluster	21
I.2.5.2.1.a.	miR-17-5p and miR-20a	22

I.2.5.2.1.b.	miR-18a.....	22
I.2.5.2.1.c.	miR-19a	23
I.2.5.2.1.d.	miR-92a.....	23
I.2.5.2.2.	Regulation of the miR-17-92a cluster.....	24
I.2.5.2.2.a.	Transcriptional regulation of the 17-92a cluster.....	24
I.2.5.2.2.b.	Posttranscriptional regulation of the miR-17-92a cluster.....	24
II.	Objective.....	27
III.	Material and Methods.....	28
III.1.	Material	28
III.1.1.	Expendable items and chemicals	28
III.1.2.	Kits	30
III.1.3.	Primers.....	30
III.1.3.1.	Primers for SYBR green qRT-PCR.....	30
III.1.3.2.	Taqman assays	31
III.1.3.3.	Primers used for generating a library for sequencing	31
III.1.4.	Small interfering RNA (siRNA)	32
III.1.5.	Antibodies.....	32
III.1.6.	Buffers	33
III.1.7.	Cell culture.....	33
III.2.	Methods.....	34
III.2.1.	Cell Culture	34
III.2.1.1.	HUVEC cultivation	34
III.2.1.2.	Exposure of HUVECs to hypoxia mimicking conditions	34
III.2.1.3.	SiRNA transfection of HUVECs	35
III.2.1.4.	Preparation of microvesicles and exosomes shed by HUVECs	35
III.2.1.5.	Nanoparticle tracking analysis (NTA)	36
III.2.2.	Molecular Biology.....	37
III.2.2.1.	RNA isolation	37
III.2.2.2.	Determination of mRNA levels.....	37
III.2.2.2.1.	Reverse Transcription of mRNAs.....	37
III.2.2.2.2.	Quantitative real time PCR (qRT-PCR) of mRNAs	38
III.2.2.3.	Determination of miR levels.....	40

III.2.2.3.1.	RT of miRs	40
III.2.2.3.2.	qRT-PCR of miRs.....	41
III.2.2.4.	In vitro transcription	42
III.2.2.5.	RNA Pulldown.....	42
III.2.2.6.	RNA immunoprecipitation	44
III.2.2.7.	Determination of the protein concentration	45
III.2.2.8.	SDS polyacrylamide gel electrophoresis (SDS-PAGE).....	46
III.2.2.9.	Western Blot	47
III.2.2.10.	Immunological detection of proteins	48
III.2.2.11.	Stripping of membranes	48
III.2.2.1.	Coomassie Staining	49
III.2.2.2.	Silver Staining	49
III.2.2.3.	In gel digest of proteins subjected to mass spectrometry.....	49
III.2.2.4.	Amplicon Sequencing.....	51
III.2.3.	Statistics.....	51
IV.	Results.....	52
IV.1.	Identification of pre-miR-92a binding proteins by RNA pulldown.....	52
IV.1.1.	Establishing of the (RIP) protocol for HUVECs.....	57
IV.2.	SND1 – a potential regulator of the miR-17-92a cluster under stress conditions	58
IV.2.1.	Confirmation of the interaction between SND1 and members of the miR-17-92a cluster	58
IV.2.2.	Under hypoxia mimicking conditions SND1 affects the maturation of miR-17-92a	60
IV.2.3.	Potential editing sites of pri-miR-17-92 are not induced upon hypoxia mimicking conditions.....	63
IV.2.4.	ADAR1 silencing does not influence the expression of the mature members of miR-17-92a.....	67
IV.3.	eIF4A2 interacts with the mature miRs of the miR-17-92a cluster but silencing of eIF4A2 does not affect its processing.....	68
IV.3.1.	eIF4A2 interacts with the mature members of the miR-17-92a cluster ...	68
IV.3.2.	Silencing of eIF4A2 does not affect the levels of miR-17-92a cluster members	70

IV.4.	Silencing of Myoferlin affects the localization of miR-92a and miR-126 and regulates the levels of pri-miR-126 and pre-miR-126	72
IV.4.1.	Myoferlin interacts with pre-miR-92a and mature miRs.....	72
IV.4.2.	Silencing of Myoferlin regulates the levels of mature miR-126 and miR-145 while not affecting other endothelial miRs.....	73
IV.4.3.	Pri-miR-126 and pre-miR-126 levels are increased in the absence of Myoferlin	75
IV.4.4.	Myoferlin interacts with pri-miR-126	76
IV.4.5.	Silencing of Myoferlin increased extracellular levels of miR-92a.....	76
IV.4.6.	Silencing of Myoferlin increases the relative number of exosomes	78
V.	Discussion	80
V.1.	Identification of pre-miR-92a binding proteins and selection of interesting candidates.....	80
V.2.	SND1 – a known regulator of RNAs with new implication in miR-17-92a maturation.....	82
V.2.1.	Silencing of SND1 under hypoxia mimicking conditions affects miR-17-92a biogenesis.....	83
V.2.2.	Hypoxia mimicking conditions do not increase the editing of pri-miRs and pre-miRs of the miR-17-92a cluster	84
V.3.	EIF4A2 – general RNA binding protein	87
V.3.1.	Half-maximal inhibition of eIF4A2 does not affect the biogenesis of the miR-17-92a cluster	87
V.4.	Myoferlin – a versatile regulator of endothelial miRs.....	88
V.4.1.	Silencing of Myoferlin does not regulate the maturation of the members of the miR-17-92a cluster	89
V.4.2.	Silencing of Myoferlin alters the export of miR-92a mediated by microvesicles or exosomes, while miR-145 was not affected.....	90
V.4.2.1.	Silencing of Myoferlin increases the relative number of exosomes.....	90
V.4.2.2.	MiR-92a levels in microvesicles or exosomes are increased after silencing of Myoferlin	91
V.4.2.3.	Myoferlin also interacts with mature miR-145.....	93
V.4.3.	Silencing of Myoferlin alters the genesis and localization of miR-126	93
V.4.3.1.	MiR-126 interacts with and its production is regulated by Myoferlin...	93
V.4.3.2.	Silencing of Myoferlin increases the levels of miR-126 in the supernatant of cells	94

VI. Conclusion	97
VII. Zusammenfassung.....	99
VIII. References.....	104
Eidesstattliche Erklärung	113
Curriculum Vitae.....	114
Acknowledgements	117

I. Introduction

I.1. Non-coding RNAs

By far not all genetic information is expressed by mRNA coding regions of the DNA. 98% of the human genome is not encoding for proteins. Therefore, these non-coding regions have been considered as “junk DNA” for a long time [1, 2]. The last years, new high throughput sequencing techniques have allowed the elucidation of the heterogeneous population of non-coding RNAs (ncRNAs, Table 1). RNAs longer than 200 nucleotides (nt) belong to the family of long non-coding RNAs (lncRNAs). They can exhibit numerous functions: The biggest family of RNAs is represented by the ribosomal RNAs (rRNAs). Together with the transfer RNAs (tRNAs) they are essential for the translation of mRNA into an amino acid sequence.

Table 1: Examples for human long (>200nt) and short (<200nt) non-coding RNAs (ncRNAs) that are implicated in numerous regulations within a human cells. lncRNA: long non-coding RNA, rRNA: ribosomal RNA, piRNA: piwi interacting RNA, tRNA: transfer RNA, snRNA: small nuclear RNA, snoRNA: small nucleolar RNA, scaRNA: small cajal bodies specific RNA, miRNA: microRNA.

ncRNA	Length [nt]	Function
<u>long</u>		
lncRNA	>200	Splicing, epigenetic regulation
rRNA	120~4700	Translation
<u>small</u>		
piRNA	24-30	Transposon silencing, heterochromatin modification, germ cell regulation
tRNA	70~100	Translation
snRNA	70~350	mRNA processing and modifications
snoRNA and scaRNA	70~300	mRNA processing and modifications
miRNA	18-22	Posttranscriptional gene silencing

The most popular example of a functional lncRNA is Xist, a lncRNA that mediates the inactivation of the second X-chromosome in females [3]. By now, numerous functions have been assigned to lncRNAs, e.g. epigenetic regulation of gene expression or splicing [4, 5] and are deregulated in disease states, e.g. MALAT1 has been shown to be involved in the pathogenesis of pulmonary tumors [6]. However, the function of many lncRNAs remains unknown. Small non-coding RNAs are shorter than 200 nucleotides. For example, small nuclear RNAs (snRNAs or U-RNAs) are located in the nucleus where they regulate the processing of mRNAs. Small nucleolar RNAs (snoRNAs) and small cajal body specific RNAs (scaRNAs), as well are able to guide modifications of other RNAs, especially methylation and pseudouridylation of rRNAs, tRNAs and snRNAs. Piwi-interacting RNAs (piRNAs) are the largest group of small non-coding RNAs. They are present in complexes with proteins and function as epigenetic gene regulators in germ cells [7]. Moreover they are implicated in transposon silencing and heterochromatin modification [8]. MicroRNAs are another large group of small non-coding RNAs, that was investigated extensively within the last two decades. The biogenesis and regulation as well as the function of miRs will be introduced in the following sections.

I.2. microRNAs (miRs)

I.2.1. Discovery of miRs

In 1993, Lee et al. [9] reported their observation from *C.elegans* that lin-4 not only encodes for a protein important for the larval development but also a small non-coding RNA of 22 nucleotides in length. This small RNA was able to repress the expression of the gene lin-14. Moreover they observed that the sequence of lin-4 is complementary to the 3'UTR of lin-14 mRNA and that binding of lin-4 to the lin-14 mRNA leads to destabilization. With this, the principle how miRs act has been described for the first time: Small non coding RNAs, later termed microRNAs (miRs), bind with a short sequence, the seed sequence, complementary to the 3'UTR of a target mRNA thereby inducing

translational inhibition and mRNA degradation. Although the seed sequence comprises only about 8 nt, miRs are specific for only few mRNAs. One miR is able to target several mRNAs and one mRNA can be targeted by different miRs. Therefore, miRs are thought to regulate a whole gene pattern rather than single genes. MiRs are predicted to target about 30% of the human genes [10]. By now more than 1100 human miRs are described in the miR database (www.microrna.org). The importance of short non-coding miRs as posttranscriptional gene regulators in physiological and pathophysiological situations has been confirmed by numerous publications.

I.2.2. Canonical biogenesis of miRs

Mammalian miRs are transcribed into primary transcripts (pri-miRs) by RNA polymerases II or III. The pri-miR forms into a hairpin of which the stem contains the mature miR sequence. The mature miR is processed out of the pri-miR within two endoribonucleolytic cleavages. First, the endoribonuclease Drosha cleaves the pri-miR into precursor miR (pre-miRs) of about 70 nt in length possessing a 3' overhang. Together with Drosha, DGCR8 (DiGeorge syndrome critical region gene 8) is part of the microprocessor complex. DGCR8 is important to lead Drosha into the correct position for cleavage. The cleavage takes place about 11 bp above the stem of the hairpin. Exportin-5 in a Ran-GTPase dependent manner shuttles the pre-miR out of the nucleus (Figure 1). In the cytoplasm, the pre-miR is further trimmed by Dicer, the second endoribonuclease. Dicer, an enzyme of the RNase III family that is able to bind and cleave dsRNAs. Dicer contains two RNase II domains and a PAZ domain [11], and splices the terminal loop from the stem of the pre-miR resulting in a duplex of 22 bp with 3' overhangs at both ends. Then, Dicer recruits the dsRNA binding protein TRBP to the complex. TRBP unwinds the dsRNA duplex. The two resulting single stranded RNAs (ssRNAs) are distinguished by the suffix "-3p" or "-5p" with respect to whether they derive from the 3' or the 5' arm of the duplex. The RNA with the higher thermodynamic stability at the 5' end is the guide miR, while the opposite strand is named miR* (miR star) and is rarely functionally important. The RNA induced silencing complex (RISC) mediates the interference of the mature miR with a target mRNA. In

addition to Dicer and TRBP, Argonaute proteins (Ago1-4) are part of the RISC; e.g. Ago2 directly interacts with the mature miR [12].

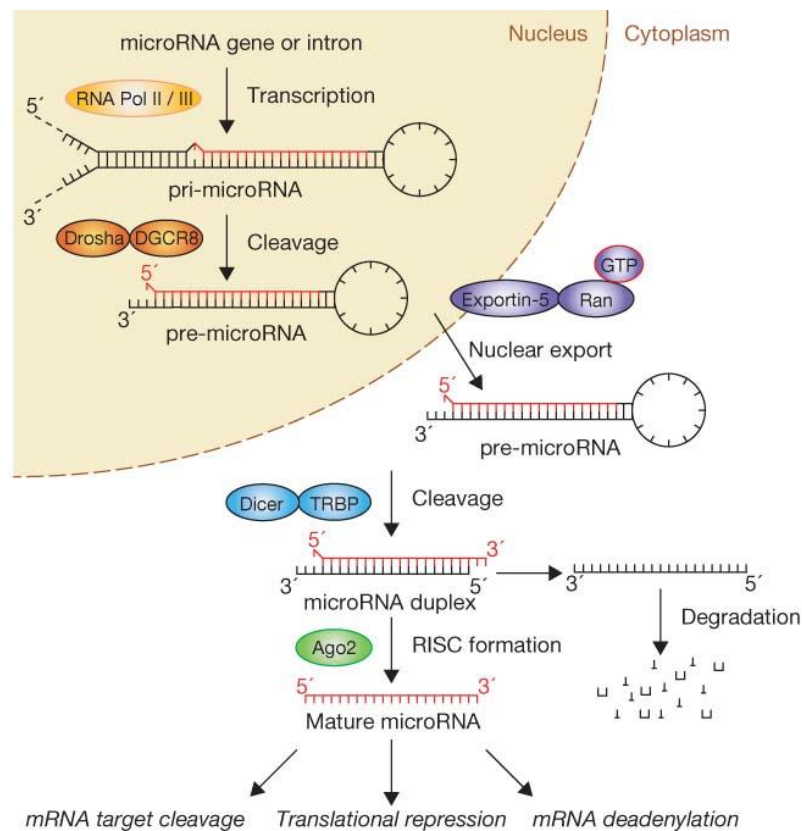


Figure 1: Canonical biogenesis of miRNAs. MiRNAs are transcribed into pri-miRs out of which Drosha excises the pre-miRs. Pre-miRs are exported into the nucleus by Exportin-5 in a Ran-GTPase dependent manner. In the cytoplasm, Dicer catalyzes the maturation of the pre-miRs into dsRNA molecules. The more stable strand is incorporated into RISC and guided to its target mRNA [13].

MiRNAs can be encoded by introns or exons and are then coexpressed with their host gene, or they are under the control of their own promoters. Moreover, about 40% of the human miRNAs are expressed in clusters. Since miRNAs of a cluster are under the control of one promoter they are transcribed as one primary transcript, which is then further processed by Drosha and Dicer. Some pre-miRs can also derive from short intronic hairpins and are therefore independent of Drosha [14]. By now, these so called mirtrons have been found in *Drosophila* [14], *C. elegans* [15], and mammals (e.g. miR-668, miR-6869) [16]. While mirtrons are independent of Drosha but still require Dicer, there are also miRNAs that only need Drosha but are Dicer independent [17]. For example, the primary transcript of miR-

451, a miR important for erythropoiesis, is cleaved into the pre-miR-451 by Drosha and then is not catalyzed by Dicer but just by Ago2 alone [17].

I.2.3. RNA interference of miRs and siRNAs

MiRs binding to the 3'UTR of target mRNA via Watson-Crick-base pairing can either induce direct cleavage of the mRNA or they induce mRNA destabilization or translational inhibition. MiRs are loaded into the RISC (RNA induced silencing complex), consisting of Dicer, Argonaute proteins and TRBP [17] and, via its seed region, attract the 3'UTR of a target mRNA. The direct mRNA cleavage is mediated by Argonaute 2 (Ago2). Prerequisite for this direct mRNA cleavage is a perfect base pairing, which can almost exclusively be found in plants but rarely in mammals. Imperfect basepairing of mammalian miRs to their target mRNA rather causes suppression of mRNA translation. When the target mRNA is located to the RISC, the 5'cap cannot be recognized by eukaryotic initiation factor 4F (eIF4F) [18]. Of note, this way of RNAi does not alter the abundance of target mRNAs but only the generation of a polypeptide.

RNAi is not restricted to miRs. Other mammalian endogenous small interfering RNAs are piRNAs and synthetic small interfering RNAs (siRNAs). They are not genome encoded (endogenous) but introduced into cells in vitro by transfection (Table 2). Structurally the miR precursor is a hairpin, while the siRNA precursor is a dsRNA. Both are matured in the cytoplasm by Dicer and loaded into RISC where they mediate their function in inhibiting protein synthesis (Figure 2). SiRNAs are designed to perfectly base pair with the target mRNA and therefore lead to direct mRNA cleavage by Ago2. In contrast to siRNAs, the base pairing of mammalian miRs to its target mRNA is hardly ever perfect. Therefore, translational suppression is considered to be the predominant way of action of miRs. Moreover, while one miRNA can target several mRNAs, siRNAs are specific for one target mRNA.

Table 2: Comparison of miRNAs and siRNAs in human cells. While there is endogenous siRNA in drosophila melanogaster [19], in human cells siRNA is not present endogenously but is used as a genetic tool that is introduced to cells by transfection.

	siRNA	miRNA
Origin	exogenous synthetic molecule, introduced to cells by transfection	endogenous genome encoded
ssRNA or dsRNA?		dsRNA
Maturation in the cell		Processed by Dicer
3' overhangs		Yes
Mediation of function		Loading into RISC
Function		Inhibition of protein synthesis
Structure of the precursor	dsRNA	hairpin
Quality of base pairing	Perfect base pairing	Imperfect base pairing in mammals
Effect on mRNA	mRNA degradation	suppression of RNA translation

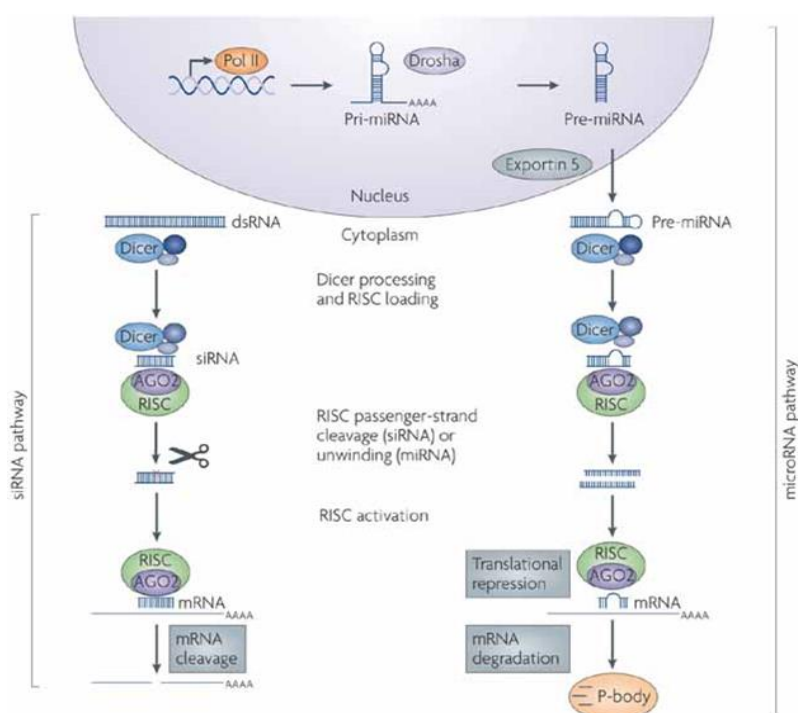


Figure 2: RNAi pathways of miRNAs and siRNAs. While hairpin pre-miRs are generated in the nucleus by Drosha and exported by Exportin-5 before they are processed by Dicer, the generation of siRNAs begins when Dicer cleaves the dsRNA into siRNAs. Both, mature siRNA and miRNA, are loaded into the RISC to bind to one (siRNA) or several (miRNA) target mRNAs by perfect (siRNA) or imperfect (miRNA) basepairing [20].

I.2.4. Regulation of miRs

As miRs are very potent posttranscriptional regulators of numerous genes they are also themselves subject of sophisticated control in order to ensure that miRs are tightly controlled not only during development but also upon stress conditions as well as in a growing number of physiological and pathophysiological situations. Regulation of miRs can take place on three levels (Figure 3): The earliest possible regulation can take place at the level of transcription of the pri-miR by RNA polymerase II or III. Promoter activators and repressors regulate the level of transcription by acting in cis or trans. Cell signaling pathways can affect miR transcription, e.g. via Ras/MAPK or TFG- β /BMP [21] as well as methylation of the promoter [22]. Moreover, the biogenesis of miRs can be regulated and, finally, the stability of miRs.

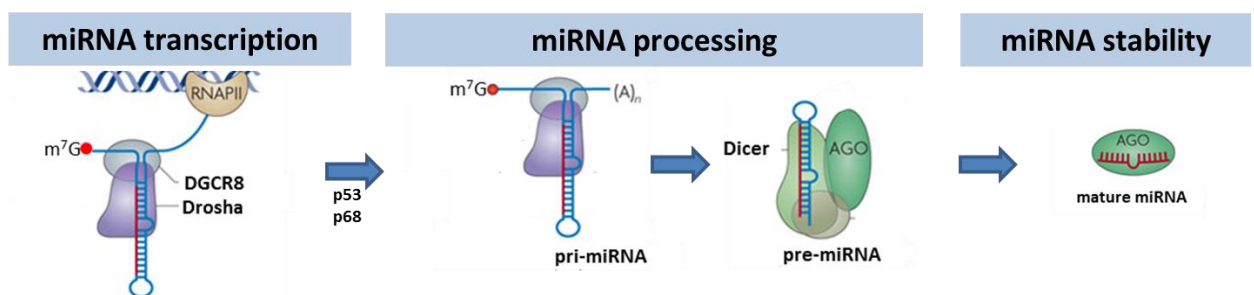


Figure 3: MiRs are regulated on different levels. The transcription is controlled via the activity of the promoter, the processing of pri-miR to pre-miR and pre-miR to mature miR can be controlled by factors interacting with Drosha, Dicer, or with the pri-miR or pre-miR. Moreover, the stability of the mature miR can be affected [23].

I.2.4.1. Regulation of the processing of miRs

MiRs are also regulated posttranscriptionally by interference with the turnover of pri-miR to pre-miR or the maturation of pre-miR to the mature miR. Several co-factors of the Drosha and Dicer processing complexes have been described which exhibit different modes of action. Some recognize certain motifs on the RNA (e.g. KSRP), others interact with the terminal loops of the hairpins within pri- or pre-miRs (e.g. hnRNP A1) or they

facilitate the trimming reaction (e.g. R-SMADs). In the following, several examples will be described in more detail.

I.2.4.1.1. Positive regulators of miR processing

I.2.4.1.1.a. DEAD box helicases p68 and p72

The DEAD box helicases p68 (DDX5) and p72 (DDX17) function as ATP dependent RNA helicases. The energy from the ATP hydrolysis is converted into energy for the unwinding of RNAs yielding in the dissociation of RNA-protein complexes. By immunoprecipitation it could be shown that p68 and p72 interact with DGCR8, a cofactor of Drosha which helps to guide Drosha to the correct cleavage site [24, 25] (Figure 4a). P68 and p72 specifically interact with a subset of pri-miRs and guide the correct trimming of the hairpin [24]. In line with this p68^{-/-} or p72^{-/-} mouse embryonic fibroblasts (MEFs) exhibit a lowered expression of miRs regulated by p68/p72. Moreover, p68 and p72 interact with SMADs, p53 and the estrogen receptor [24].

I.2.4.1.1.b. SMADs

SMADs are signal transducers of the TGF β signaling pathway: Upon binding of ligands, e.g. TGF β or bone morphogenetic proteins (BMPs), to the TGF β receptor (TGF β R) I or II, the receptors TGF β RI and TGF β RII interact and form heterodimers. In this activated form, TGF β RI activates R-SMADs which bind to Co-SMADs and then enter the nucleus where they bind to a conserved sequence, the SMAD binding element. By recruitment of other transcription factors the R-SMADs-Co-SMADs complex mediates transcriptional activation or repression. Interestingly, research of the past decade has demonstrated that the TGF β induced signaling not only acts on the regulation of promoters but also as a posttranscriptional regulator of miR processing. SMADs appeared to play a role in the regulation of miRs since BMP4 or TGF β stimulation of vascular smooth muscle cells (VCMCs) induced the expression of miR-21. This leads to a reduced expression of the programmed cell death protein 4 (PCDP4) while contractile smooth muscle genes are

induced [26]. This implies the BMP/TFG β dependent induction of miR-21 expression. However, knock down of the effector proteins R-Smads did not influence the pri-miR-21 transcription but only the levels of pre-miR-21 and the mature miR-21 (Figure 4b). Further experiments identified Smads as posttranscriptional regulators of miR processing. Smads interact with p68 and/or Drosha within the microprocessor complex and facilitate the binding of pri-miRs to Drosha by recognizing the Smad binding element in pri-miRs. The stimulation of VSMCs with TFG β or BMP4 facilitates the miR-21 maturation thereby indirectly inducing the contractile phenotype of VSMCs [26].

There is also a small subset of miRs present in VSMCs that is rapidly down regulated upon stimulation with TGF β or BMP4 [27]. This indicates that R-Smads not only facilitate Drosha processing but also repress maturation of some miRs, e.g. by promoting the dissociation of the Drosha complex from pri-miRs.

I.2.4.1.1.c. P53

The transcription factor p53 is not only crucial for the transcriptional regulation of genes involved in cell cycle control and apoptosis but also positively regulates the biogenesis of certain miRs, e.g. miR-16-a and miR-143/145 in response to DNA damage [28]. These miRs are associated with the suppression of cell growth and are part of the tumor suppressive program governed by p53. The mode of action is similar to that observed with R-Smads upon TGF β signalling. Suzuki et al. showed that in response to DNA damage in cancer cells, p53 associates with the DEAD box helicase p68 leading to an increased maturation of certain pri-miRs (Figure 4c). In line with this, when p53 was mutated, Drosha could not interact with p68, resulting in a widespread down regulation of miRs [28].

I.2.4.1.1.d. BRCA1

Breast cancer 1 (BRCA1) is a tumor suppressor that plays a role in DNA repair. Inherited mutations of BRCA1 or BRCA2 are associated with a predisposition for breast and ovarian

cancer [29]. BRCA1/2 mutations go in line with dysregulation of some miRs. It turned out that BRCA1 is able to interact with the Drosha microprocessor complex, DDX5 [30], Smad3 [31], p53 [32], as well as with the root of the stem loop of pri-let7a, pri-miR-16, pri-miR-145 and pri-miR-34a [30]. Thereby BRCA1 facilitates Drosha mediated pri-miR processing of miRs that are dysregulated under cancer conditions [30] (Figure 4d).

I.2.4.1.1.e. KSRP

The KH-type splicing regulatory protein (KSRP) has first been described to be involved in mRNA decay. It recognizes single strand mRNA elements that are AU rich via its four KH elements. By now, it is known that KSRP is also involved in the processing of miRs. It is part of both, the nuclear Drosha complex and the cytoplasmic Dicer complex and therefore regulates the turnover of pri-miRs as well as pre-miRs and represents a link between the two endonucleolytic cleavages catalyzed by Drosha and Dicer. Criteria for the interaction of KSRP with pri- or pre-miRs are the presence of G-rich sequences and the accessibility of the RNA. MiRs that harbor this motive include the let-7 family and miR-20a [33]. KSRP acts as a coactivator of miR processing by recruiting specific pri- and pre-miRs to Drosha and Dicer and facilitating the trimming (Figure 4e). The precursor of pre-let-7a is an attractive target of KSRP as it contains a G-rich stretch and provides steric accessibility at the terminal loop of the hairpins [33]. Pre-miR-21, which lacks a G-rich stretch, is also bound by KSRP because it offers a well accessible 3D structure at its terminal loop.

I.2.4.1.1.f. hnRNP A1

The heterogeneous nuclear ribonucleoprotein A1 (hnRNP A1) has been described to be involved in the maturation of miR-18a, a member of the miR-17-92a cluster. HnRNP A1 acts only in the nucleus where it binds to the terminal loop of miR-18a within the pri-miR-17-92 transcript and thereby facilitates further processing by Drosha [34, 35]. By interacting with the terminal loop of pri-miR-18a hnRNP A1 enables a conformation of the hairpin that is favoured by Drosha (Figure 4f). Therefore, the terminal loop of pri-miR-18a

is of major importance for the efficient processing [35]. HnRNP A1 has also affinity for the precursor of let-7a, however, its impact on the maturation of let-7a is different from its function regarding pri-miR-18a: KSRP normally facilitates the turnover of let-7a [36]. HnRNP A1 antagonizes the binding of KSRP [37]. In line with this, levels of hnRNP A1 negatively correlate with mature let-7a levels and depletion of hnRNP A1 processing of pri-let-7a [38].

I.2.4.1.1.g. Autoregulation

MiRs are not only regulated by proteins that bind to pri- or pre-miRs or the processing proteins, but also the microprocessor complex itself can exhibit aberrant functions. Argonaute proteins have been shown to interact with the primary transcript of pri-let7, thereby promoting downstream processing [39]. This interaction is supported by mature let-7 that binds specifically a conserved site within the pri-let7 and thereby creating a positive feedback loop [39] (Figure 4g).

I.2.4.1.1.h. TDP-43

The TAR DNA binding protein 43 (TDP-43) is a homologous of the hnRNPs and is located in the nucleus [40]. In patients suffering from neurodegenerative diseases such as amyloid lateral sclerosis, TDP-43 is mutated and therefore accumulates in cytoplasmic aggregates [41]. Under diseased states certain miRs are dysregulated. Interestingly, TDP-43 was shown to interact with the Drosha complex and thereby facilitates the processing of miRs that play a role in neuronal outgrowth, e.g. miR-558-3p, miR-574-3p, miR-132 and miR-143 [42] (Figure 4h). In absence of TDP-43 or under disease conditions when TDP-43 is abnormally distributed these miRs are reduced [42]. Taken together, TDP-43 is an example of how the tightly controlled regulation of miR processing is crucial for the prevention of diseases.

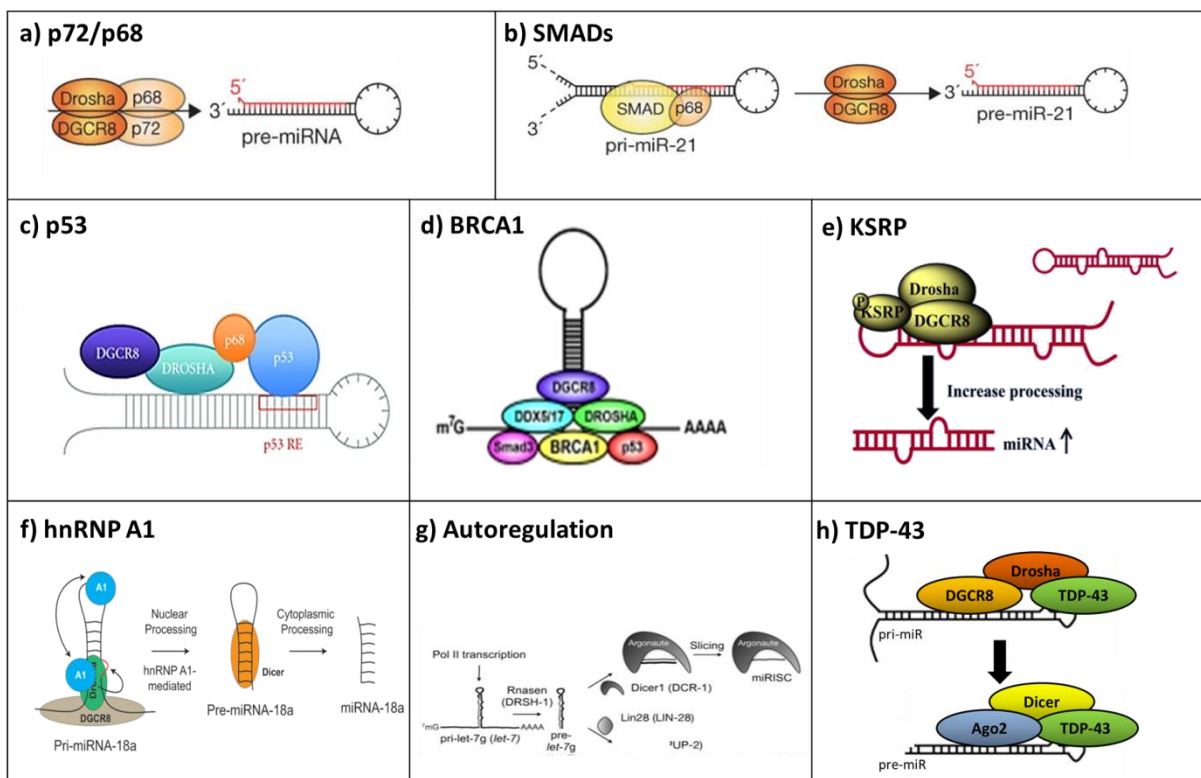


Figure 4: Positive effectors of miR maturation. a) The DEAD box helicases p68 and p72 guide the correct trimming of pri-miRs by Drosha [13], b) SMADs facilitate the binding of Drosha to pri-miRs [13], c) p53 mediates Drosha processing by enabling the interaction of Drosha with p68. RE=response element [43], d) BRCA1 interacts with numerous members of the microprocessor complex and with pri-miRs, thereby promoting Drosha processing [30], e) KSRP recognizes G-rich stretches in the terminal loop of pre-miRs and pri-miRs and thereby facilitates Drosha and Dicer processing [44], f) HnRNP A1 interacts with the terminal loop of pri-miR-18a, thereby bringing pri-miR-18a in a conformation favored by Drosha [38], g) Mature let-7 is able to induce the interaction of pri-let7 and thereby establishing a positive feedback loop [39], h) TDP-43 interacts with Drosha and facilitates further Drosha processing [42].

I.2.4.1.2. Negative regulators of the processing of miRs

I.2.4.1.2.a. TUT4

TUT4, a terminal uridyl transferase, specifically acts on pre-miRs that harbor a GGAG motif in their terminal loop. The terminal loops of pre-let-7a, pre-miR-107, pre-miR-143, pre-miR-200c exhibit this motif and is bound by TUT4. TUT4 adds a polyuridine tail to the 3' end of these pre-miRs which leads to a blockage of further processing by Dicer (Figure 5a). Moreover 3' polyuridylation triggers pre-miR decay by recruitment of exonucleases [45]. Binding of TUT4 to these pre-miRs can exclusively take place in the presence of Lin28. While TUT4 is widely expressed, Lin28 is restricted to undifferentiated cells. As let7a promotes stem cell differentiation, the presence of Lin28 in stem cells assures the maintenance of the undifferentiated state by enabling the uridylation of pre-let7a [46].

I.2.4.1.2.b. IRE1 α

IRE1 α is an endoribonuclease of the endoplasmic reticulum (ER) that is activated upon ER stress and induces apoptosis. ER stress occurs when the amount of proteins that need to be folded over scopes the capacity of the ER and many unfolded proteins are enriched. IRE α forms oligomers which autophosphorylate each other. Activated IRE1 α splices the mRNA of Xbp1, a transcription factor regulating the adaption to ER stress [47]. Moreover, under ER stress, IRE α cleaves the pre-miRs pre-miR-17, pre-miR-34a, pre-miR-96 and pre-miR-125b by a mechanism that is distinct from Dicer cleavage, thereby creating different cleavage sites (Figure 5b). Under basal conditions these miRs target the mRNA of Caspase2. When the maturation of caspase2 targeting miRs is disturbed, caspase2 is increased and induces mitochondrial apoptosis. Therefore, the posttranscriptional regulation of a subset of miRs by IRE α enables the adaption of the cell to ER stress [48].

I.2.4.1.2.c. ADARs

Adenosine deaminases acting on RNA (ADARs) bind to dsRNAs and convert adenosine into inosine (A-to-I) by deamination. Inosine is recognized as Guanosine resulting in a change of A-T pairing to G-C pairing and therefore in a change from Adenosine to Guanosine on the one strand and Uridine to Cytidine on the other strand. Being dsRNAs, a subset of pri-miRs and pre-miRs can be the subject of editing. This tiny change of the sequence can either cause a block of further processing [49], or it can change the mRNA targets of the mature miR. It has been shown that when pri-miR-142 is A-to-I edited it cannot be further processed by Drosha but is degraded by SND1, a component of the RISC [50] (Figure 5c).

I.2.4.1.2.d. Hormones

Upon estrogen treatment of uteri or human breast cancer cells an inhibition of miR expression has been observed. First, it has been speculated that the promoters of miRs exhibit estrogen response elements. Unexpectedly, estrogen stimulation did not affect the levels of pri-miRs but only reduced the levels of pre-miRs. Further experiments confirmed that miR expression is regulated by estrogen not at the levels of transcription but by interference with the miR processing machinery. The estrogen receptor ER α directly interacts with two DEAD box helicases belonging to the microprocessor complex, p68 and p72. Activation of ER α by its ligand estrogen (E2) even increased the interaction with the microprocessor complex because of additional interaction of ER α with Drosha. Under this condition Drosha is not able to process pri-miRs (Figure 5d). This blockage of miR biogenesis explains the observed stabilization of mRNAs that are potential miR targets upon estrogen treatment [51].

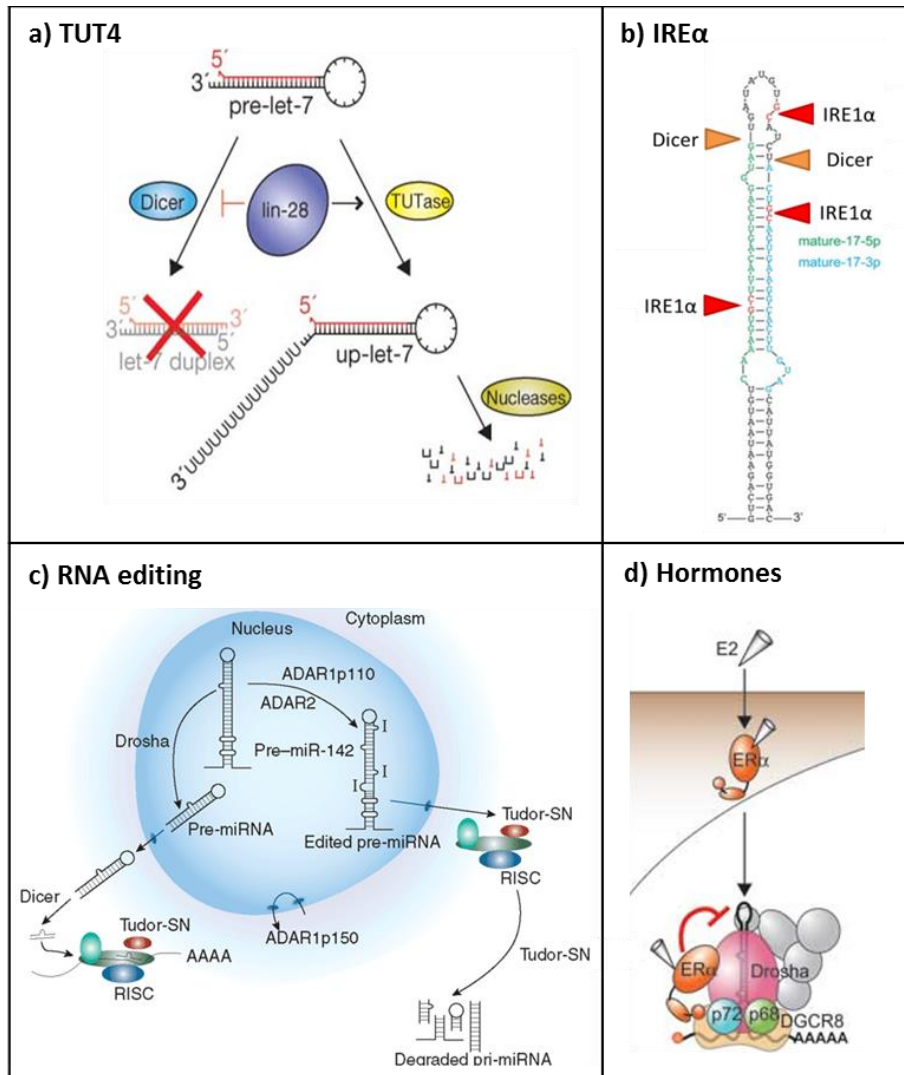


Figure 5: Negative regulators of miR processing. a) TUTase4 polyuridylation of pre-let-7 and thereby initiates miR degradation [13], b) Upon ER stress IRE1 α cleaves pre-miRNAs at different sites than Dicer, thereby inducing the degradation of these RNAs (picture adapted from [48]), c) ADAR1 and ADAR2 catalyze the deamination Adenosine in pri-miRNAs and pre-miRNAs (A-to-I editing). Edited pri- and pre-miRNAs are degraded by Tudor-SN (SND1) [52], d) Upon activation, the Estrogen receptor ER α interacts with the microprocessor thereby inhibiting further pri-miR maturation [53].

Table 3: Summary of known regulators of miR maturation.

	Name	Interaction partner	Mechanism	Effect	Examples	Ref.	
Positive regulators	a) p68, p72	DGCR8	Positions Drosha for binding pri-miRs	+	all miRs	24, 25	
	b) SMADs	Drosha	Facilitates binding of Drosha to pri-miRs via the SMAD binding element	+/-	miR-21	26,27	
	c) p53	p68	Enables interaction of p68 with Drosha	+	miR-15, miR-16-1, miR-143/145	28	
	d) BRCA1	members of the microprocessor complex and with the stem loop of pri-miRs	Facilitates Drosha processing of pri-miRs	+	let-7a, miR-16, miR, 145, miR-34a	29-32	
	e) KSRP	GC-rich ssRNAs, part of Dicer and Drosha, needs steric accessibility to TL	Facilitates Drosha and Dicer processing	+	Let-7, miR-20, miR-21	33	
	f) hnRNP A1	TL of pre-miR and pri-miR	Conformational change facilitates Drosha processing	+	miR-18a, let-7a	34-38	
	k) Autoregulation	Ago2	Mature let-7 together with Ago facilitates pri-let7 processing, positive feedback loop	+	Let-7	39	
	h) TDP-43	Drosha	Facilitates Drosha processing	+	miR-558, miR-574, miR-143	40-42	
	Negative regulators	a) TUT4	Pre-miRs with GCAG motif in TL	Uridylation of terminal loops prevents Dicer processing	-	Let-7a, miR-107, miR-143, miR-200c	45, 46
		b) IRE1 α	Pre-miRs (upon ER stress)	Promotes alternativ cleavage of pre-miRs, degradation of miRs, apoptosis	-	miR-17, miR-34a, miR-96, miR-125b	47, 48
c) ADARs		dsRNA	A-to-I editing of pri- and pre-miRs prevents further processing	-	Pri-miR-142	49, 50	
d) Estrogen receptora		Competitive binding to p68, p72 and Drosha	Prevents Drosha processing	-	all miRs	51	

I.2.4.2. Regulation of mature miRs

The function of mature miRs can be regulated in various ways. Their functionality can be regulated by the availability of target mRNAs, which can act as a decoy for miRs or by competitive non coding RNAs that bind to miRs and thereby inhibit their binding to target mRNAs [54]. MiRs can also be trapped as they are bound to circular RNAs (ciRs), so called molecular sponges. Interestingly, ciR-7 contains numerous miR-7 binding sites thereby serving as a decoy for miR-7 which can no longer interact with target mRNAs [55]. Another way of preventing the interaction of a miR and its target mRNA is by binding of the target mRNA to the RNA binding protein Dnd1 so that the mRNA is protected from miR binding [56]. Moreover, miRs can be regulated via their localization. Mature miRs are generally found in the cytoplasm bound to RISC, but there is also evidence for subcellular localization, e.g. to nucleoli [57], mitochondria [58] at the rough ER [59] or endolysosomes (multivesicular bodies) [60]. Recent publications indicate that miRs can also be found extracellularly in almost all tested body fluids. They can be protected from RNases either by proteins or by the membrane of apoptotic bodies, shedding vesicles or exosomes (for revision see [61]). Binding to proteins has been observed under atheroprotective low shear stress, miR-126 is released from ECs in an Ago2 bound form and is taken up by SMCs and controls gene expression of SMCs in a paracrine manner. This leads to an increased turnover of SMCs [62]. Apoptotic bodies are 1-4 μm in diameter and are produced upon apoptosis [63]. Shedding vesicles or microvesicles are smaller in size (0.1-1 μm) and are released by budding of the plasma membrane [64]. For example, miRs can act as mediators between ECs and SMCs. Hergenreider et al. showed that the transcription factor Klf2 activates the promoter of miR-143/145 in endothelial cells and that miR-143/145 is transported from ECs to SMCs via extracellular vesicles, thereby enabling the atheroprotective phenotype of the endothelium [65] (Figure 6).

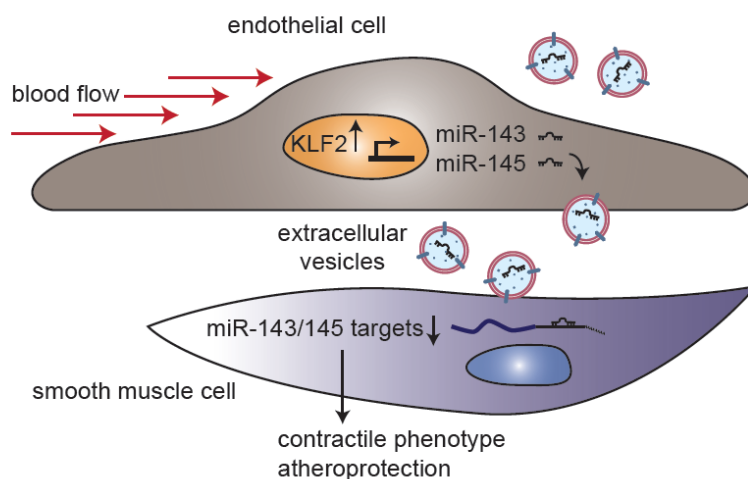


Figure 6: MiR-143 and miR-145 are expressed by endothelial cells upon laminar flow and function as atheroprotective signals that are shuttled in vesicles to recipient smooth muscle cells. (Copyright Eduard Hergenreider)

1.2.5. MiRs in endothelial cells

Endothelial cells (ECs) form the most inner layer of blood vessels, forming the barrier between the blood and the tissue and are in direct contact with the circulating blood. To the periphery ECs are covered by smooth muscle cells (SMCs), pericytes and fibroblasts. Another function of the endothelium, besides providing a special separation, is the coordination of the communication of blood cells and circulating factors with the surrounding tissue. The endothelium also controls the blood pressure by adjusting the diameter of the vessels by vasoconstriction or vasodilation induced by SMCs. Endothelial dysfunction can further contribute to atherosclerotic diseases, e.g. coronary artery disease. In order to prevent thrombosis, the healthy endothelium exposes fibrinolytic substances as heparin sulfate to its surface. Moreover, endothelial cells control and contribute to the formation of new blood vessels from existing ones, a process termed angiogenesis. Angiogenesis is induced by the vascular endothelial growth factor (VEGF) and takes place when a tissue is insufficiently supplied with oxygen and when new vessels are needed to counteract ischemia. Aberrant angiogenesis is associated with various diseases, e.g. tumor progression [66]. Due to the impact of the endothelium on the

survival of an organism, endothelial cells need to be controlled tightly. Numerous studies showed that certain miRs function as potent regulators of the endothelium, e.g. miR-126, miR-17-92a, miR-130a, miR-223, miR-296 and miR-378, as well as miR-221/222 and let7. MiR-126 and the members of the miR-17-92a cluster are very well characterized and will be described in more detail on the next pages. Not only endothelial cells but also SMCs are controlled by miRs. The miR-143/145 family is essential for the functional contractile phenotype of SMCs. MiR-143/145 deficient mice lack the ability of vasoconstriction and vasodilation and are prone to exhibit neointimal lesions. ACE, the angiotensinogen-to-angiotensin converting enzyme, is targeted by miR-143/145. Silencing of ACE interferes with the ability of SMCs to narrow down the vessel diameter and therefore to a lowering of blood pressure [67].

I.2.5.1. miR-126

MiR-126 is one of the highest expressed miRs in endothelial cells. It is encoded within intron 7 of *Egf7*. MiR-126 expression is induced by activation of the *Egf7* promoter, either via the transcription factors ETS1 and ETS2, or epigenetically by methylation of the promoter [68]. *Egf7*, which encodes miR-126, regulates the migration of ECs as well as the integrity of capillary tubes, both in vitro [69] and in vivo [70]. The depletion of miR-126 in mice caused a phenotype of vascular leakage, edema and hemorrhages, and leads to lethality in some of the miR-126 depleted mice embryonically lethal [70, 71] (Figure 7). *Spred1* is a validated target of miR-126. It inhibits MAP kinase signaling, which is essential for the signal transduction that is normally induced by binding of VEGF to its receptor. Therefore, due to an increase of *Spred1* mRNA in the absence of miR-126, angiogenesis is hampered [70].

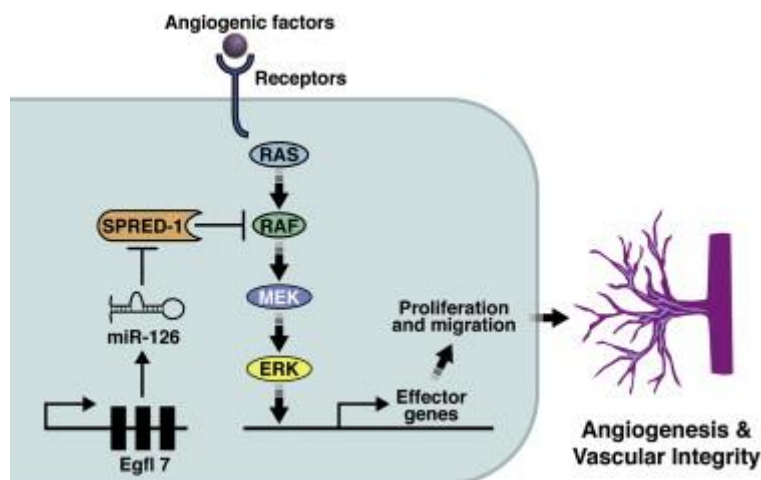


Figure 7: MiR-126 regulates angiogenesis. Upon binding of VEGF or FGF to the receptor on endothelial cells, the MAPK signaling pathway is induced which induces the expression of pro-angiogenic genes. SPRED1 inhibits this effect as long as it is not silenced by miR-126 [70].

Another target of miR-126 is the mRNA of the miR-126 host gene Egf7 [72]. In the context of tumorigenesis miR-126 plays a bivalent role: On the one hand, miR-126 can act as a tumor suppressor by interfering with cell proliferation and migration. In line with this it was shown that patients with primary breast cancer and high levels of miR-126 displayed higher survival than patients with low miR-126 levels [73]. In mice with breast cancer and low levels of miR-126 the retroviral restoration of miR-126 levels could suppress tumor growth and metastasis [73]. In addition to breast cancer, miR-126 is reduced in colorectal cancer [74], gastric cancer [75], bladder and prostate cancer [76], cervical cancer [77] and lung cancer [78]. On the other hand, miR-126 induced angiogenesis also promotes the growth of tumors [79].

1.2.5.2. The miR-17-92a cluster

The miR-17-92a cluster is a polycistronic cluster encoded on chromosome 13 open reading frame 25. It comprises seven mature miRs, miR-17-5p (in the following miR-17), miR-17-3p, miR-18a, miR-19a, miR-20a, miR-19b and miR-92a, which are under the control of one promoter and transcribed as one primary transcript. Although all members of the miR-17-92a cluster are transcribed simultaneously, they exhibit different functions.

1.2.5.2.1. Functions of the miR-17-92a cluster

The miR-17-92a cluster has first been described in the context of tumorigenesis of B-cell lymphomas [80] and is therefore also called oncomir-1 [81-83]. By now, it has been described in numerous types of tumors, e.g. colon cancer [84], lung cancer [85], breast cancer [86] or glioma [87]. However, also additional functions have been assigned to the miR-17-92a cluster (Figure 8). It is conserved among species and is highly expressed in endothelial cells. Depletion of miR-17-92a in mice was lethal during embryogenesis or shortly after birth due to hypoplastic lungs or defects in the ventricular septum as well as defective B-cell development [88].

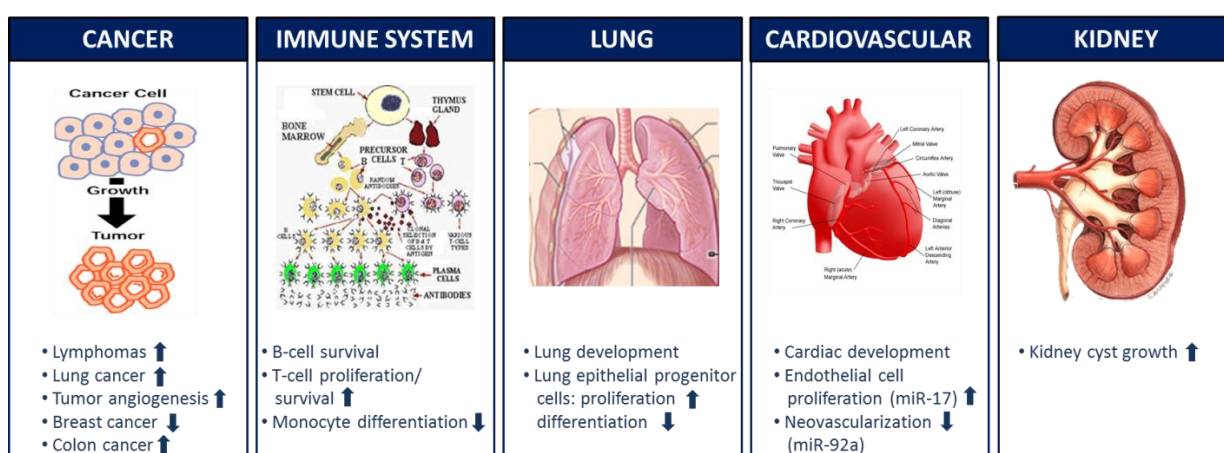


Figure 8: Functions of the miR-17-92a cluster. The first described function of miR-17-92a was related to tumorigenesis and therefore this family also is named “oncomir-1”. By now it has been described in numerous conditions of health and disease (picture adapted from [89]).

I.2.5.2.1.a. miR-17-5p and miR-20a

MiR-17-5p (miR-17) and miR-20a differ in as little as two nucleotides. Since their seed sequences differ in only one nucleotide, they have many targets in common. Both exhibit tumor promoting functions as they target tumor repressive factors such as the cell cycle regulator p21. Interestingly, they reveal bivalent roles as they are also able to act tumor suppressive by targeting the cell cycle promoter cyclin D1 [90] or the transcription factor E2F [91, 92]. Whether miR-17 and miR-20a act as tumor promoters or suppressors appears to be dependent on the cellular context [93]. Additional functions of miR-17 and miR-20a refer to the regulation of monocyte differentiation [94] as well as the regulation of the cardiopulmonary system. They are highly expressed during the development of the lung. Silencing of miR-17 had beneficial effects on mice suffering from pulmonary hypertension [95]. P21 seems to be the relevant target for this effect by preventing lung vascular and right ventricular remodeling [95]. Both miR-17 and miR-20a impede angiogenesis by targeting pro angiogenic genes such as Janus kinase 1 (Jak1) [96] or fibronectin, thereby impairing cell adhesion, migration and proliferation [97]. In the heart, miR-17 targets tissue inhibitor of metalloproteases 1 and 2 (TIMP1 and 2) thereby impairing cardiac matrix remodeling after myocardial infarction [98]. Moreover, it was shown that miR-17 and miR-20a control the self-renewal capacity of neural stem cells (NSCs) by targeting Trp53inp1, a downstream component of p53 [99].

I.2.5.2.1.b. miR-18a

Tumor angiogenesis by suppressing the release of anti angiogenic factors from tumor cells is promoted by miR-18a [82]. Moreover, miR-18a was shown to be involved in immune reactions, as it is able to be involved in the destruction of cartilage and chronic joint inflammation in the course of rheumatoid arthritis by enhancing the signaling of NFκB [100]. Interestingly, miR-18a appears to be an applicable biomarker for oesophageal squamous cell carcinoma (ESCC) [101] as well as for colorectal cancer [102].

I.2.5.2.1.c. miR-19a

MiR-19a often acts in concert with miR-18a and is mainly responsible for the oncogenic potential of miR-17-92a as it targets regulators of apoptosis, e.g. the pro apoptotic Bim1 or the tumor suppressor PTEN [103]. For example, in T-cell lymphoblastic leukemia (T-ALL) miR-19a, by targeting Bim and Pten, alone is able to promote leukaemogenesis [104]. It was shown that deletion of miR-17-92a impaired cardiomyocytes proliferation [105]. Interestingly, when miR-17-92a was overexpressed in embryonic, postnatal or adult hearts, miR-19a, together with the other cluster members, was inducing cardiomyocyte proliferation, thereby enabling cardiac repair [105].

I.2.5.2.1.d. miR-92a

MiR-92a is highly expressed in numerous tumor types but also under physiological conditions in cardiac fibroblasts, cardiomyocytes, lymphocytes, and hematopoietic stem cells. The highest levels of miR-92a can be found in endothelial cells. By targeting proangiogenic factors, miR-92a interferes with angiogenesis. Targets of miR-92a include the integrin subunit αv , a factor important for cell migration and cell-matrix interactions [106, 107] [108], Rap1, a protein important for mediating angiogenesis, as well as sirtuin 1 (SIRT1), a histone deacetylase modulating sprouting angiogenesis during vascular growth and other angiogenic functions. In ischemic tissues of animal models miR-92a is increased. Interestingly, in animals that suffered from acute myocardial infarction or hind limb ischemia, the specific inhibition of miR-92a by administration of antagomirs to the animals supports the functional recovery by inducing angiogenesis in ischemic tissue. Therefore, miR-92a represents a potential target in the treatment of ischemic diseases [109]. Applying the miR-92a inhibitor LNA-92a to pig that underwent percutaneous ischemia, followed by reperfusion, confirmed the beneficial effects of miR-92a silencing [110]. Another study showed that miR-92a is upregulated by oxidated low-density lipoprotein (oxLDL) in atheroprone areas of low shear stress and thereby contributes to

the formation of atherosclerotic lesions [111]. In mice that were conditionally overexpressing miR-17-92a in the heart and SMCs cardiomyopathy and arrhythmia were observed. These pathologies appear to be induced by downregulation of the mRNAs of Connexin43 and PTEN [112].

I.2.5.2.2. Regulation of the miR-17-92a cluster

I.2.5.2.2.a. Transcriptional regulation of the 17-92a cluster

First insights into the regulation of the miR-17-92a cluster came from studies in human B-cells and myeloid leukemia cells where the oncogene c-Myc stimulates the transcription of the cluster [113, 114]. In neuroblastoma and medullablastoma cells the c-Myc homologue N-MYC contributes to the upregulation of miR-17-92a [115-117]. Other transcriptional activators are Cyclin D1 and E2Fs, which are also targets of miR-17 and miR-20a, thereby creating a negative feedback loop [90, 118, 119]. Similarly it has been shown that the miR-17/miR-20a target AML1 activates miR-17-92a transcription in hematopoietic progenitor cell (HPCs) which in turn promotes the differentiation of HPCs. The negative feedback loop of miR-17 and miR-20a helps to fine tune the activity of AML1 [120].

I.2.5.2.2.b. Posttranscriptional regulation of the miR-17-92a cluster

The polycistronic miR-17-92a cluster is transcribed as one primary transcript. However, data generated during my master thesis as well as findings from others [113, 115, 121] [116] showed that the mature members can be expressed differentially. For example, during endothelial differentiation of murine embryonic stem cells (mESCs), the primary transcript and the mature miR-92a were reduced with ongoing differentiation for 11 days, while the expression of the other mature cluster members was increasing with differentiation [122]. This gave a hint on the presence of factors that function in addition to transcriptional effectors in a way that they influence the posttranscriptional regulation

of the miR-17-92a cluster on the level of Drosha and Dicer processing [26, 34, 123-125]. So far the mechanism underlying the differential posttranscriptional regulation of the individual members of the miR-17-92a cluster is mainly unclear. Only a few factors controlling the maturation of certain members of the cluster have been described (Figure 9). HnRNP A1 is a protein specifically binding to the miR-18a hairpin within the primary transcript thereby facilitating the Drosha cleavage (for details see I.2.4.1.1.f). Another interesting factor acting specifically on the regulation of one cluster member is KSRP. It interacts with the precursor of miR-20a and facilitates the processing by Dicer in mammalian cells (for details see I.2.4.1.1.e) while not affecting the other cluster members. MiR-17 is negatively regulated by splicing of IRE α upon ER stress, as described in I.2.4.1.2.b)

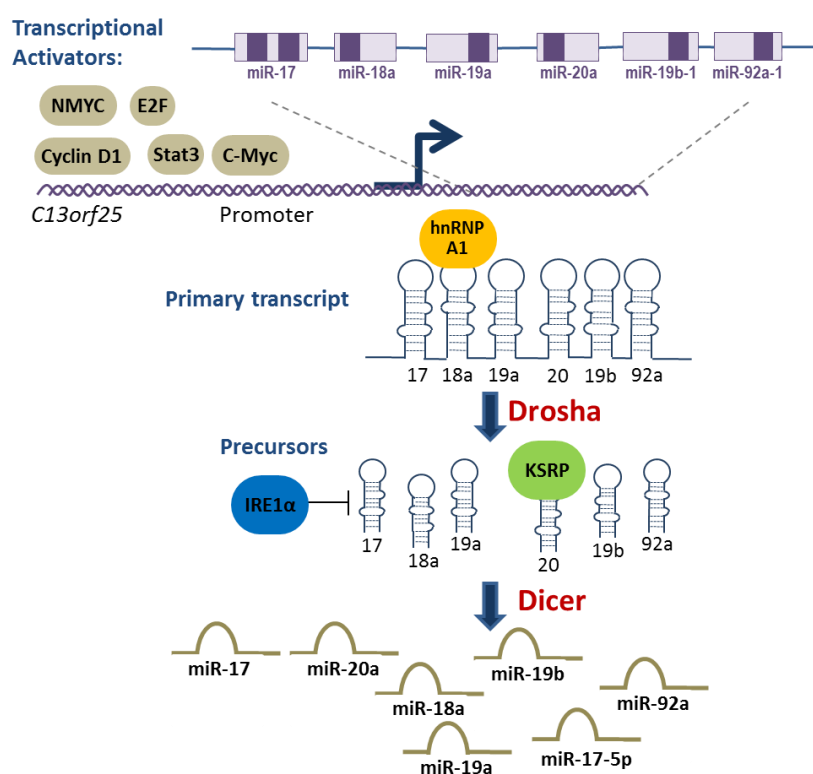


Figure 9: Known regulation of the miR-17-92a cluster. The transcription of the pri-miR transcript is controlled by the transcriptional activators NMYC, c-Myc, E2F, Cyclin D1, and Stat3 [90, 114, 116, 117]. Moreover, hnRNPA1 acts specifically on pri-miR-18a, thereby facilitating further Drosha processing [38]. KSRP interacts with the terminal loop of pre-miR-20a which enhances Dicer processing [36]. IRE1 α is a negative regulator since under endoplasmic reticulum stress it cuts pre-miR-17 differentially to Dicer, leading to the degradation of pre-miR-17[48] (Figure adapted from [89])

Another example of how the differential regulation of miR-17-92a cluster members is caused came from electron microscopy pictures that were taken by Chaulk et al. [126]. They show in HEK cells that the pri-miR-17-92 transcript forms a globular tertiary structure in which the 3' end is hidden within the core of the globe. The hairpins of miR-19b and miR-92a are less accessible than miR-17, miR-18a and miR-19a, which form the outside of the structure and are therefore expressed at lower levels. Moreover, this helps to understand why miR-92a mediates antiangiogenic effects while the other members of the miR-17-92a cluster are supporting angiogenesis. It might be of therapeutic interest to modulate the 3D structure of pri-miR-17-92, in order to induce the maturation of pro- or antiangiogenic members of the miR-17-92a cluster [126].

II. Objective

Since their discovery 20 years ago, it has been demonstrated that miRs are important regulators of nearly all cellular processes. The miR-17-92a cluster comprises seven mature members (miR-17-5p, miR-17-3p, miR-18a, miR19a, miR-20a, miR-19b, miR-92a) and is highly expressed in endothelial cells. By now, numerous functions have been assigned to the miR-17-92a cluster, e.g. the regulation of the immune system [103], lung development [88] and cancer [93]. Moreover, its members mostly impair angiogenesis [96]. MiR-17-92a is a polycistronic cluster that is transcribed as one primary transcript. Drosha cleaves the pri-miR-17-92 transcript into the individual pre-miRs that are exported into the cytoplasm and processed into a dsRNA of about 21 nucleotides in length. From this sequential maturation it would be assumed that all mature members of miR-17-92a are representing the levels of pri-miR-17-92 and that the individual mature members are equally expressed. However, previous experiments showed that mature miRs of miR-17-92a are differentially expressed during endothelial differentiation of murine embryonic stem cells [122] and after hind limb ischemia in mice [109]. This gives a strong hint on the presence of posttranscriptional regulation of miR-17-92a. Interestingly, it has been shown that hnRNP A1 specifically interacts with the miR-18a hairpin within the pri-miR-17-92, thereby facilitating further Drosha processing [34]. The cluster member miR-92a is of crucial importance for angiogenesis and it was shown that the inhibition of miR-92a enhances the recovery after myocardial infarction in mice [109] as well as in pig [110]. As the regulation of miR-92a is of great therapeutic potential, the understanding of the posttranscriptional regulation of this miR should be elucidated in more detail. Therefore, the aims of this study were

1. To identify pre-miR-92a interaction partners in endothelial cells by RNA pulldown and subsequent mass spectrometry analysis.
2. To characterize interesting pre-miR-92a binding proteins and their implication in the regulation of the miR-17-92a cluster and other endothelial miRs.

III. Material and Methods

III.1. Material

III.1.1. Expendable items and chemicals

Table 4: Expendable items and chemicals.

Item/Chemical	Company
Acrylamide Bromophenol blue DTT Glycerol Hydrochloric acid TBE-Buffer Phenol-Chloroform-Isoamylalcohol Sodium chloride	Applichem, D-Darmstadt
96 well reaction plate (for qRT-PCR)	Applied Biosystems, Carlsbad, CA, USA
5 ml polycarbonate tubes for ultracentrifugation	Beckman Coulter
Ultrapure water	B. Braun, D-Melsungen
Bradford reagent	BioRad, D-Munich
Disposable serological pipette, wrapped	Cornig, NY, USA
Reaction tubes (0.5, 1.5, 2 ml)	Eppendorf, D-Hamburg
Random Hexamer Primers RiboLock RNase Inhibitors	Invitrogen, Canada-Burlington
ECL western blotting detection Amersham Hyperfilm ECL	GE healthcare, D-München
15 ml and 50 ml tubes T 75 cell culture flask Cell scraper 6 well cell culture plate	Greiner bio one, D-Frickenhausen

6 cm dish

Trypsin (10x)	Invitrogen, D-Karlsruhe
DMEM	
1 kb DNA-Ladder	
10 mM dNTP Mix	
fetal calf serum (FCS)	
Lipofectamine RNAiMax	
MuLV-Reverse-Transcriptase (200 U/ μ l)	
4-12% Novex-Gels	
5x Reverse transcriptase buffer	
TEMED	
HEPES	
TCA	

AgNO ₃	Merck, D-Darmstadt
Aquacide	

Polyvinylidenfluorid Membrane	Millipore, Billerica, MA, USA
-------------------------------	-------------------------------

BSA	PAA laboratories, A-Pasching
PBS	

Glycerol	Roth, D-Karlsruhe
SDS	
TRIS	
Phenol	

Acetic acid	Sigma Aldrich, D-Taufkirchen
Acetone	
EDTA	
Ethanol	
Formaldehyde	
Isopropyl alcohol	
Methanol	
Potassium chloride	
Sodium acetate	
Sodium Hydroxyde	
Sodium-m-periodate	
β -mercaptoethanol	
Triton-X	
Tween-20	
DFO	

Pipettips	Starlab, D-Ahrensburg
-----------	-----------------------

III.1.2. Kits

Table 5: Kits.

Kit	Company
QIAfilter Plasmid Mini Kit QIAfilter Plasmid Midi Kit QIAfilter Plasmid Maxi Kit QIA filter Plasmid Giga Kit miRNeasy Mini Kit AllPrep RNA/Protein Kit QiaQuick Gel extraction it Max Tract High Density Tubes	Qiagen, D-Hilden
Colloidal blue staining	Invitrogen, D-Darmstadt
MagnaRIP Kit	Millipore, D-Darmstadt

III.1.3. Primers

III.1.3.1. Primers for SYBR green qRT-PCR

Table 6: Primer sequences used in qRT-PCR (ordered from Sigma-Aldrich, D-Taufkirchen).

Target		Sequence (5' - 3')
Pri-miR-17-92a	For	CCAATAATTCAAGCCAAGCAA
	Rev	AAATAGCAGGCCACCATCAG
Pre-miR-17	For	TGTCAAAGTGCTTACAGTGCAG
	Rev	ACCATAATGCTACAAGTGCCTTC
Pre-miR-18a	For	GGTGCATCTAGTGCAGATAGTGA
	Rev	TGCCAGAAGGAGCACTTAGG
Pre-miR-19a	For	CCTCTGTTAGTTTTGCATAGTTG
	Rev	CAGGCCACCATCAGTTTTG
Pre-miR-20a	For	CGACTAAAGTGCTTATAGTGCAG
	Rev	TGCTCATAATGCAGTAGATAACTAAAC
Pre-miR-92a	For	TCTACACAGGTTGGGATCGG
	Rev	CGGGACAAGTGCAATACCATA
Pri-miR-126	For	GCCTCATATCAGCCAAGAAGG
Pre-miR-126	For	TGGCGACGGGACATTATTAC

	Rev	GGACGGCGCATTATTACTCA
SND1	For	CCGAACGCAGCTCCTACTAC
	Rev	ATAGTGGGCCAGACCTTCT
eIF4A2	For	CTCAATACGAGGCGCAAGGTGGA
	Rev	GGTCCATGTCACCATGCAGAGCAG
Myoferlin	For	AAAAGCTTGAGCCCATTTC
	Rev	CATGGTGGCTGAATGAAACA
ADAR1	For	TGCTGCTGAATTCAAGTTGG
	Rev	CCCCAACTTTTGCTTGGTAA
P0	For	TCGACAATGGCAGCATCTAC
	Rev	ATCCGTCTCCACAGACAAGG

III.1.3.2. Taqman assays

Table 7: Taqman Assays (Applied Biosystems, Carlsbad, CA, USA).

Taqman assay ID	Target Sequence (5' - 3')
U6 snRNA	GUGCUCGCUUCGGCAGCACAUUACUAAAAUUGG AACGAUACAGAGAAGAUUAGCAUGGCCCUUGCGC AAGGAUGACACGCAAUUCGUGAAGCGUCCAUA UUUUUACUGCCCUCCAUGCCCUGCCACAAACGC UCUGAUAAACAGUCUGUCCUGUCUCUCUCCUGCU GCUCCUAUGGAAGCGAAGUUUCCGCUCCUGCAG AAAGCAAAGUUACGACUCAGAGACGGCUGAGGAU GACAUCAGCGAUGUGC
Hsa-miR-17	CAAAGUGCUUACAGUGCAGGUAG
Hsa-miR-18a	UAAGGUGCAUCUAGUGCAGAUAG
Hsa-miR-19a	UGUGCAAUCUAUGCAAACUGA
Hsa-miR-20a	UAAAGUGCUUAGUGCAGGUAG
Hsa-miR-92a	UAUUGCACUUGUCCGGCCUGU
Hsa-miR-126	UCGUACCGUGAGUAAUAAUGCG

III.1.3.3. Primers used for generating a library for sequencing

Table 8: Primers for generation of amplicons used in next generation sequencing (Sigma-Aldrich, D-Taufkirchen).

Pri-miR/pre-miR		Sequence (5' - 3')
Pri-miR-17-92a	For	GAAGAGCCACCACTTCCAGT
	Rev	GCAACCCCAAAGTGAAATG
Pre-miR-17	For	TGCAAAGTGCTTACAGTGCAG

	Rev	ACCATAATGCTACAAGTGCCTTC
Pre-miR-18a	For	TAAGGTGCATCTAGTGCAGATAGT
	Rev	TGCCAGAAGGAGCACTTAGG
Pre-miR-19a	For	CCTCTGTTAGTTTTGCATAGTTGC
	Rev	CAGGCCACCATCAGTTTTG
Pre-miR-20a	For	AAAGTGCTTATAGTGCAGGTAGTG
	Rev	TGCTCATAATGCAGTAGATAACTAAAC
Pre-miR-92a	For	CACAGGTTGGGATCGGTTGC
	Rev	CCAAACTCAACAGGCCGGGA

III.1.4. Small interfering RNA (siRNA)

Table 9: Sequence of siRNA control (siCo) (Sigma-Aldrich, D-Taufkirchen).

siRNA control	Sequence (5' - 3')
siFirefly luciferase	Sense: CGUACGCGGAAUACUUCGA Antisense: UCGAAGUAUUCGCGUACG

Table 10: SiRNAs. Flexitube siRNA (Qiagen, D-Hilden)

siRNA name	Target Sequence (5' - 3')
siSND1	ATCCACCGTGTTCAGATATA
siEIF4A2_3	TTGCTCAAGCTCAGTCAGGTA
siMyof	CAAGCTGATCTCCCTGCTAAAA

III.1.5. Antibodies

Table 11: Antibodies used for Western Blot and RIP.

Antibody	Species	Company
secondary antibody goat α-rabbit	Goat	Jackson ImmunoResearch, UK-Newmarket
Secondary antibody rabbit α-mouse	Rabbit	Jackson ImmunoResearch, UK-Newmarket
SND1	Rabbit	Abcam, UK-Cambridge
eIF4A2	Rabbit	Abcam, UK-Cambridge
Ago2	Mouse	Millipore, D-Darmstadt
Myoferlin	Mouse	Abcam, UK-Cambridge

III.1.6. Buffers

Table 12: Composition of the buffers.

Buffer	Composition
10x TBE	25 mM EDTA, 890 mM Tris-Base, 890 mM Boric acid, pH 8,0 (adjust with acetic acid)
50x TAE	1 mM EDTA, 400 mM sodium-acetate, 800 mM Tris-Base, pH 8 (adjust with acetic acid)
TBS	250 mmol/l Tris (pH 8), 750 mmol/l NaCl, 12,5 mmol/l KCl
TBST	TBS + 0,2 %Tween (v/v)
Running buffer Western Blot	25 mmol/l Tris, 192 mmol/l Glycin, 1 % SDS
Resolving buffer Western Blot	1,5 mol/l Tris pH 8, 0,4 % SDS
Stacking buffer Western Blot	0,5 mol/l Tris pH 6,8, 0,4 % SDS
RNA Pulldown buffer	20 mM Tris-HCl pH 7.9, 6% (v/v) Glycerol, 0.1 M KCl, 0.2 mM EDTA, 0.5 mM DTT

III.1.7. Cell culture

Human umbilical vein endothelial cells (HUVECs) were purchased from Lonza (B-Verwies).

Table 13: Endothelial basal medium (EBM) (Invitrogen, D-Darmstadt).

Medium	Composition
EBM full	EBM plus: 10% v/v FCS (Boehringer Ingelheim) 10 µg/ml rhEGF 10 µg/ml 1 µg/ml Hydrocortisone 1µg/ml 50 µg/ml Gentamycin sulfate 50 µg/ml 3 µg/ml Bovine brain extract

III.2. Methods

III.2.1. Cell Culture

III.2.1.1. HUVEC cultivation

Human umbilical vein endothelial cell (HUVECs) were cultivated in endothelial basal medium (EBM, purchased from Gibco, Invitrogen, D-Karlsruhe) that was supplemented with hydrocortisone, bovine brain extract, epidermal growth factor and 10% fetal calf serum (Invitrogen, D-Karlsruhe). The cells were kept at 37°C and 5% CO₂. The medium was changed every other day, except otherwise mentioned. For passaging the cells were washed with PBS and detached by addition of 0.025% Trypsin-EDTA. The activity of trypsin was stopped using EBM full medium. The cells either passaged or counted using a Neubauer counting chamber and seeded at the desired density. For the transfection with siRNA, 5*10⁵ cells were seeded into 6 cm wells one day in advance to the transfection.

III.2.1.2. Exposure of HUVECs to hypoxia mimicking conditions

In order to mimic hypoxic stress, HUVECs were treated with 100 µM Deferoxamine (DFO, Sigma-Aldrich, D-Taufkirchen) which was added to the medium of the cells (EBM). DFO functions as a Fe²⁺ chelator and is able to stabilize the hypoxia inducible factor HIF1α [127]. The transcription factor HIF1α exerts the adaptive processes to promote the survival of the cell under conditions of low oxygen. The cells were exposed to DFO for up to 96 hrs. If the incubation was longer than 48 hrs, the medium was changed every other day and fresh DFO was added.

III.2.1.3. SiRNA transfection of HUVECs

HUVECs were seeded at 70-80% confluency. Small interfering RNA (siRNA) was transferred into the cells by lipofection. HUVEC were incubated in serum free OptiMEM (Invitrogen, D-Karlsruhe) to ensure efficient uptake of the siRNA (purchased from Qiagen, D-Hilden, for sequences see chapter material). SiRNA was first packed into lipid vesicles and then added to serum depleted cells. In detail, 250 μ l OptiMEM was mixed with 60 μ M siRNA (Mix1) and another 250 μ l OptiMEM was mixed with 5 μ l RNAiMax Lipofectamine (Mix2, Invitrogen, D-Karlsruhe). Then Mix1 (OptiMEM and siRNA) was added to Mix2 (OptiMEM and Lipofectamine RNAiMax) and incubated for 15 min at room temperature. Subsequently, the mixture was added dropwise to the cells, which have been overlaid with 2.5 ml OptiMEM. After 4 hrs of starvation the medium was aspirated and substituted by full EBM. The efficiency of the knockdown was determined via qRT-PCR and Western Blot analysis. As a negative control siRNA targeting firefly luciferase, an artificial gene, was used.

III.2.1.4. Preparation of microvesicles and exosomes shed by HUVECs

For the investigation of HUVEC shed microvesicles and exosomes the cells were incubated in vesicle precleared endothelial basal medium in order to ensure that no more bovine vesicles from the fetal calf serum were present in the medium. Therefore, EBM was centrifuged at 140,000 x g for 90 min at 4°C. The supernatant was transferred into a fresh tube and stored at 4°C. For the investigation of the influence of a protein on the formation of vesicles, $5 \cdot 10^5$ HUVECs were seeded and the next day transfected with siRNA or treated with a drug. The cells were incubated with 4 mL EBM for 72hrs. Then the supernatant of the cells was first centrifuged at 4,000 rpm for 10 min at 4°C to precipitate dead cells. From the remaining medium 200 μ l were mixed with Qiazol ("Supernatant") and 3.5 ml was centrifuged for 1 hr at 140,000 x g for 1 hr to precipitate vesicles. The pellet was washed once with 3 ml PBS and again centrifuged for 1 hr at 140,000 x g at 4°C.

Finally the pellet was either resuspended in Qiazol or used for Nanoparticle tracking analysis.

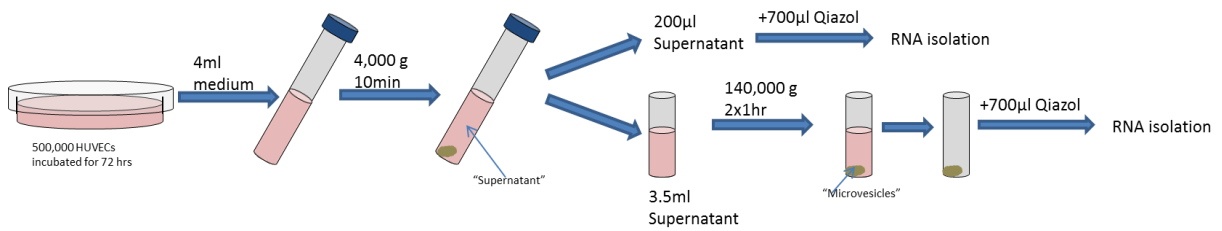


Figure 10: Preparation of supernatant and microvesicles and exosomes of HUVECs after incubation of 72 hrs.

III.2.1.5. Nanoparticle tracking analysis (NTA)

In order to determine the size and amount of vesicles in the supernatant of cells, the pre-cleared supernatant (15 min 4,000 rpm, 4°C) was diluted 1:10 in vesicle free media (medium was cleared by centrifugation for 90 min at 140,000 x g, 4°C) and loaded into the Nanosight NS500 according to the manufacturer's instruction. The sample was focused and the camera level was adjusted at position 10-12 so that 20-200 particles could be seen in the visual field. Then the movement of the particles was recorded in 10 movies each 10 seconds in duration. For the analysis of the movies the threshold was set to 8-10. The threshold was not changed between different samples. The analysis of the raw data was performed with Microsoft Excel 2010.

III.2.2. Molecular Biology

III.2.2.1. RNA isolation

RNA was isolated using Qiazol and the miRNeasy RNA extraction kit from Qiagen (D-Hilden) which are designed to also allow the extraction of small RNAs. Therefore, the cells were washed once with PBS before lysis in 700µl Qiazol. The RNA extraction was either continued immediately or the cells were kept frozen at -80°C. For the isolation of RNA from microvesicles or supernatant, 3 µl of *c.elegans* miR-47 was spiked in at this point. 140 µl Chloroform was added to the phenol-cell-mixture. After centrifugation for 15 minutes at 12,000 x g, the aqueous phase (approximately 350 µl) was transferred into a fresh tube and mixed with 525 µl 100% ethanol in order to precipitate the RNA. Then, the mixture was loaded onto miRNeasy kit (Qiagen, D-Hilden) columns to immobilize the RNA. According to the manufacturer's protocol, the RNA was washed several times and remaining DNA was digested by DNase. Finally, the RNA was eluted with 30-50 µl H₂O (for the elution of RNA isolated from the supernatant/from microvesicles only 12 µl H₂O were used for the elution). The concentration of RNA was determined by Nanodrop (Peqlab, D-Erlangen).

III.2.2.2. Determination of mRNA levels

III.2.2.2.1. Reverse Transcription of mRNAs

In order to reverse transcribe mRNA into cDNA, the following reaction was set up according to the manufacturers protocol (Table 14) (Invitrogen, D-Karlsruhe).

Table 14: Reverse transcriptase reaction set up. All reagents were purchased from Invitrogen (D-Karlsruhe).

Reagent	Volume [μ l]
H2O	0.5
Buffer II	2
MgCl ₂	4
dNTPs (10 mM)	1
Random Hexamers	1
MuLV RT	1
RNase Inhibitor	0.5
RNA (50 ng/ μ l)	10

Table 15: Thermocycler protocol for the reverse transcription of mRNAs.

Step	Temperature [$^{\circ}$ C]	Duration [min]
1	20	10
2	43	75
3	99	5
4	4	Pause

III.2.2.2.2. Quantitative real time PCR (qRT-PCR) of mRNAs

QRT-PCR was used to determine the levels of certain genes. By using primers designed to specifically amplify a reverse transcribed mRNA, a primary miRNA, or a precursor miRNA the expression level could be determined. SYBR green was used for the detection of PCR products because it intercalates into double stranded DNA strands. P0 was used as a house keeping control.

Table 16: SYBR green qRT-PCR reaction set up. All reagents were purchased by Applied Biosciences (D-Darmstadt).

Reagent	Volume [μ l]
SYBR green master mix Fast	10
Forward primer [10 μ M]	1
Reverse primer [10 μ M]	1
cDNA (diluted 1:8)	8

Table 17: Thermocycler protocol for the reverse transcription of mRNAs.

Step	Temperature [$^{\circ}$ C]	Duration [min:s]	
1	95	00:20	
2	95	00:03	Steps 2-3 were repeated 40x
3	60	00:30	
4	95	00:15	
5	60	1:00	
6	95	00:15	

III.2.2.3. Determination of miR levels

III.2.2.3.1. RT of miRs

In order to determine the expression of mature miRNAs Taqman assays specific for each miRNA were used according to the manufacturer's protocol (Life Technologies, D-Darmstadt).

Table 18: Reverse transcription of miRs. Reaction set up for Taqman assays. All reagents were purchased from Applied Biosystems (D-Darmstadt).

Reagent	Volume [μ l]
RT Primer	3
dNTPs 100 mM	0.15
Multiscribe RT	1
RNase Inhibitor	0.19
Buffer 10x	1.5
H ₂ O	4.16
RNA (2 ng/ μ l)	5

Table 19: Thermocycler Protocol for Taqman Reverse Transcription.

Step	Temperature [°C]	Duration [min]
1	16	30
2	42	30
3	85	5
4	4	Pause

III.2.2.3.2. qRT-PCR of miRs

The levels of miRs were determined via qRT-PCR using miR-specific Taqman Assays (Applied Biosystems, D-Darmstadt).

Table 20: Thermocycler Protocol for qRT-PCR of miRs. All reagents were purchased from Applied Biosystems (D-Darmstadt).

Reagent	Volume [μ l]
Primer (20x)	1
Taqman Fast Master Mix	10
H2O	6
Reverse transcribed miRNA	3

Table 21: Thermocycler protocol for the qRT-PCR of miRs with Taqman Assays (Applied Biosystems, D-Darmstadt).

Step	Temperature [°C]	Duration [min:s]
1	50	2:00
2	95	2:00
3	95	00:05
4	60	00:20

III.2.2.4. In vitro transcription

For the cloning of pre-miR-92a into a pGEM-T vector (Promega) the sequence CUUUCUACACAGGUUGGGAUCGGUUGCAAUGCUGUGUUUCUGUAUGGUAUUGCACUUGUC CCGGCCUGUUGAGUUUGG (Sanger miR base) with flanking Apal restriction sites was ligated into a pGEM-T vector. This insertion occurred in both correct and reverse orientation. In the following, the incorrectly inserted pre-miR-92a served as a negative control. The two constructs were in vitro transcribed according to the run-off transcription with T7, as described previously [128].

III.2.2.5. RNA Pulldown

To identify RNA binding proteins we used published RNA pulldown protocols which were applied to endothelial cells [34, 35, 38, 129].

Protein preparation: Proteins from 10^6 HUVECs were isolated with the AllPrep Kit from Qiagen (D-Hilden) according to the manufacturer's protocol. This ensured that the proteins remain in their native and active state and are supposed to be still able to interact with RNA. The proteins were dialyzed overnight in pulldown buffer (20 mM Tris-HCl pH7.9, 6% (v/v) Glycerin, 0.1M KCl, 0.2 mM EDTA, 0.5 mM DTT) using a cellulose tube (type 20/32 inch, Roth, D-Karlsruhe) and were concentrated for the pulldown by incubation of the closed cellulose tube in a water soaking material (Aquacide, Merck, D-Darmstadt).

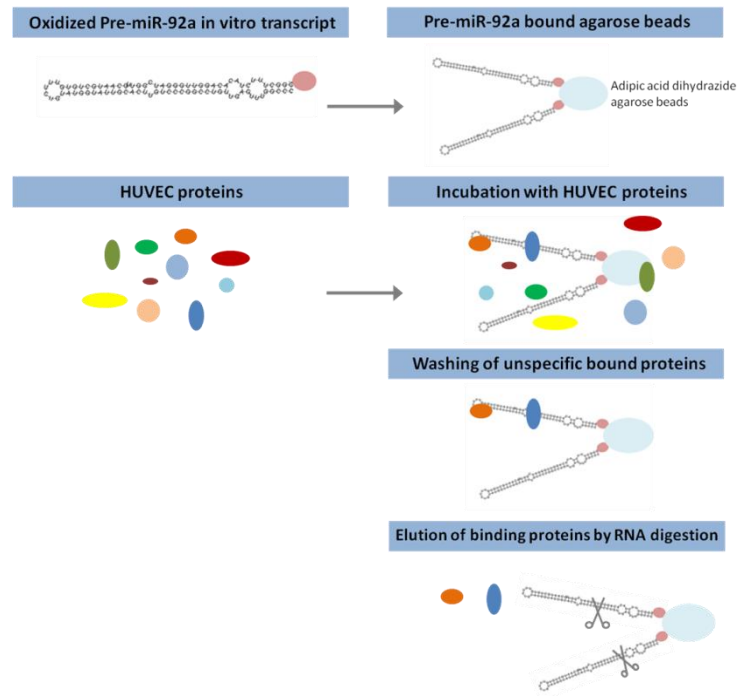


Figure 11: Schematic depiction of the RNA pulldown used for the identification of pre-miR-92a binding proteins. Pre-miR-92a was oxidized with sodium-m-periodate and immobilized with adipic acid dihydrazide agarose beads. After incubation with native proteins from HUVECs and several washings, the proteins bound to pre-miR-92a or the control sequence (pre-miR-92a in the reverse orientation) was eluted by addition of RNases.

RNA preparation: 500 pmol in vitro transcribed RNA was denatured at 95°C and then allowed to renature on ice for 10 min. To covalently link the RNA to adipic acid dihydrazide agarose beads (Sigma-Aldrich, D-Taufkirchen) RNA was oxidized with 5mM sodium-m-periodate (Sigma-Aldrich, D-Taufkirchen) in 0.1 M NaOAc, pH 5.0 in a final volume of 200 µl and incubated for 1 hr at room temperature in dark. Then, the RNA was precipitated with ethanol and resuspended in 100 µl 0.1 M NaOAc. To prepare the beads for the immobilization of the RNA, 200 µl 50% slurry adipic acid dihydrazide agarose beads were washed 4 times with 1.5 ml 0.1 M NaOAc pH5, then resuspended in 300 µl 0.1 M NaOAc pH5 and mixed with the RNA. The binding of the RNA to the beads took place over night at 4°C and rotating. The next day, the beads were washed 3 times in 1 ml 2M KCl and four times in 1 ml pulldown buffer containing 1.5 mM MgCl₂. The washed RNA coupled beads were mixed with 500 µg native HUVEC proteins. The binding of the proteins to the immobilized RNA took place during an incubation of 30 min at room temperature and under rotation. After washing four times with 1 ml pulldown buffer

containing 1.5 mM MgCl₂ and twice with 1 ml water, the proteins were eluted by the addition of a mixture of RNases V1 (5 units), A (2500 units), and T1 (5000 units) in 50 µl elution buffer (20 mM Tris-HCl pH7.9, 100 mM NaCl, 5 mM MgCl₂) for 30 min at 37°C under shaking. The eluted proteins were precipitated with trichloroacetic acid (TCA) and resuspended in loading dye for subsequent SDS-PAGE.

III.2.2.6. RNA immunoprecipitation

In order to confirm the interaction of proteins and RNA that were detected in the RNA pulldown, an RNA immunoprecipitation was performed. Therefore, the MagnaRIP Kit (Millipore, D-Darmstadt) was used according to the manufacturer's protocol. Antibodies against the protein of interest were immobilized to magnetic beads. Per condition 1.5 10⁶ HUVECs were detached from flasks using trypsin and pelleted via centrifugation at 800 rpm for 3 minutes. The cell pellet was washed once with PBS and then stored at -80°C until the experiment or immediately used. The pellet was mixed with 1 ml of 0.1% Formaldehyde and incubated for 30 minutes on ice to allow cross linking of the RNA-protein interactions present in the cells. The reaction was stopped by addition of 10 ml cold PBS, centrifuged at 800 rpm for 3 minutes and again washed once with PBS. Then, the pelleted cells were lysed using the kit's buffer. After 45 minutes incubation on ice, the lysate was centrifuged at 14,000 rpm and the cell debris free supernatant was mixed with the antibody coupled beads in IP buffer (from the kit) for overnight incubation at 4°C under rotation. A 10% fraction was kept as an input control and was also kept overnight at 4°C in IP buffer provided with the MagnaRIP Kit (Millipore, D-Darmstadt). The beads were washed 6 times and from the last washing 50 µl were used for a control western blot. Then, proteins were digested during incubation with proteinase K at 55°C for 30 min. In order to extract the eluted RNA from the supernatant of the beads, the supernatant was mixed with the equal volume of Phenol-Chloroform-Isoamylalcohol (Applichem, D-Darmstadt) and tRNA (Yeast tRNA, Invitrogen, D-Darmstadt) to improve the precipitation efficacy. After centrifugation for 10 min at 14,000 rpm at room temperature the aqueous phase was mixed with the equal volume of Chloroform-Isoamylalkohol 24:1 and centrifuged for another 10 min at 14000 rpm to wash out remaining phenol. The aqueous

phase was mixed with 2.5 vol 100% Ethanol and 0.1 vol 3M NaOAc to precipitate the RNA and incubated at -80°C for 1 hour or overnight. After centrifugation for 30 min at 14000 rpm, the pellet was washed with 75% Ethanol, again centrifuged for 15 min at 14000 rpm and finally dried and resuspended in 15 µl water.

III.2.2.7. Determination of the protein concentration

The protein concentration was determined spectrometrically via the Bradford assay. Therefore, 798 µl water was mixed with 200 µl Bradford reagent (BioRad, D-Munich) and 2 µl of the protein solution. For a blank control, water instead of protein solution was added. Under acidic conditions Coomassie blue G250 is binding to proteins and thereby its absorption maximum from 465 to 595 nm. The turnover is proportional to the protein content and can be measured by the Smartspec 300 Photometer (BioRad, D-Munich). The protein concentration was calculated with a reference calibration line that had been set up with bovine serum albumin (BSA). After protein extraction with the AllPrep Kit (Qiagen, D-Hilden), the protein concentration was not measured with the Bradford reagent because the components of the Elution buffer interfere with the colorimetric reaction. Therefore, the protein content after using the AllPrep Kit was determined directly with the Nanodrop Spectrometer at 260 nm and 280 nm and calculated with formula: $\text{conc [mg/ml]} = (1.55 \cdot A_{280}) - (0.76 \cdot A_{260})$.

III.2.2.8. SDS polyacrylamide gel electrophoresis (SDS-PAGE)

Proteins of different sizes were separated according to their electrophoretic mobility in a sodium dodecyl sulphate polyacrylamide gel which served as a molecular sieve within an electric field. The proteins move within this electric field dependent on their weight or length of the polypeptide chain as well as on the folding, presence of posttranscriptional modifications and other factors. Before the proteins underwent PAGE they were denatured in order to overcome its secondary structure and can move within the electric field mainly due to its length. Therefore, the proteins were heated in a loading buffer that contains DTT and SDS for 5 min at 95°C. SDS binds amino acids and adds the negative charge to the denatured proteins while breaking up non-covalent bonds and dithiothreitol (DTT) is used to reduce disulfide bonds. The gel is generated by acrylamide-bisacrylamide polymerization. To initiate this reaction APS (Ammonium Persulphate) and TEMED (N,N,N,N-tetramethylethyldiamin) to enable the start of this radicalic reaction. The gel consists of two phases. The upper phase is the stacking gel in which the proteins run first and then enter the resolving gel which is denser and the actual separation can take place. While the proteins pass the stacking gel, the voltage is set 80 V, as soon as they entered the resolving gel it was increased to 120 V.

Table 22: Composition of the resolving gel with 8% or 10% acrylamide used for SDS-PAGE.

	8%	10%
H2O	7.1 ml	6.1 ml
Resolving Buffer (1.5 M Tris pH8, 0.4% SDS)	3.75 ml	3.75 ml
Acrylamide30% [ml]	4 ml	5 ml
APS 10% [µl]	150 µl	150 µl
TEMED [µl]	6 µl	6 µl

Table 23: Composition of the stacking gel used for SDS-PAGE.

Reagent	Volume
H ₂ O	5.45 ml
Stacking Buffer (0.4 M Tris pH 6.8, 0.4% SDS)	2.5 ml
Acrylamide30%	1.7 ml
APS 10%	125 µl
TEMED	12.5 µl

III.2.2.9. Western Blot

The proteins that were separated via SDS-PAGE were blotted from the gel onto a polyvinylidendifluorid-membrane (PVDF). First, the PVDF-membrane was activated by incubation in methanol for 1 minute. Then the membrane together with the whatman papers and the gel was set up as depicted in Figure 12. The transfer of proteins was achieved at 20 W for 90 min.

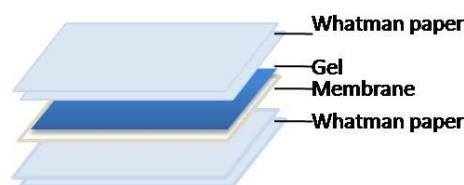


Figure 12: Arrangement of the Western Blot. Two Whatman papers are placed on the bottom toward the anode. On top first the activated membrane and then the gel is stacked. Towards the cathode another two sheets of Whatman paper is placed.

Table 24: Running buffer for wet blot.

Reagent	Amount
Tris	25 mM
Glycin	192 mM
SDS	1%

III.2.2.10. Immunological detection of proteins

Proteins that were immobilized to the PVDF membrane were determined via antibodies. Primary antibodies were specific against the epitopes of the proteins of interest which in turn were recognized by their IgG by secondary antibodies. The presence of the protein of interest can be measured indirectly because the secondary antibody is linked to a horseradish peroxidase (HRP). By addition of a substrate and hydrogen peroxide (Millipore, D-Darmstadt) HRP catalyzes the enzymatic reaction by which the substrate gets oxidized. After exposing the membrane to a chemiluminescent signal these electrons loose its energy in form of light of 428 nm, thereby blackening an X-ray film or is recorded with the Fluorchem M machine using the digital darkroom software (Biorad, D-München).

In detail, after blotting, the PVDF membrane was incubated in blocking solution (3% skim milk powder in TBS-Tween) for one hour to block unspecific binding of antibodies to the membrane. Next, the primary antibody was diluted in blocking solution and incubated on the membrane over night at 4°C and under rotation. After washing 3 times for 15 minutes with TBS-Tween, the secondary antibody was diluted in blocking solution and incubated on the membrane for 1 hr at room temperature. Then, the membrane was again washed 3 times 15 min in TBS-Tween. Addition of the substrate (Immobilon Western, Millipore Merck, D-Darmstadt) enabled the detection of the chemiluminescent signal either by a software (FluorChem and Axiovision, Zeiss) or by exposing to an X-ray film.

III.2.2.11. Stripping of membranes

In order to use one membrane for several antibodies, the previous antibody had to be removed. Therefore, the membranes were incubated at 55°C for 30 minutes.

Table 25: Composition of the stripping buffer.

Reagent	Amount
---------	--------

Tris	62.5 mM
SDS	2%
β-mercaptoethanol	0.1 M

III.2.2.1. Coomassie Staining

Proteins in a gel or on a membrane were visualized with coomassie blue using the colloidal blue staining kit (Invitrogen, D-Darmstadt) according to the manufacturer's instruction with 12 hrs incubation of the gel in the staining solution.

III.2.2.2. Silver Staining

In order to visualize proteins in a polyacrylamide gel, silverstaining was performed. For fixation of the proteins, the gel was incubated overnight in fixing solution (50% (v/v) Methanol, 12% (v/v) acetic acid, 80 µl/100 ml formaldehyde). The next day, the gel was washed 3 times for 20 minutes in washing solution (50% (v/v) Ethanol) and incubated for 2 minutes in solution I (0.1g Na₂S₂O₃ x 5 H₂O ad 500 ml H₂O). After washing 3 times for 40 seconds in H₂O, the gel was placed into Solution II (0.3g AgNO₃, 100 µl formamide, ad 125 ml H₂O). After three additional washing steps (3 times 40 seconds with H₂O), the staining was developed in solution III (15 g Na₂S₂O₃, 70 µl formaldehyde, 2.5 ml solution I, ad 125 ml H₂O). When bands become visible, the development was stopped by addition of acetic acid. After 5 minutes, the gel was washed with H₂O for several times to remove the acetic acid. For the documentation, the gel was dried and/or scanned.

III.2.2.3. In gel digest of proteins subjected to mass spectrometry

In order to identify the proteins binding to pre-miR-92a or the control sequence they were subjected to mass spectrometry. The eluted proteins were separated via precasted 4-12% gradient gels (1 mm Novex gels, Invitrogen, D-Darmstadt) in MOPS running buffer

pH 7.7 (0.1 M MOPS, 0.1 M Tris, 6.9 mM SDS, 2.05 mM EDTA, filtered with a 2 μ m filter). The proteins in the gel were stained with colloidal Coomassie (III.2.2.1). The complete lanes of proteins fished with pre-miR92a and the control sequence were each cut into small pieces with a sterile scalpel and transferred into a fresh tube. The fragments were washed twice with 100 μ l 50 mM Ammoniumbicarbonate 50% EtOH for 20 minutes at room temperature. For dehydration the fragments were incubated for 10 min in 100% EtOH and then dried via speed vac for 5 min. Then the proteins were reduced by incubation in 100 μ l 10 mM DTT for 45 min at 56°C on a thermomixer and alkylated in order to block free sulphhydryl groups using 100 μ l 55 mM iodacetamide and incubation for 30 min at RT in dark. Then again the fragments were washed in 100 μ l of 50 mM Ammoniumbicarbonate for 15 min at RT and dehydrated in 100 μ l 100% EtOH for 15 min at RT. After an additional washing step with 100 μ l 50 mM ammoniumbicarbonate for 15 min at RT the gel pieces were dehydrated twice with 100 μ l 100% EtOH for 15 min at RT. For the digestion of the proteins they were incubated with 40 μ l of 12 ng/ μ l Trypsin (Sequencing grade modified Trypsin, Promega, D-Mannheim) in 50 mM ammoniumbicarbonate for 15 min at 4°C allowing the pieces to swell again. The digestion took place over night at 37°C. The next day the supernatant was transferred to a fresh tube. For the extraction of proteins the gel pieces were incubated with 100 μ l of 30% acetonitrile/3% trifluoroacetic acid (TFA) for 20 min at RT. The supernatant was combined with the supernatant from the overnight digest. Next, the gel pieces were incubated twice with 100 μ l 70% acetonitrile for 20 min at RT and the supernatant was combined with the supernatant from the steps before. Then, the gel pieces were incubated twice in 100 μ l 100% acetonitrile for 20 min at RT and the supernatant was combined with the other supernatants. Stage Tips were prepared using 0.2 ml pipette tips and 2 layers of C18 silica material. To equilibrate the stage tips they were first washed with 20 μ l Methanol and centrifuged at 2600 rpm for 2 min, then washed with 20 μ l of Buffer B (800 ml Acetonitrile, 5 ml Acetic acid, ad 1 l aqua dest.) and centrifuged at 2600 rpm for 2 min and finally washed twice with 20 μ l of buffer A (5 ml Acetic acid ad 1 l aqua dest.) and centrifuged at 2600 rpm for 2 min. The collected supernatants were dried down to 80 μ l using the Speed Vac at 30°C and mixed with 80 μ l of Buffer A* (2 ml acetonitrile in 40 ml 1% TFA) and loaded on Stage tips. After centrifugation at 2600 rpm for 4 min, the tips were washed with 20 μ l buffer A and centrifuged again at 2600 rpm for 2 min. Access

liquid was removed with a syringe and the tips were stored at 4°C. The proteins were measured mass spectrometrically with an LTQ-Orbitrap XL as previously described [130]. Label free protein quantification was performed using MaxQuant Software tool [131].

III.2.2.4. Amplicon Sequencing

In order to detect potential RNA A-to-I editing sites, RNA from HUVECs grown under different conditions were reverse transcribed into cDNA for next generation sequencing. PCR amplicons were created using specific primers (Table 8, page 31) and send out to MWG Eurofins (D-Ebersberg) for further preparation. Using different bar code linkers the amplicons of the different conditions were pooled and subjected to unidirectional next generation sequencing on Roche GS junior with Titanium series chemistry. The data was bioinformatically analyzed by David John according to the pipeline described by Ramaswami et al. [132].

III.2.3. Statistics

Data are depicted as mean \pm standard error of the mean (SEM). The raw data were processed via Microsoft Excel 2010. The data were compared in GraphpadPrism™ (GraphPad Software, Sand Diego, CA, USA) or Microsoft Excel using the student's t-test . Data were considered statistically significant when $p < 0.05$.

IV. Results

IV.1. Identification of pre-miR-92a binding proteins by RNA pulldown

Previous studies from my master thesis and from others revealed that the members of the miR-17-92a cluster are differentially regulated under certain conditions such as hypoxia, hind limb ischemia and acute myocardial infarction although they derive from one primary transcript. This strongly suggests the presence of factors that posttranscriptionally regulate the maturation from pri-miR-17-92 to the individual mature members of the cluster. In order to identify potential binding proteins of pre-miR-92a, an RNA pulldown protocol has been established for HUVECs during my master thesis [122]. First, the pre-miR-92a sequence was in vitro transcribed and immobilized to agarose beads. Native proteins were isolated from HUVECs with the help of the AllPrep Kit from Qiagen and incubated with the pre-miR-bound beads. By addition of RNases A1, V, and T1, the proteins bound to pre-miR-92a or the control sequence were eluted. The eluted proteins were sorted according to their size via SDS-PAGE and the proteins were silver stained subsequently. After silver staining, more proteins could be detected in the elution fraction from pre-miR-92a than from the control sequence (pre-miR-ctrl.) (Figure 13).

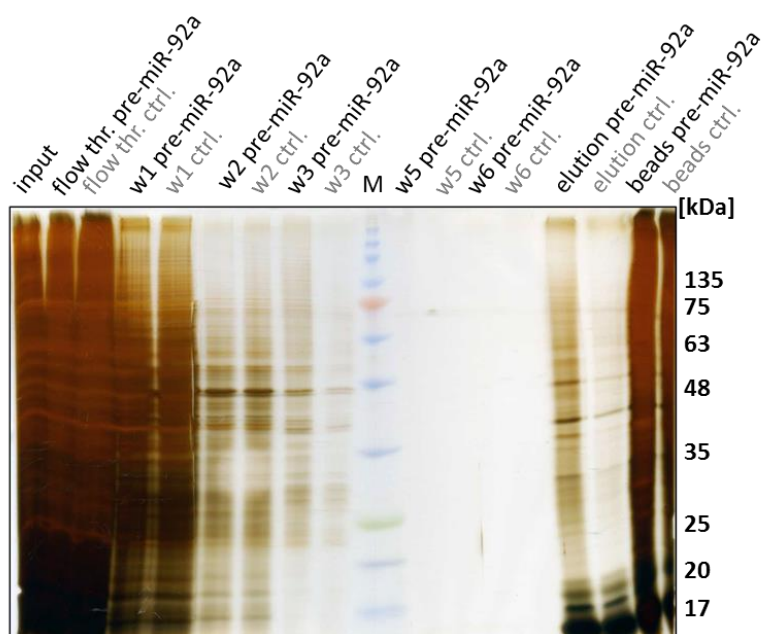


Figure 13: RNA Pulldown. 12% SDS-PAGE with proteins bound to pre-miR-92a or a pre-miR-Co after elution with RNases. M=Page Ruler pre-stained protein ladder (Thermo Scientific), input: HUVEC lysates before addition of the beads (same volume as used for the pulldown), TCA precipitated, flow thr: Flow through after 30 minutes incubation with pre-miR-92a/pre-miR-Co coupled beads, TCA precipitated, w1-6: washing fractions, TCA precipitated, Elution: Supernatant after incubation with RNases A, T1 and V. beads: agarose beads after incubation with RNases A, T1 and V, ctrl: control sequence.

In order to identify specific binding partners of pre-miR-92a, the eluted proteins were subjected to mass spectrometry after the RNA pulldown. To do so, the eluted proteins also underwent SDS-PAGE and were then Coomassie stained. In collaboration with Marcus Krüger from the Max Planck Institute in Bad Nauheim, the proteins were subjected to in-gel digestion with trypsin and extracted from the gel. Then, the proteins were analyzed by mass spectrometry with an LTQ-Orbitrap XL as previously described [130] and label free protein quantification was performed with the MaxQuant Software tool [131]. The experiment was overall repeated four times. The four experiments were pooled and in total 962 proteins were identified by mass spectrometry analysis (Figure 14a). Of those, 791 proteins were at least in one of the four experiments enriched for binding to pre-miR-92a in comparison to pre-miR-Co. Among them, 95 were predicted to interact with RNA and 64 of the identified proteins were shown to bind to other nucleotides (Figure 14b). The criteria for the selection of potential regulators of pre-miR-92a processing were a low p-value for the difference of binding to pre-miR-92a and the

binding to the control sequence in the four experiments, as well as a high ratio of pre-miR-92a to control, indicating a high and specific affinity of pre-miR-92a to the respective proteins. In Figure 14a, all proteins from the four experiments were plotted according to their p-value and the ratio of binding to pre-miR-92a and the control sequence. For example, 6-phosphofructokinase (6-PFK) was highly enriched to pre-miR-92a in each of the 4 experiments (Figure 14a and c, 6-PFK is labeled as 1). However, since it is a crucial enzyme of glycolysis and not yet described in the context of RNAs it was not selected for further investigation in this study.

C1-tetrahydrofolate synthase and integrin alpha V was highly enriched only in the last two experiments. 60S ribosomal protein L5 and splicing factor Serine/Arginine 10 are considered to be more general RNA binding proteins. Delta(3,5)-delta(2,4)-dienoyl-CoA isomerase is involved in the mitochondrial fatty acid oxidation and therefore not likely to get access to nuclear or cytoplasmic located pre-miRs.

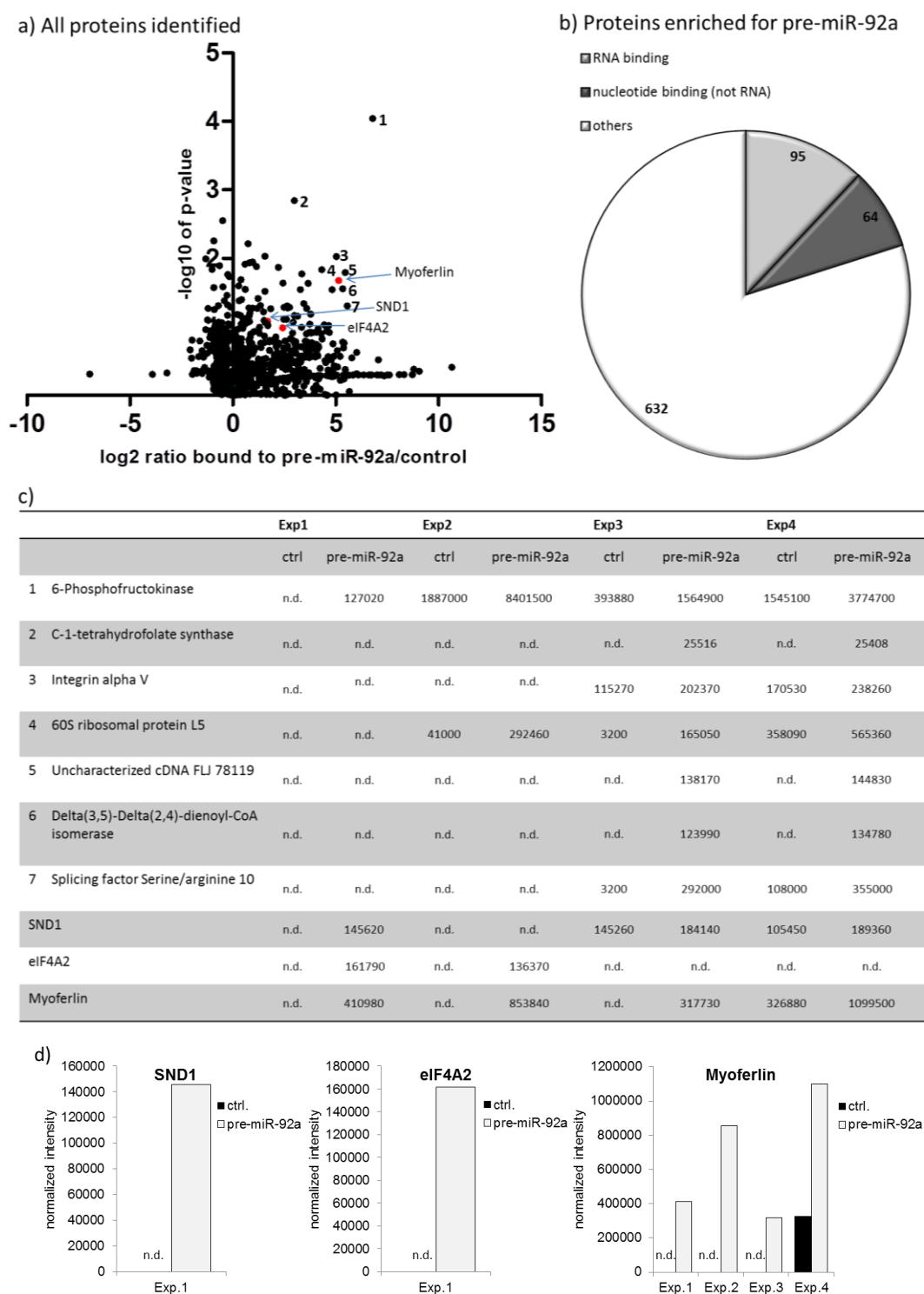


Figure 14: Analysis of pre-miR-92a binding proteins. a) Plot of all proteins identified by mass spectrometry from four different RNA pulldown experiments. Depicted are the p-values and the ratio of the normalized intensity of the proteins bound to pre-miR-92a and the control sequence. For proteins that were not detectable in the control fractions, zero substitution was performed to allow the calculation of the ratio pre-miR-92a to control. The red labeled proteins and numbers 1-7 are described in c) and d). b) Number of proteins that were at least in one of the four experiments enriched to pre-miR-92a. c) Normalized intensities of the interesting proteins in the four different experiments. d) Normalized intensities of the proteins that were further characterized. n.d.: not detected.

After the first experiment, Staphylococcal nuclease domain containing protein 1 (SND1) and eukaryotic initiation factor 4A2 (eIF4A2) were chosen as potential candidates for the regulation of miR-17-92a. Both were highly enriched to pre-miR-92a and absent in the control fraction in this first experiment (Figure 14a, red dots, and d). In the additional three experiments, SND1 was absent in experiment 2, but enriched to pre-miR-92a in the last two experiments. In addition to experiment 1, eIF4A2 was present and enriched to pre-miR-92a in experiments 1 and 2, but not detectable in Experiments 3 and 4 (Figure 14c and d). Both proteins were chosen because they have already been described as interaction partners of RNA: SND1 is a known component of the RNA induced silencing complex (RISC), as well as a regulator of spliceosome assembly and splicing activity [133]. Moreover, it is involved in the degradation of edited pri-miRs transcripts and pre-miRs [49, 134]. EIF4A2, the eukaryotic translation initiation factor, is an RNA helicase of the DEAD box family that unwinds RNA [135-137] and, like the miR-17-92a cluster, is dysregulated in cancer tissues [138].

After having analyzed the RNA pulldown experiments 2, 3, and 4, Myoferlin appeared as another interesting candidate for the regulation of miR-17-92a (Figure 14d). It was highly enriched to pre-miR-92a in each of the four pull down experiments and was not detectable in the control sample in three out of four experiments. Myoferlin is a transmembrane protein that is highly expressed in skeletal and cardiac muscles [139] as well as in endothelial cells, where it regulates sprouting angiogenesis by influencing the expression of VEGFR2 [140]. Moreover, it is implicated in membrane fusion events and during patching of injured cell membrane [141].

Before analyzing SND1, eIF4A2 and Myoferlin regarding their impact on the miR-17-92a cluster, the interaction between the candidates and pre-miR-92a was confirmed by RNA immunoprecipitation. Moreover, the interaction with the mature members of miR-17-92a or other endothelial miRs was assessed.

IV.1.1. Establishing of the (RIP) protocol for HUVECs

RIP with the selected pre-miR-92a binding proteins was performed in order to confirm the interaction with pre-miR-92a. As a negative control we used IgG, whereas Ago2, a well described interaction partner for mature miRs [142], served as positive control. The respective antibodies were coupled to magnetic beads and incubated with HUVEC lysates over night at 4°C on a rotator to allow protein-RNA complexes to bind to the respective antibodies. The next day, the bound RNA was eluted by proteinase K digestion of the proteins. RNA was isolated by organic extraction followed by ethanol precipitation. In order to improve the amount and quality of the eluted RNA, the RIP protocol was further adapted: First, more cells were used per sample. Instead of two T75 flasks, four T75 flasks with 90-100% confluence were used (approximately $2.2 \cdot 10^7$ cells). Moreover, before lysing of cells, RNA-protein interactions were cross linked by 0.1% formaldehyde. For the normalization of the results, a 10% input control was taken before adding the lysates to the antibody carrying beads, and the input was also incubated in the IP buffer over night at 4°C to monitor potential degradation. Additionally, the RNA extraction was improved. To ensure an efficient precipitation of RNA from the elution fraction, tRNA from yeast was added as carrier for RNA before addition of phenol-chloroform-isoamylalcohol. For the subsequent reverse transcription and the qRT-PCR maximal amounts of RNA or cDNA were used. The RIPs were additionally controlled at the level of the binding of proteins to the antibodies before proteinase K digestion. 50 µl of the beads were subjected to SDS-PAGE and subsequent western blot in order to ensure the binding of the proteins to the respective antibodies.

IV.2. SND1 – a potential regulator of the miR-17-92a cluster under stress conditions

IV.2.1. Confirmation of the interaction between SND1 and members of the miR-17-92a cluster

In order to confirm the interaction of SND1 with pre-miR-92a, RIP with SND1 was performed. The band in the last lane of Figure 15 is indicating that SND1 was successfully precipitated with the SND1 antibody.

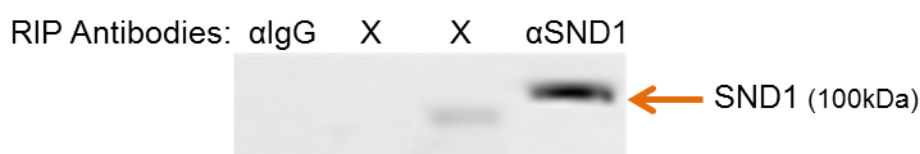


Figure 15: Efficiency of the protein binding to the antibody during RIP. Before the Proteinase K digestion, 50 μ l of the last washing fraction were subjected to 10% SDS-PAGE, Western Blotting and detection of SND1 in order to control the efficient binding of SND to its antibody. IgG: Immunoglobuline G, negative control, X: a different experiment.

The RNA that was extracted from the complexes that bound to IgG or the antibodies against SND1 or Ago2, was analyzed by qRT-PCR for the determination of the presence of pre-miR-92a to confirm the results from the RNA-pulldown. Moreover, the interaction of SND1 with the pri-miR-17-92 transcript and the mature members of miR-17-92a was controlled. SND1 not only interacts with pre-miR-92a (Figure 16b) but also with the pri-miR-17-92 transcript (Figure 16a) and the mature members of the cluster: miR-17, miR-18a, miR-19a, miR-20a, and miR-92a (Figure 16c). Since Ago2 is a known component of the RNA induced silencing complex (RISC), it was used as a positive control for the binding of mature miRs. The highest interaction was found between Ago2 and all tested mature miRs (Figure 16d). For example, miR-20a is 8.3 times more bound by Ago2 than by SND1, and the binding of miR-92a to Ago2 is still 4.9 times more compared to the interaction

with SND1 (Figure 16c and d). Moreover, pri-miR-17-92 was found to slightly interact with Ago2 (Figure 16a), while no interaction with pre-miR-92a could be detected (Figure 16b).

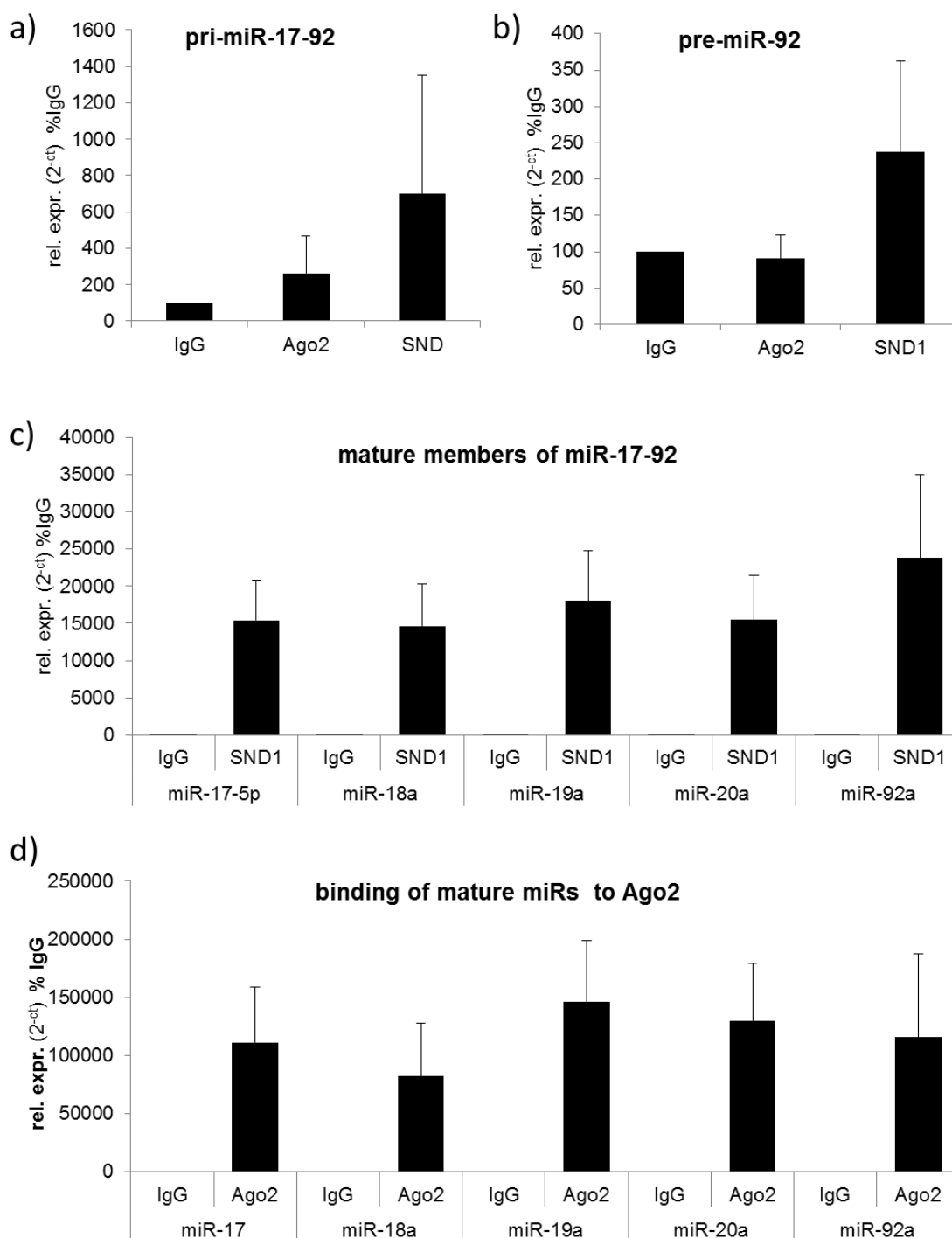


Figure 16: RIP with SND1 and Ago2. Antibodies against SND1, Ago2 or IgG were immobilized to magnetic beads and incubated with HUVEC lysates. Proteins were digested by Proteinase K and the RNA was precipitated from the supernatant and analyzed by qRT-PCR. a) Binding of pri-miR-17-92 to IgG, Ago2 and SND1, b) binding of pre-miR-92a to IgG, Ago2 and SND1, c) binding of the mature miR-17-92a cluster members to IgG and SND1. d) Binding of the mature miR-17-92a members to Ago2. Data are depicted as mean \pm SEM. n=4.

IV.2.2. Under hypoxia mimicking conditions SND1 affects the maturation of miR-17-92a

Having confirmed the interaction of SND1 with pre-miR-92a and, moreover, having detected the interaction of SND1 with the mature members of the miR-17-92a cluster, the influence of SND1 on the processing of the miR-17-92a cluster was investigated. SiRNA was used to silence SND1 expression. SND1 was efficiently down regulated by siRNA against SND1 at 48, 72 hrs and 96 hrs compared to control siRNA treated cells (Figure 17a).

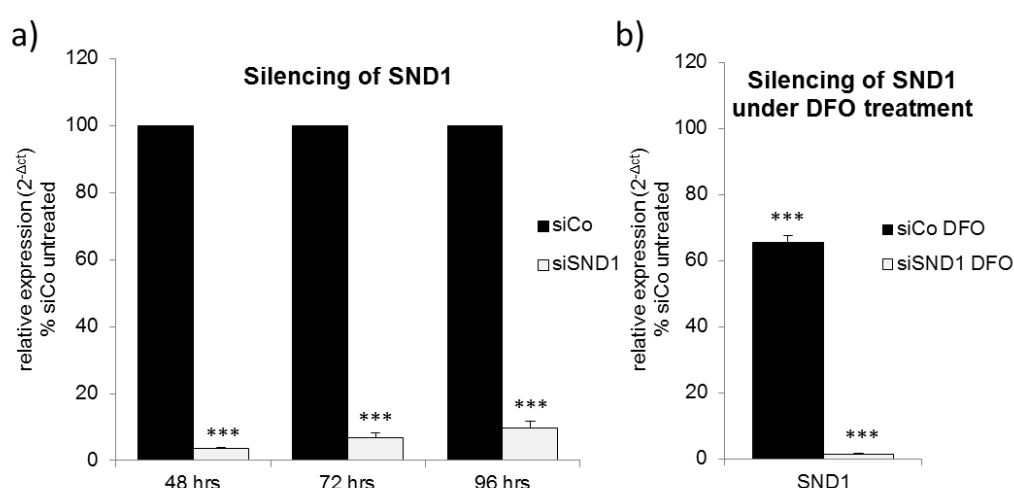


Figure 17: Silencing efficiency of siSND1. a) Time course of expression of SND1 48, 72 and 96 hrs after transfection with 60 nM siSND1, n=5-7, b) HUVECs were transfected with 60 nM siSND1 or siCo. After 24 hrs, 100 μ M DFO was added. 96 hrs after transfection RNA was extracted and mRNA expression levels were analyzed by qRT-PCR. Data are depicted normalized to RPLP0 as mean \pm SEM, n=5, DFO: Deferroxamin 100 μ M, ***p<0.001.

Under basal conditions, neither the level of the primary transcript nor the levels of pre-miR-17, pre-miR-18a, pre-miR-19a or pre-miR-20a were affected by the knock down (Figure 18a and b “-DFO”). Pre-miR-92a was slightly, but not statistically significantly elevated. The mature cluster members miR-17, miR-18, and miR-19a were not affected (Figure 18c “-DFO”). MiR-20a was slightly upregulated while miR-92a was slightly down

regulated. However, these findings were not significantly different from the control group. Therefore, silencing of SND1 under basal conditions does not appear to have an impact on the expression and maturation of miR-17-92a.

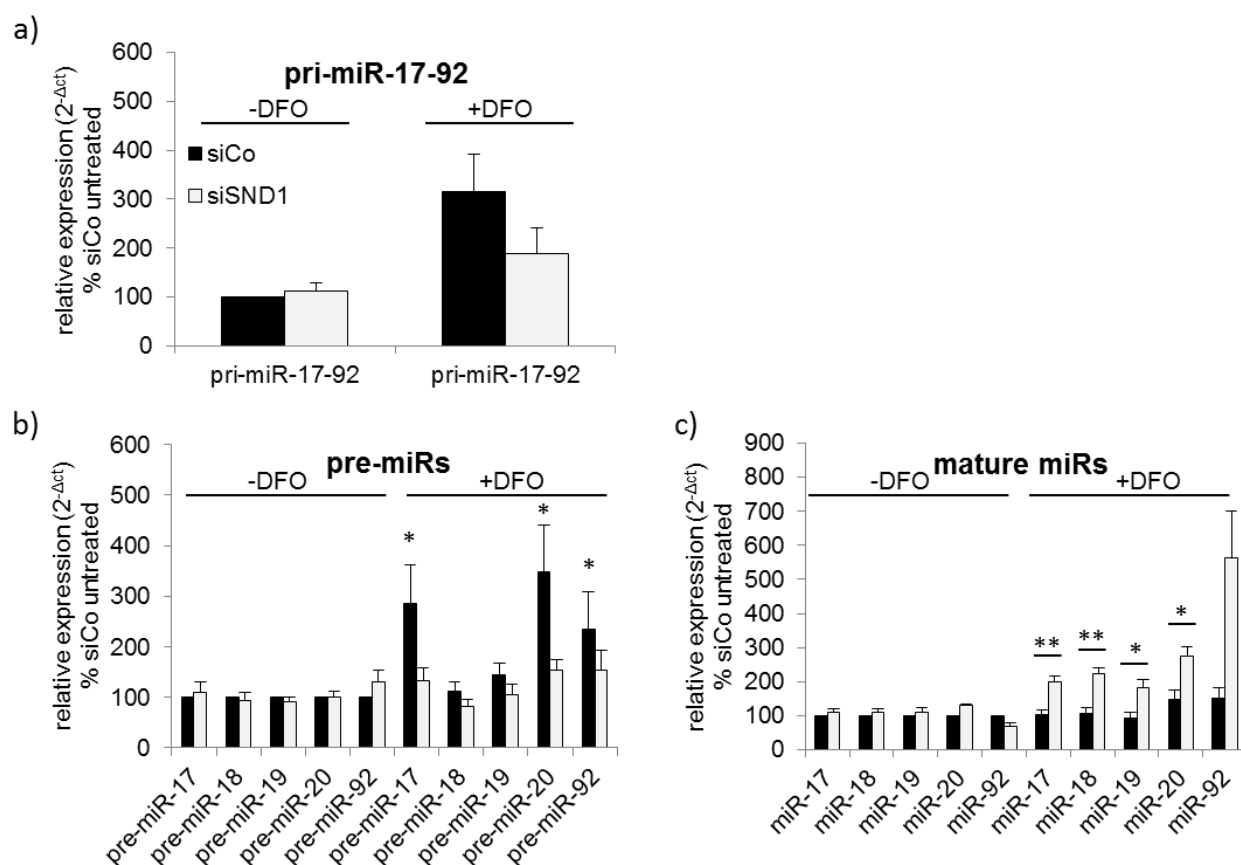


Figure 18: Effect of SND1 silencing 96 hrs after transfection of 60 nM siSND1. a) pri-miR-17-92 levels after transfection, b) pre-miR levels, c) mature miRs. Data are normalized against U6 snRNA and depicted as mean \pm SEM. n=3-5. *p<0.5, **p<0.01. DFO: Deferoxamin, 100 μ M. n=3-7.

Since it has been described that the cluster miR-17-92a is differentially regulated under conditions of low oxygen, e.g. in hind limb ischemia or after acute myocardial infarction [109], the effect of SND1 silencing under hypoxia mimicking conditions was explored. Therefore, HUVECs were transfected with siRNA against SND1 and then treated with 100 μ M of the iron ion chelator Deferoxamin (DFO) to mimic hypoxia. Silencing of SND1 was also successful under these hypoxia mimicking conditions (Figure 17b). Next the maturation of miR-17-92a was analyzed: After 96 hrs, DFO alone led to an increase of the pri-miR-17-92 transcript to 316 \pm 76% compared to the levels in untreated control cells (Figure 18a, black bars). Moreover, the precursors pre-miR-17 (285 \pm 78%), pre-miR-20a

(348±92%) and pre-miR-92a (234±39%) were significantly enriched under hypoxia mimicking conditions, while pre-miR-18, pre-miR-19a, as well as all mature miR-17-92a cluster members were not affected by the treatment (Figure 18b, black bars). Additional silencing of SND1 reduced the DFO mediated increase of pri-miR-92a to 189±52% (Figure 18a, gray bars). Also pre-miR-17 (134±52%), pre-miR-20a (153±22%) and pre-miR-92a (153±39%) were reduced compared to DFO treatment alone. Pre-miR-18a and pre-miR-19a again were not affected. Interestingly, all mature cluster members were clearly elevated under combined DFO and siSND1 treatment (Figure 18b and c, gray bars). Therefore, silencing of SND1 under hypoxia mimicking conditions seems to lower the effects of DFO on the pri-miR-17-92 transcript and the pre-miRs while elevating the mature miR levels. To illustrate the effects on the processing of pre-miRs to mature miRs the ratios of pre-miRs to mature miRs was calculated. A ratio of more than 1 indicates a block in the processing when pre-miR is accumulating and the levels of mature miRs are relatively lower. If more pre-miRs are processed into the mature form, the level of pre-miRs is decreasing while the mature form increases. Thus, the ratio will be smaller than 1. As shown in Figure 19, a significantly reduced ratio of pre-miRs to mature miRs (e.g. miR-17: 0.27±0.075; miR-92: 0.20±0.1) indicates an increase in the miR maturation in the absence of SND1 under hypoxia mimicking conditions by up to 5 fold indicating that SND1 blocks pre-miR processing.

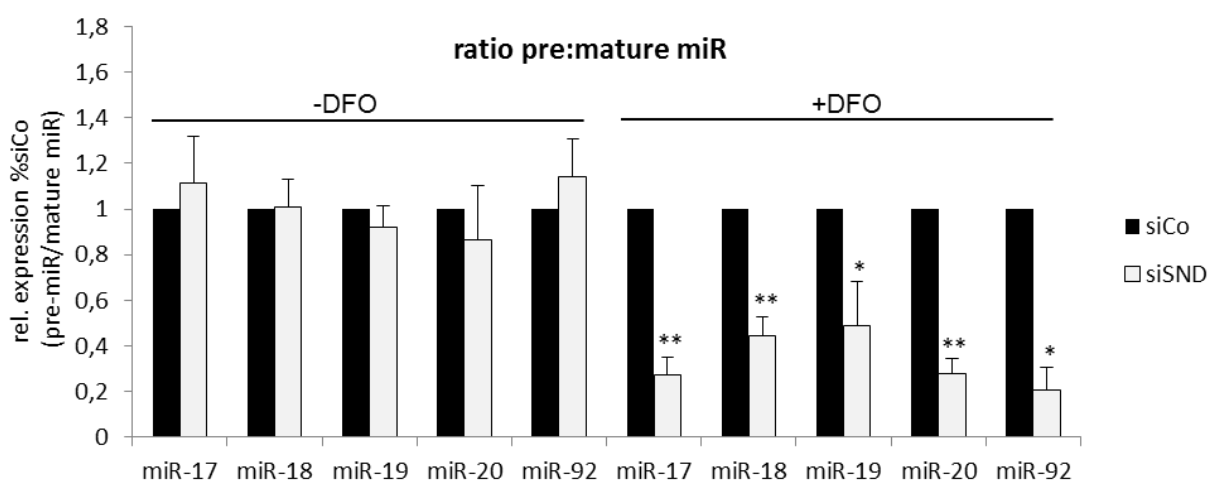
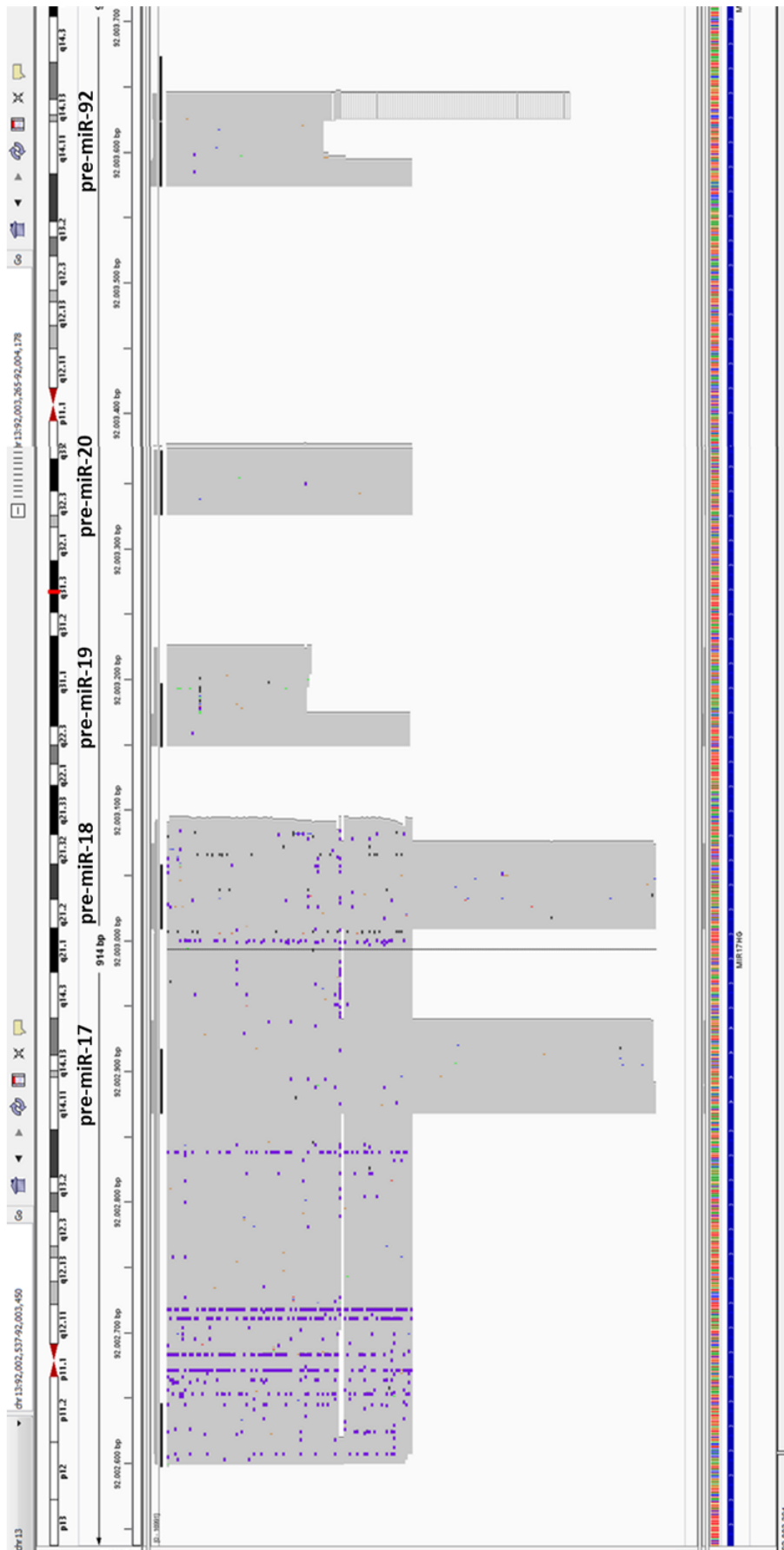


Figure 19: Effect of silencing SND1 under basal and hypoxia mimicking conditions on the ratio of pre-miRs to mature miRs. A ratio <1 indicates increased processing of pre-miR to mature miR. Data are depicted as mean ±SEM, n=3-7, *p<0.05, **p<0.01, DFO: Deferoxamin, 100 µM.

IV.2.3. Potential editing sites of pri-miR-17-92 are not induced upon hypoxia mimicking conditions

Since SND1 has been described to both interact with and degrade A-I-edited pri-miRs and pre-miRs [49, 134] and to mediate their degradation, next it was investigated whether those miRs that are regulated by siSND are edited under hypoxia mimicking conditions and therefore are degraded by SND1 under siCo conditions. This hypothesis was further supported by a finding by indicating that hypoxia increases the rate of occurrence of RNA editing events [143]. Therefore, we analyzed the occurrence of editing events in a part of the pri-miR-17-92 transcript and in the precursor miRs. RNA from HUVECs that were treated with either siCo or siSND1 and DFO was converted to cDNA. With primers specific for a 5' section of the pri-miR-17-92 transcript or the pre-miRs, the respective regions were amplified and further processed by MWG Eurofins (D-Ebersberg). After addition of specific bar code sequences the amplicons were sequenced on GS Junior Titanium Series Chemistry. The bioinformatics analysis was performed with the help of David John (member of the working group of Shizuka Uchida at the Institute for cardiovascular regeneration, University Frankfurt) according to a pipeline described by Ramaswami et al [132]. Deamination of adenosine by ADAR1 or ADAR2 forms an inosine ("A-to-I-editing"). In contrast to adenosine, inosine is not able to base pair with thymidine but only with cytidine. Therefore, during reverse transcription of RNA into cDNA inosine gets substituted by guanine. An A-to-I editing event appears as adenosine-to-guanosine substitution after deep sequencing of reverse transcribed RNA. The number of A-to-G substitutions was counted in order to see whether the combined treatment of HUVEC with siSND and DFO leads to an increase in potential editing sites and to a block of the degradation of these edited RNA due to the absence of SND1. Figure 20 shows the analyzed sequences and the reference genome hg19 provided by the integrative genomics viewer (IGV) software. In the upper part of Figure 20 the genetic locus of chromosome 13q13-q32, the area that encodes for miR-17-92, can be seen. The gray area marks the matching sequences. Nucleotides that do not match the reference genome are indicated blue for cytidine, red for thymidine, green for adenosine, orange for guanosine and purple for single base insertions. On the bottom of the figures the reference sequence is illustrated using the color code for the individual nucleotides.

a) SiCo



b) siSND DFO

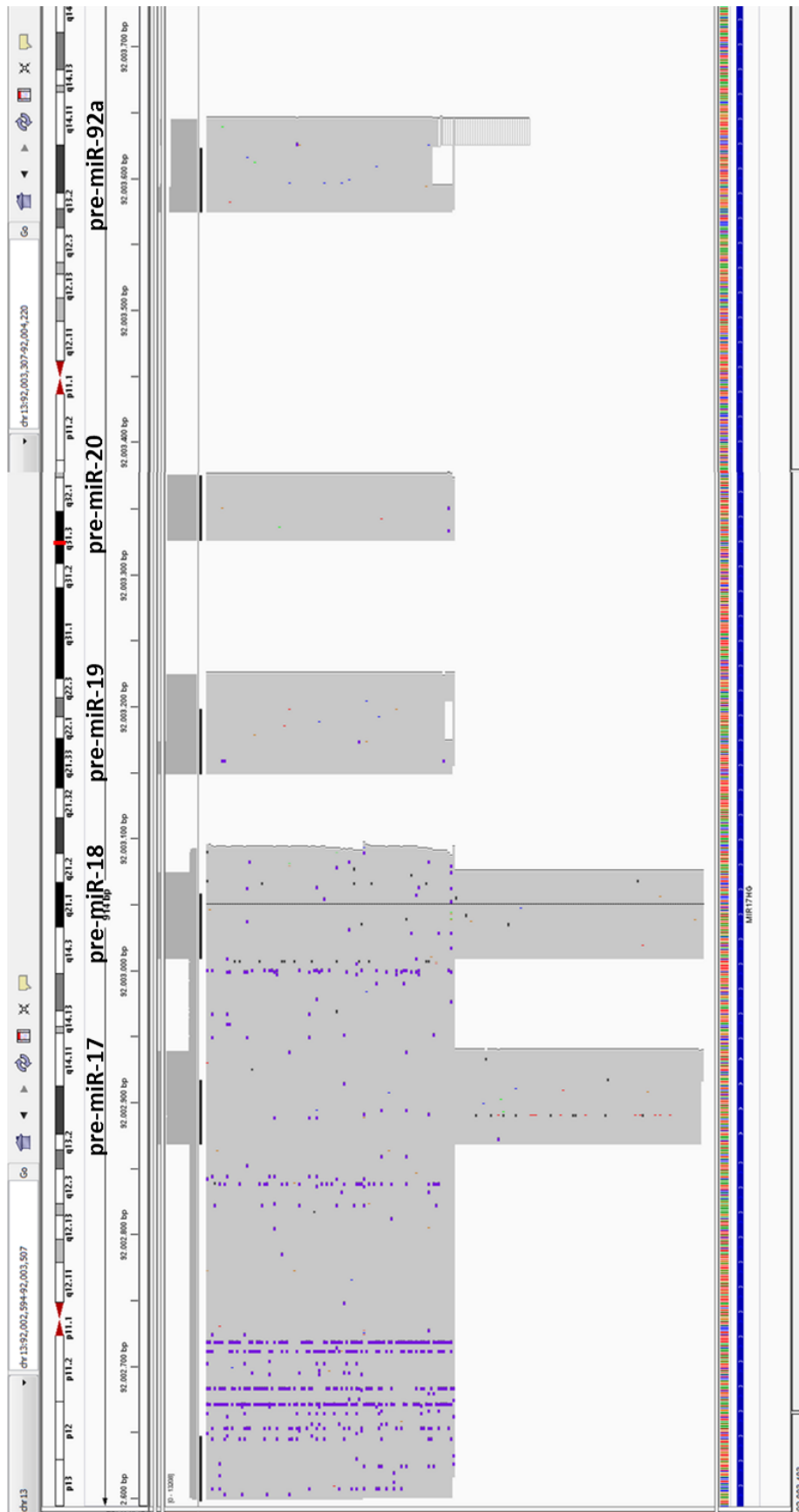


Figure 20: Depiction of the deep sequencing reads for pri-miR-17-92 and the precursors to the reference genome of chromosome 13q13-q32, the genomic locus or miR-17-92a. RNA was isolated and reverse transcribed. RNA was extracted from HUVEC 96 hrs a) after siCo transfection under basal conditions, b) after siSND1 transfection under hypoxia mimicking conditions (DFO 100 μ M). Gray: matching areas, green: Adenosine, orange: Guanosine, red: Thymidine, blue: Cytidine, purple: single base insertions.

A potential editing site appears in Figure 20 as an orange mark (guanosine) at a site where the reference genome at the bottom of the screen shot is green (adenosine). A summary of the counted potential editing sites is given in Table 26.

Table 26: A-to-G substitutions in miR-17-92a intermediates. Quantification of A-to-G substitutions in pri-miR-17-92a_5' and pre-miRs of miR-17-92a in HUVECs treated with control siRNA (siCo) or siSND and DFO (100 μ M). cDNA was amplified with specific primers and sequenced by MWG Eurofins (D-Ebersberg).

	siCo	siSND DFO
Pri-miR-17-92a_5'	28	18
Pre-miR-17	2	1
Pre-miR-18	3	1
Pre-miR-19	3	3
Pre-miR-20	1	-
Pre-miR-92	1	1
Total	38	24

In siCo treated cells in a total of 38 A-to-G substitutions were identified, while in siSND1 and DFO treated cells 24 A-to-G substitutions could be found.

IV.2.4. ADAR1 silencing does not influence the expression of the mature members of miR-17-92a

In parallel to the next generation sequencing approach, we analyzed by qRT-PCR whether editing by ADAR1 might influence miR levels. Since ADAR1 is the enzyme that mainly mediates RNA editing in HUVECs (unpublished Data K. Stellos, Institute for cardiovascular regeneration, D-Frankfurt), we addressed whether ADAR1 regulates the expression of processing of members of miR-17-92a under conditions of SND1 silencing or mimicking of hypoxia. ADAR1 or SND1 were silenced by siRNA under hypoxia mimicking conditions and the levels of the mature members of miR-17-92a were analyzed. SiADAR1 treatment reduced ADAR1 mRNA expression compared to siCo treated cells (Figure 21a). By qRT-PCR the levels of the mature miR-17-92a members were analyzed and are depicted in Figure 21b as percentage of the levels in siCo treatment without DFO. The expression of miR-18, miR-19a, and miR-20a was not affected by siADAR1 while miR-92a was slightly but not significantly elevated (Figure 21) in contrast to the strong elevation of the cluster members after silencing of SND1 compared to silencing of SND1 under basal conditions (Figure 18).

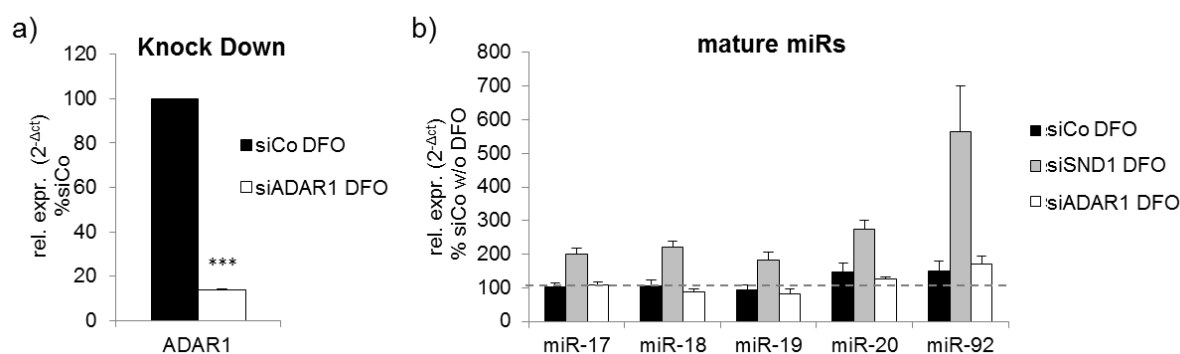


Figure 21: Silencing of ADAR1 under hypoxia mimicking conditions. a) ADAR1 expression 96 hrs after siADAR1 treatment (for silencing efficiency of siSND1 see Figure 17), b) Effect of silencing ADAR1 under hypoxia mimicking conditions (DFO 100 μ M) on the expression of the mature miRs of the miR-17-92a cluster compared to siCo treated cells under normoxic conditions. Data are depicted as mean \pm SEM, n=3, *p<0.05, ***p<0.001.

Together with the deep sequencing analysis, the unaffected levels of the mature miRs in the absence of ADAR1 indicate that ADAR1 does not seem to increase the editing of pri-miR-17-92a_5' or any of the pre-miRs of the miR-17-92a cluster under hypoxia mimicking conditions.

IV.3. eIF4A2 interacts with the mature miRs of the miR-17-92a cluster but silencing of eIF4A2 does not affect its processing

IV.3.1. eIF4A2 interacts with the mature members of the miR-17-92a cluster

In order to confirm the interaction of eIF4A2 with members of the miR-17-92a cluster, RIP was performed. Figure 22 depicts a fraction of the last washing fraction before proteinase K digestion and RNA elution. The band in the last lane proves that eIF4A2 was efficiently bound to its antibody. The non-specific band shows the reaction of the secondary anti-mouse antibody with the heavy chain of the murine antibodies against eIF4A2 and murine IgG.

RIP Antibodies: α IgG X α eIF4A2

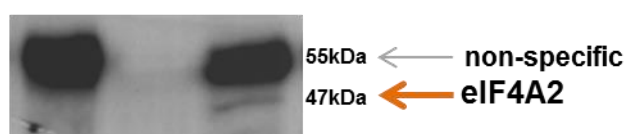


Figure 22: RIP with eIF4A2. Control for the binding of eIF4A2 to its antibody. Western Blot (10% SDS-PAGE) with eIF4A2 specific antibodies shows a fraction of the last wash fraction before the proteins were digested in order to elute the bound RNA. X=lane with a different experiment.

Compared with the RNA bound to the negative control IgG, no binding of eIF4A2 to pri-miR-17-92 and pre-miR-92a could be detected (Figure 23a and b). However, an enrichment of the mature cluster members in complexes with eIF4A2 was measured

(Figure 23c). Although it was shown by RNA pulldown that eIF4A2 interacts with pre-miR-92a, this result could not be confirmed under conditions where the RNA-protein interaction takes place within the cell. By RIP only an interaction of eIF4A2 with the mature miR-17-92a cluster members could be detected.

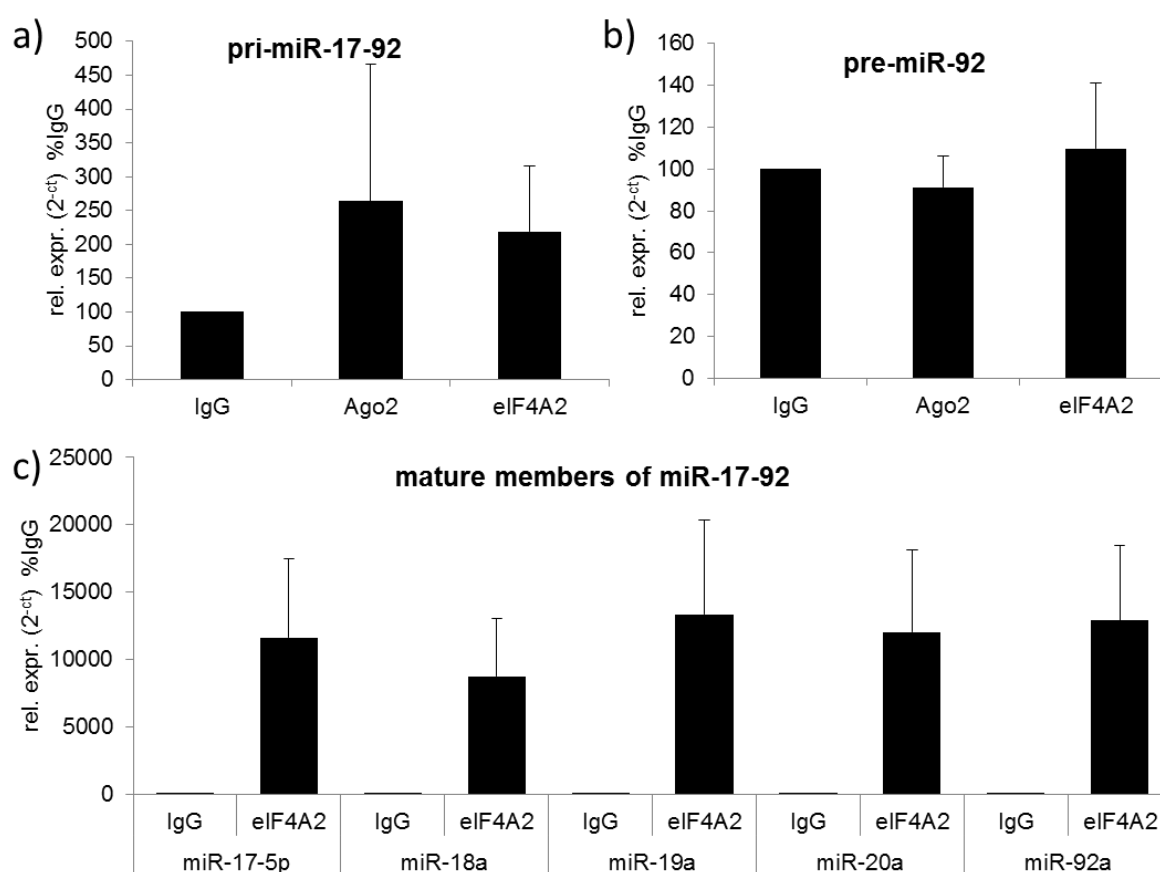


Figure 23: RIP with eIF4A2. Antibodies against eIF4A2, Ago2 or IgG were immobilized to magnetic beads and incubated with HUVEC lysates. Proteins were digested by Proteinase K and the RNA was precipitated from the supernatant and analyzed by qRT-PCR. a) Binding of pri-miR-17-92 to IgG, Ago2 and eIF4A2, b) binding of pre-miR-92a to IgG, Ago2 and eIF4A2, c) binding of the mature miR-17-92a cluster members to IgG and eIF4A2. (The respective binding to Ago2 can be found in Figure 16d (Section IV.2.1). Data are depicted as mean \pm SEM, n=3.

IV.3.2. Silencing of eIF4A2 does not affect the levels of miR-17-92a cluster members

As eIF4A2 was shown to interact with the mature members of the miR-17-92a cluster in the RIPs, the role of eIF4A2 as a potential regulator of the maturation of these miRs was investigated. In order to silence eIF4A2 mRNA, HUVECs were transfected with siRNA against eIF4A2 via lipofection. After 48 hrs RNA was isolated and qRT-PCR was performed to confirm the efficiency of the knock down. Four different siRNA were tested and the most efficient silencing effect was obtained with siRNA siEIF4A2_3 (reduction to 45% compared to eIF4A2 levels in siCo treated cells, Figure 24a). Therefore, this siRNA was used for further experiments. Within four experiments with siEIF4A2_3 an average knock down to 46% was achieved (Figure 24b).

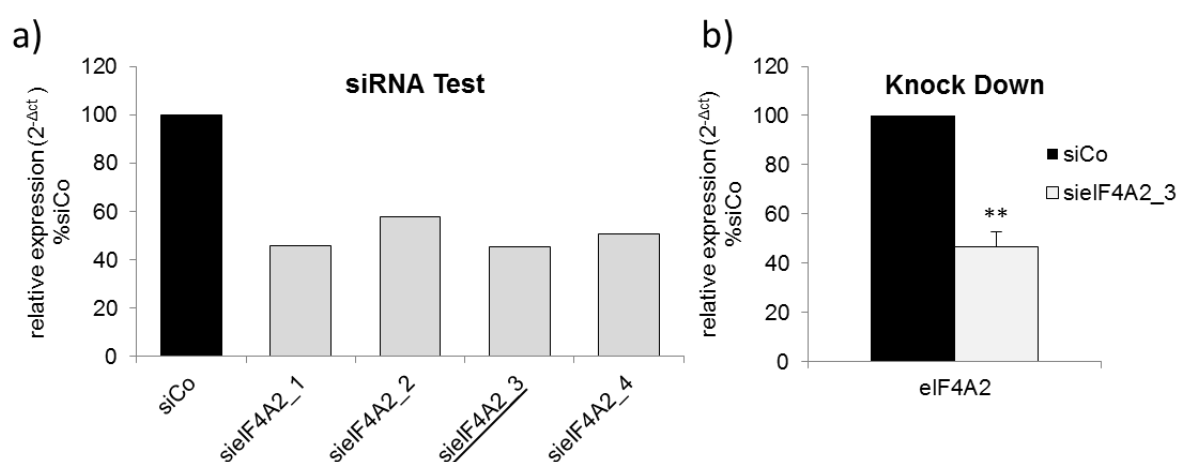


Figure 24: siRNA mediated silencing of eIF4A2. a) siRNA test for silencing of eIF4A2. 4 different siRNA were tested and the mRNA levels of eIF4A2 were determined 48 hrs after transfection. n=1, underlined: siRNA that had the strongest silencing effect, b) for further experiments siEIF4A2_3 was used. Data are depicted normalized to RPLP0 as mean \pm SEM, n=4, **p<0.01.

To test whether silencing of eIF4A2 has an influence on the expression of the miR-17-92a cluster members, the levels of pri-miR-17-92, the precursor miRs and the mature miRs was measured after silencing of eIF4A2.

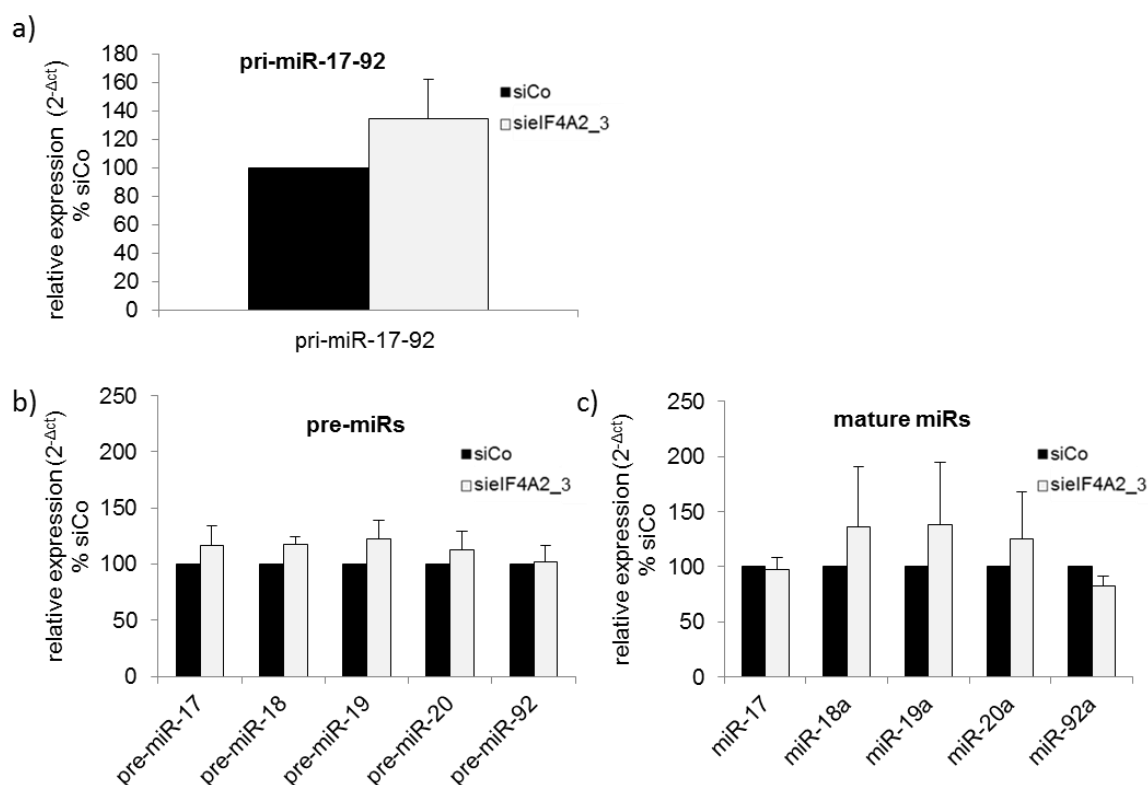


Figure 25: Effect of silencing of eIF4A2 on the maturation of the miR-17-92a cluster. 48 hrs after transfection of sielF4A_3, the expression levels of pri-miR-17-92 (a), pre-miRs (b), and mature miRs of miR-17-92a (c) were analyzed. Data are depicted normalized to RLPP0 (pri-miR-17-92 and pre-miRs) or snRNA U6 (mature miRs) as mean \pm SEM. n=4-5.

Silencing of eIF4A2 slightly elevated the levels of the pri-miR-17-92, pre-miR-17, pre-miR-18a, pre-miR-19a and pre-miR-20a (Figure 25a and b). Moreover, a slight upregulation of the mature miRs miR-18a, miR-19a and miR-20a was detected, whereas miR-92a was slightly downregulated to 82% in the absence of eIF4A2 (Figure 25c). However, none of these changes was significantly different from the expression levels in control siRNA treated cells.

Together, these data indicate that eIF4A2 seems to be a general RNA binding protein that is also able to interact with members of miR-17-92a but that does not significantly influence the expression and biogenesis of the miR-17-92a cluster.

IV.4. Silencing of Myoferlin affects the localization of miR-92a and miR-126 and regulates the levels of pri-miR-126 and pre-miR-126

IV.4.1. Myoferlin interacts with pre-miR-92a and mature miRs

RIP with Myoferlin was performed in order to confirm the interaction of Myoferlin with pre-miR-92a that has been identified before via RNA pulldown and mass spectrometry. QRT-PCR of the RNA eluted from the RIP confirmed the interaction of Myoferlin with pre-miR-92a (Figure 26a).

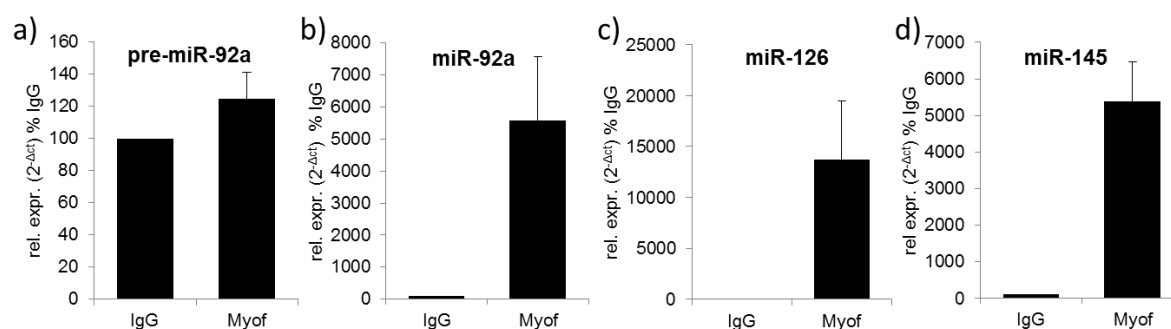


Figure 26: RIP with Myoferlin. Antibodies against Myoferlin or IgG were immobilized to magnetic beads and incubated with HUVEC lysates. Proteins were digested by Proteinase K and the RNA was precipitated from the supernatant and analyzed by qRT-PCR. Binding of a) pre-miR-92a and the endothelial miRs miR-92a (b), miR-126 (c), and miR-145 (d), compared to binding to IgG. Data are depicted as mean \pm SEM, n=3-4.

Compared to the amount of RNA that was bound by IgG, pre-miR-92a was precipitated with Myoferlin. However, this interaction appears to be weak, as pre-miR-92a was only 1.24 fold higher enriched to Myoferlin than with the negative control IgG (Figure 26a). Mature miR-92a was enriched in the Myoferlin IP compared to IgG (Figure 26b). In order to analyze whether Myoferlin acts as a general miR interaction partner in HUVECs, the

endothelial highly enriched miR-126 was analyzed in the RNA eluted from RIP. MiR-126 was detected in the eluted RNA from Myoferlin RIP and found to be enriched (Figure 26c). The interaction of miR-126 was 2.4-fold higher than with miR-92a and even 110-fold higher compared to Myoferlin with pre-miR-92a. Myoferlin has been described to be involved in the organization of the cell membrane and the fusion of vesicles with injured sites of the membrane [141]. Therefore, the levels of miR-145, a miR described to be released from HUVECs in vesicles [65], were also measured in the elution fraction of the RIP. MiR-145 was also found to interact with Myoferlin (Figure 26d). However, the interaction of miR-126 with Myoferlin was 2.5-fold higher than with miR-145.

IV.4.2. Silencing of Myoferlin regulates the levels of mature miR-126 and miR-145 while not affecting other endothelial miRs

Having shown that the mature miRs miR-92, miR-126 and miR-145 interacts with Myoferlin, next the impact of silencing of Myoferlin on the expression of these miRs was investigated. Therefore, siRNA against Myoferlin (siMyof) was used to silence its expression.

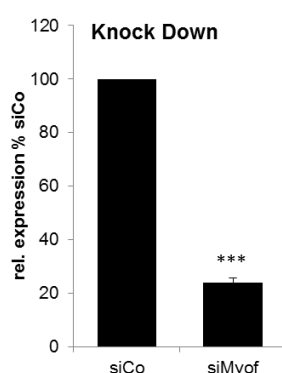


Figure 27: Silencing efficiency of siMyof. HUVECs were transfected with 60 nM siMyof. 72 hrs after transfection RNA was extracted and mRNA expression levels were analyzed by qRT-PCR. Data are depicted normalized to RLPP0 as mean \pm SEM, n=35, ***p<0.001.

The silencing of Myoferlin was efficient as the mRNA levels were reduced to $24\pm 1.8\%$ (Figure 27), but neither the levels of miR-92a nor of the other members of the miR-17-92a cluster was affected (Figure 28). Although interacting with pre-miR-92a and the mature cluster members, Myoferlin did not influence the expression of miR-92a or the other mature members of miR-17-92a. Therefore, under these conditions Myoferlin does not seem to regulate the processing of miR-17-92a.

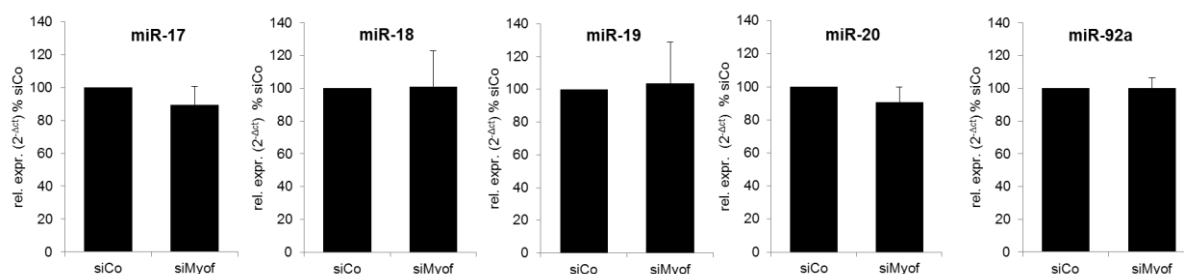


Figure 28: Effect of silencing of Myoferlin on the expression of the mature members of miR-17-92a. HUVECs were transfected with 60 nM siMyof. 72 hrs after transfection RNA was isolated. MiR-levels were determined by specific taqman miR assays (life technologies, D-Darmstadt). Data are depicted normalized to snRNA U6 as mean \pm SEM. n=8.

However, the endothelial enriched miR-126 was significantly increased in absence of Myoferlin to $133\pm 9.4\%$ compared to siCo, while miR-145 was significantly reduced to $81\pm 4.6\%$ (Figure 29). Additionally, miR-150 was tested because it has been observed to be exported by vesicles under specific conditions (unpublished data by Dr. Nicolas Ja e, Institute for cardiovascular regeneration, Frankfurt). MiR-150 was slightly reduced but not significantly affected by silencing of Myoferlin (Figure 29).

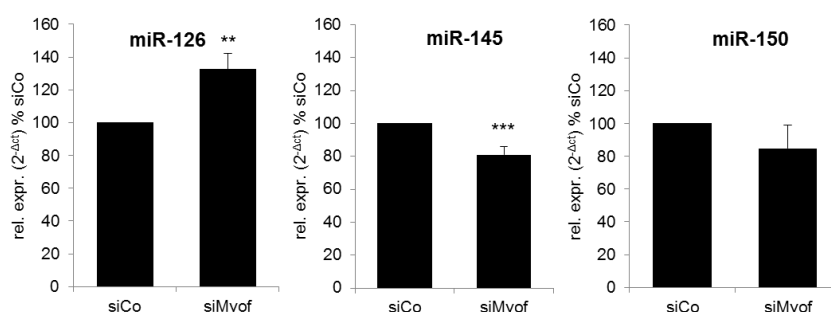


Figure 29: Effect of silencing of Myoferlin on the expression of miR-126, miR-145 and miR-150. HUVECs were transfected with 60 nM. 72 hrs after transfection RNA was isolated. MiR-levels were determined by specific Taqman miR assays (Life Technologies, D-Darmstadt). Data are depicted normalized to snRNA U6 as mean \pm SEM, n=8, **p<0.01, ***p<0.001.

IV.4.3. Pri-miR-126 and pre-miR-126 levels are increased in the absence of Myoferlin

The strongest effect of silencing of Myoferlin was seen for miR-126. The increase of miR-126 and the interaction of Myoferlin with miR-126 raised the question whether Myoferlin has an impact on the maturation of miR-126. Therefore, the intermediate products of miR-126 processing, namely pri-miR-126 and pre-miR-126, were analyzed by qRT-PCR in HUVECs after transfection with siRNA against Myoferlin (siMyof). Interestingly, both pri-miR-126 and pre-miR-126 were significantly decreased in the absence of Myoferlin to $34\pm 8.1\%$ and $39\pm 10.1\%$, respectively (Figure 30).

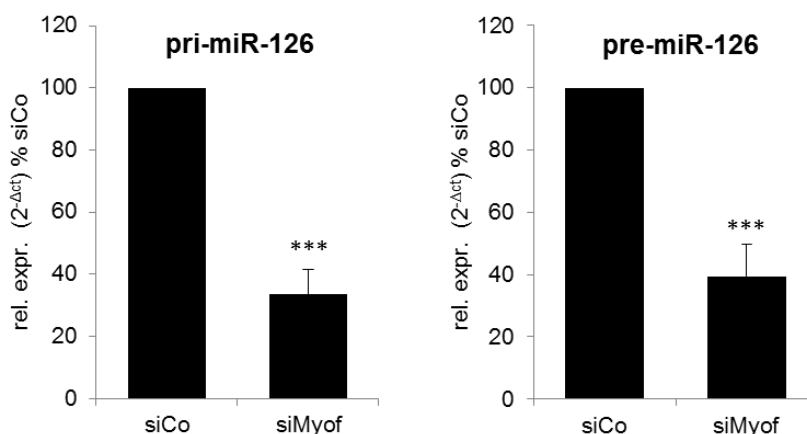


Figure 30: Effect of silencing of Myoferlin on the levels of pri-miR-126 and pre-miR-126. HUVECs were transfected with siMyof. 72 hrs after transfection RNA was isolated. Data are depicted normalized to RPLP0 as mean \pm SEM, n=5, ***p<0.001.

IV.4.4. Myoferlin interacts with pri-miR-126

Since the processing of miR-126 is differentially regulated in the absence of Myoferlin, it was next tested whether Myoferlin interacts with pri-miR-126. RIP revealed that indeed, pri-miR-126 is interacting with Myoferlin (Figure 31). However, the binding of the mature miR-126 to Myoferlin was still 9.7-fold higher.

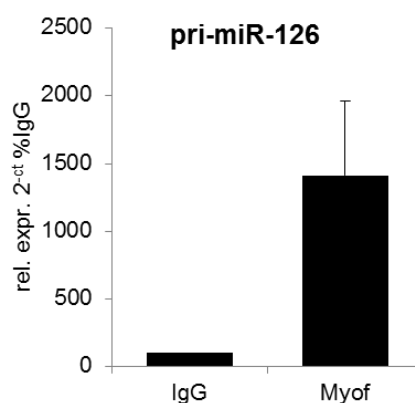


Figure 31: RIP with Myoferlin. Antibodies against Myoferlin or IgG were immobilized to magnetic beads and incubated with HUVEC lysates. Proteins were digested by Proteinase K and the RNA was precipitated from the supernatant and analyzed by qRT-PCR to determine the binding of pri-miR-126 to α Myof compared to binding to IgG. Data are depicted as mean \pm SEM. n=4.

IV.4.5. Silencing of Myoferlin increased extracellular levels of miR-92a

Myoferlin has been described to be involved in the rearrangement of membranes, e.g. after injury of the membrane, Myoferlin mediates the patching of the membrane by fusion of the membrane with vesicles [141]. As Hergenreider et al. showed, HUVECs release microvesicles that carry miRs to recipient cells, e.g. miR-143/145 are transported to SMCs [65]. Therefore, we investigated whether Myoferlin might control the shedding of vesicles. In order to test this hypothesis, RNA from the pre-cleared (10 min, 4000*g, 4°C) supernatant of HUVECs transfected with siCo or siMyof was isolated. Next, the pre-cleared supernatants were centrifuged at 140,000*g for 1 hr and the microvesicles containing pellet was subjected to RNA isolation. As a control, c.elegans-miR-47, that has

no homologue in HUVECs, was spiked in to ensure the quality of the RNA isolation. Results from qRT-PCR showed that in the absence of Myoferlin miR-92a is enriched to $139\pm 17\%$ in the supernatant (Figure 32a) and increased to $220\pm 55.2\%$ in the pelleted microvesicles (Figure 32b). In contrast, miR-126 is enriched only in the supernatant ($246\pm 70.3\%$) and its concentration is not changed in the microvesicles ($95\pm 5.8\%$, Figure 32). MiR-150 and miR-145 levels in the supernatant or the microvesicles were not significantly changed in the absence of Myoferlin (Figure 32).

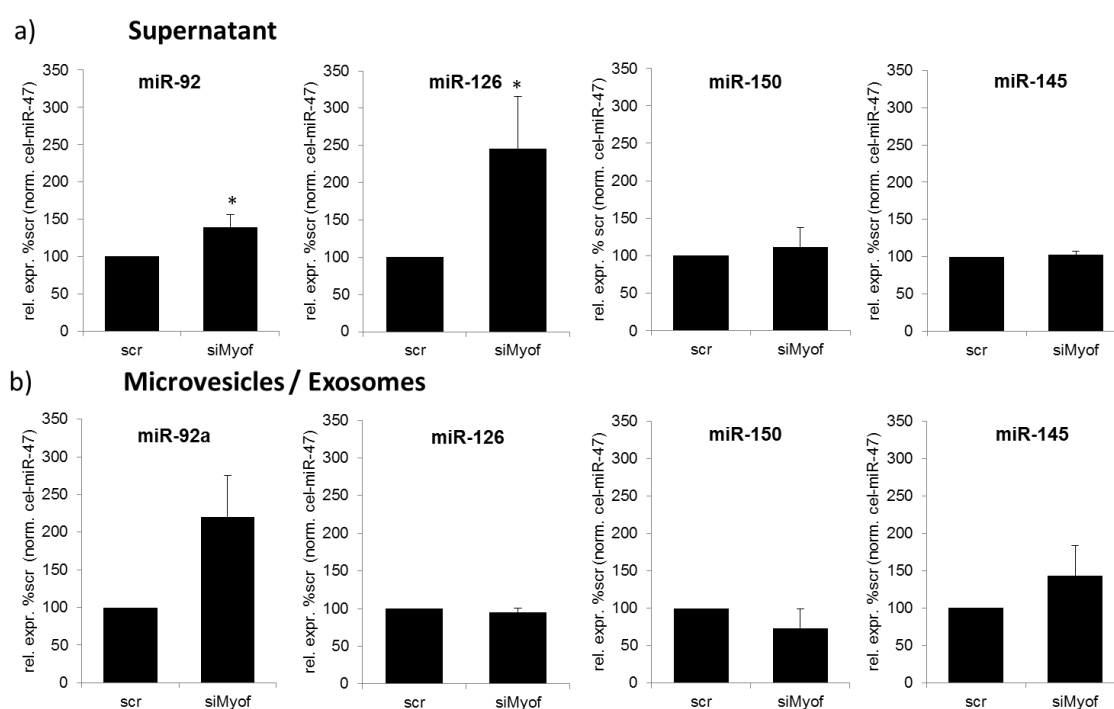


Figure 32: Effect of silencing of Myoferlin on the levels of miRNAs in the supernatant or extracellular microvesicles and exosomes of HUVECs. HUVECs were transfected with 60 nM of siCo or siMyof. After 72 hrs the supernatant was centrifuged for 10 min, $4000\times g$, $4^{\circ}C$. 200 μl of the supernatant from this step were mixed with 700 μl Qiazol (“supernatant”). The rest was subjected to ultra centrifugation at $140,000\times g$, 1 hr, $4^{\circ}C$. The pellet was washed with PBS and again centrifuged $140,000\times g$, 1 hr, $4^{\circ}C$ and finally resuspended in Qiazol for RNA isolation (“microvesicles/exosomes”). a) miR levels determined in the supernatant of HUVECs 72 hrs after siRNA transfection, b) miR-levels were determined in the microvesicle and exosomes after pelting of the supernatant. Data are depicted as mean \pm SEM, $n=8-14$, $*p<0.05$.

IV.4.6. Silencing of Myoferlin increases the relative number of exosomes

The differential levels of miR-92a in the microvesicles of siMyof treated cells led to the assumption that Myoferlin might regulate the shedding of vesicles by HUVECs. To determine the number and size of vesicles, the use of the nanoparticle tracking analysis (NTA) using the Nanosight laser was established for the use with HUVECs. Microvesicles were prepared from HUVECs via differential centrifugation as described for Figure 32. Then, the particles were analyzed under Brownian motion by a laser. Silencing of Myoferlin did not change the number of vesicles (Figure 33a). The size of most particles detected after siCo treatment was 110 nm, which is the expected size of exosomes (Figure 33b, blue line). After silencing of Myoferlin, a slight shift of this peak was observed. In the pelleted supernatant from siCo treated cells, $26.8 \pm 7.6\%$ of the particles were smaller than 100 nm, while after silencing of Myoferlin only $17.7 \pm 3.3\%$ of the measured particles had a diameter of less than 100 nm.

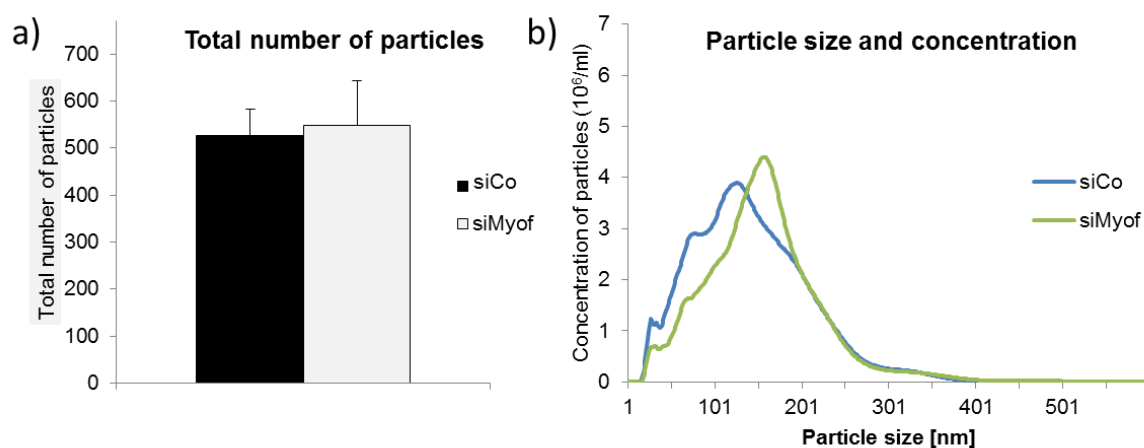


Figure 33: Nanoparticle tracking analysis after silencing of Myoferlin. HUVECs were transfected with 60 nM of siCo or siMyof. After 72 hrs the supernatant was centrifuged for 10 min, $4000 \times g$, $4^\circ C$. Then, the supernatant from this step was subjected to ultra centrifugation at $140,000 \times g$, 1 hr, $4^\circ C$. The pellet was washed with PBS and again centrifuged $140,000 \times g$, 1 hr, $4^\circ C$ and finally diluted 1:10 and analyzed by nanoparticle tracking analysis using the Nanosight laser and the Nanosight software. a) Total number of particles shed by HUVECs, b) Concentration of particles per size. $n=3$.

Together, Myoferlin performs a complex role in the regulation of the tested endothelial miRs. It is a weak interaction partner of pre-miR-92a while exhibiting higher interaction with the mature miRs miR-92a, miR-126, miR-145 and pri-miR-126. Myoferlin could not be found as a regulator of the processing of miR-92a, but there are strong hints that Myoferlin has an impact on the levels of pri-miR-126 and pre-miR-126. The localization of miR-92a is regulated in absence of Myoferlin since under these conditions miR-92a is detected in the extracellular fraction. However, nanoparticle tracking analysis showed that Myoferlin does not regulate the amount of vesicles and only slightly changes the size of the vesicles. The increase of miR-126 in the supernatant but not in the microvesicles indicates that miR-126 is not exported in microvesicles, but rather protected from extracellular degradation through different mechanisms

V. Discussion

The miR-17-92a cluster is highly expressed in endothelial cells and comprises seven mature members: miR-17-3p, miR-17-5p (miR-17), miR-18a, miR-19a, miR-20a, miR-19b, and miR-92a. It is a polycistronic cluster since all members share one promoter and are transcribed as one common primary transcript. Interestingly, although all members of the cluster derive from the same pri-miR, the mature members of miR-17-92a are under various conditions present at differential levels. During endothelial differentiation of murine embryonic stem cells for example, the pri-miR-17-92 transcript and miR-92a are decreasing with ongoing differentiation, while the mature members miR-17, miR-18a, miR-19a and miR-20a are increasing [122]. Together with findings from others this strongly suggests that the miR-17-92a cluster is regulated posttranscriptionally.

V.1. Identification of pre-miR-92a binding proteins and selection of interesting candidates

Aiming at the identification of potential regulators of the processing of pre-miR-92a, a RNA pulldown with pre-miR-92a as a decoy was established during the preceding master thesis [122]. In vitro transcribed pre-miR-92a was immobilized to agarose beads and incubated with lysates from HUVECs. As a negative control, the pre-miR-92a sequence in the reverse orientation was used. After binding of proteins from the lysate to pre-miR-92a or the control sequence, proteins were eluted from the beads by RNase digestion. The stable binding of the RNA to the beads has been controlled before in the master thesis [122]. Eluted proteins were characterized by Mass Spectrometry. In four experiments, 962 different proteins could be identified of which 9 proteins were enriched to pre-miR-92a in all four experiments and 791 were binding to pre-miR-92a in at least one of the four experiments. 20% of the proteins that were shown to bind to pre-miR-92a in at least

one experiment were described as nucleic acid interaction partners, among them were 12% proteins with predicted RNA binding activity. There were also unspecifically bound proteins, such as Keratins that were eluted in equal amount from pre-miR-92a and the control sequence. These Keratins are present in endothelial cells as part of the cytoskeleton [144], however, it is also possible, that these keratins are contaminants that derive from the user.

EIF4A2, a eukaryotic initiation factor, and SND1, a known component of RISC, were bound by pre-miR-92a in the first experiment, but not reproducibly detected in the following three experiments. However, we started to analyze eIF4A2 and SND1 after the first experiment since the additional RNA pulldown experiments took additional 6 months. The third candidate, Myoferlin is a known regulator of angiogenesis [140] and raised our interest after statistical analysis of all four RNA pulldown experiments.

In addition to Myoferlin, there were also other proteins significantly enriched in all pulldown experiments, such as 6-Phosphofruktokinase (6-PFK) and Integrin alpha V. 6-PFK is important for glycolysis in all cell types [145]. It is described that 6-PFK mRNA is regulated by miRs, but 6-PFK has no described function in interacting with RNAs [146]. However, it might be interesting to elucidate whether 6-PFK is implicated in the regulation of miR, especially under conditions that change the metabolism of HUVECs, such as mechanic shear stress. Similarly, Integrin alpha V is known to be targeted by miRs but so far no implication in the regulation of miRs has been described [147].

The heterogeneity between the four RNA pulldown experiments can be explained by the biology of endothelial cells which are primary cells and therefore more prone to variations than immortalized cell lines. Moreover, the identification of RNA binding proteins via RNA pulldown is a method of high complexity that can be influenced by differences in the batches of recombinant pre-miR-92a, that were reproduced by in vitro transcription twice during the four experiments. Of note, mass spectrometry is a non-quantitative method and therefore does not allow the determination of absolute protein levels. For quantitative genomics, the method of stable-isotope labelling of amino acids in cell culture (SILAC) or ICAT (isotope-encoded affinity tags) can be used [148]. These approaches are based on the comparison of proteins from cells that were fed with amino

acids with heavy isotopes (^2H , ^{13}C or ^{15}N) to cells that were fed with amino acids with normal isotopes (H , ^{12}C or ^{14}N) and thereby distinguish unspecifically bound proteins.

The interaction of the interesting candidates with pre-miR-92a in the RNA pulldown could be confirmed via RNA immunoprecipitation (RIP) in the case of two out of three candidates. Only the interaction of eIF4A2 and pre-miR-92a could not be confirmed. Of note, the interaction of SND1 and Myoferlin with pre-miR-92a was also very weak compared to the levels of the mature miRs bound by SND1 and Myoferlin. This can be explained by the differences of the two methods: While the RNA pulldown is an *ex vivo* approach that uses relatively high numbers of recombinant pre-miR-92a and protein-extracts from HUVECs, the RNA-protein interaction observed in the RIP takes place within living cells, where the endogenous pre-miRs underlie a rapid turnover. Moreover, during the RIP the formation of large protein complexes may influence the accessibility of the pre-miR. For instance, since it is known that eIF4A2 together with several different eIFs form a complex to bind mRNA, this complex formation might interfere with the accessibility of eIF4A2 for pre-miR-92a intracellularly.

V.2. SND1 – a known regulator of RNAs with new implication in miR-17-92a maturation

SND1 (staphylococcal nuclease domain containing protein 1, also called p100, Epstein-Barr virus encoded transcription factor 1 or Tudor-SN1) is highly conserved among species and consists of five staphylococcal nuclease (SN) domains and a Tudor domain. It is a known component of the RNA induced silencing complex (RISC) [50] and has been described as a cofactor during tumorigenesis [149]. Moreover, SND1 is highly upregulated in colorectal adenoma [150]. More recently, a role for SND1 as an RNase specific for Inosine containing dsRNAs has been described as it degrades edited pri-miRs and pre-miRs [49]. Interestingly, SND1 is also a regulator of angiogenesis since it inhibits angiogenesis in a chicken chorioallantoic membrane assay as well as in endothelial cells [151]. The binding of SND1 to pre-miR-92a in the RNA pulldown could be confirmed by RIP. Additionally, an interaction of SND1 with the pri-miR-17-92 transcript as well as with

all the mature members of miR-17-92a was detected, while only a small amount of miR-126 was interacting with SND1 (data not shown n=2). Ago2 served as a positive control in all RNA pulldown experiments because it is an essential component of RISC where it binds miRs and enables the guidance of a miR to its target mRNA [142]. In line with this, the strongest interaction was observed between the mature members of the miR-17-92a cluster and Ago2. Of note, the interaction of miRs with SND1 and Ago2 cannot be compared directly, because the IP efficiency of the two antibodies might differ. To enable a comparison between the binding to SND1 and Ago2, the levels should be compared to the input. When the data were reanalyzed and compared to the input, the difference between binding of miR-92a to Ago2 ($272.3 \pm 214\%$) and SND1 ($87.8 \pm 38\%$) becomes obvious.

Although the interaction of SND1 with the mature miRs of the miR-17-92a cluster seems to be reproducible, it cannot be ruled out that this interaction is indirect. It is also conceivable that SND1 is present in a complex with other proteins of which one directly interacts with miRs. For example, according to the string analysis (www.string-db.org), PRPF8 is a potential interaction partner of SND1 with described ability to bind RNA [152]. Still, it is also likely that SND1 interacts with pre-miR-92a directly since it has been shown to directly interact with other dsRNAs [153] mediated by two SN domains functioning as a clamp for the dsRNA.

V.2.1. Silencing of SND1 under hypoxia mimicking conditions affects miR-17-92a biogenesis

We further investigated the effect of SND1 on the biogenesis of the miR-17-92a cluster using small interfering RNA (siRNA) mediated SND1 knockdown and subsequent analysis of miR levels by qRT-PCR. Under basal conditions, silencing of SND1 did not significantly influence the levels of pri-miR-17-92, the pre-miRs or the mature miRs. However, since studies from other members of the institute showed that under hypoxic conditions a differential expression of miR-17-92a cluster members could be observed, we tested the effect of SND1 silencing after exposing endothelial cells to the hypoxia mimicking agent DFO for 96 hours. DFO alone induced an increase in pri-miR-92a as well as pre-miR-17,

pre-miR-20a and pre-miR-92a. The levels of the mature miRs were not significantly altered. The observation that the mature miRs are not decreasing while the pre-miRs are accumulating can be explained by the fact that the mature miRs are very stable and, thus, effects of decreased processing cannot yet be seen. Taken together, under hypoxia mimicking conditions, the miR processing of the miR-17-92a cluster was reduced.

Interestingly, when the treatment with DFO was combined with the silencing of SND1, the effects of DFO alone on pri-miR-17-92 were reversed: The pri-miR-17-92 transcript, as well as pre-miR-17, pre-miR-20a and pre-miR-92a decreased. Simultaneously, all mature members of miR-17-92a were significantly increased. The effects of siSND1 in combination with DFO treatment can be summarized by calculating the ratio of pre-miR to mature miR. Under hypoxia mimicking conditions, siSND1 significantly decreases this ratio to less than 1, indicating a strong increase in the processing of pre-miRs and an enrichment of mature miRs. This indicates that SND1 is involved in the DFO dependent impairment of the maturation of pre-miRs into mature miRs. It has been shown by others that hypoxia mediates a transcriptional repression of Dicer and Dicer mRNA half-life which causes an inhibition of miR processing [154]. To test whether SND1 is involved in the down-regulation of Dicer, the effect of siSND1 on Dicer expression was analyzed. However, the hypothesis could not be confirmed because siSND1 did not affect Dicer mRNA levels neither under basal nor under hypoxia mimicking conditions (data not shown).

V.2.2. Hypoxia mimicking conditions do not increase the editing of pri-miRs and pre-miRs of the miR-17-92a cluster

It has been described that hypoxia induces the Adenosine-to-Inosine (A-to-I) conversion [143]. Moreover, it is known that SND1 plays a role in degrading edited pri- and pre-miRs [49]. Therefore, it is conceivable that hypoxia mimicking conditions might lead to the generation of edited pri-miR-17-92 and edited pre-miRs that are then degraded by SND1. In the absence of SND1 the edited RNAs might not be degraded and therefore might be more efficiently processed. It can also be speculated that under conditions, where edited

pre-miRs cannot be degraded, they have an increased affinity to Dicer. To elucidate whether editing takes place, ADAR1, the adenosine deaminase acting on RNA 1 that regulates most of the A-to-I editing in endothelial cells (unpublished data from Konstantinos Stellos, institute for cardiovascular regeneration, Frankfurt), was silenced by siRNA and the effects on the mature miR-17-92a cluster members were assessed. Next generation sequencing was performed to quantify potential editing sites in the miR-17-92a cluster in order to see whether under hypoxia mimicking conditions and in the absence of SND1, more potential editing sites can be seen. It has been expected that DFO increases the number of potential editing sites and that after DFO treatment in combination with silencing of SND1 these miRs are not degraded. However, next generation sequencing revealed that a 5' part of pri-miR-17-92 and the pre-miRs of miR-17-92a under basal conditions only showed few Adenosine to Guanosine (A-to-G) substitutions and did not reveal more A-to-G substitutions after treatment with DFO but a slightly reduced number of editing sites. It is conceivable, that the change of A-to-G in the nucleotide sequence does not necessarily represent an A-to-I editing event but also single nucleotide polymorphisms (SNPs). Of note, hypoxia induces a whole cascade of adaptive processes, while DFO mainly functions by stabilizing HIF-1 α [127]. It would be worthwhile testing the effects of silencing of SND1 under real hypoxia (<1% oxygen). Another possible explanation is that pri-miR and pre-miRs are actually edited but are degraded by other factors than SND1, so that the silencing of SND1 alone does not prevent the degradation of these modified RNAs.

Interestingly, previous studies postulated that SND1 is located to stress granules that are formed upon a stress stimulus [155]. Since DFO is a strong stress stimulus for the cell, it is tempting to speculate that after DFO treatment, SND1 is located to stress granules in a complex with the bound pre-miRs that are then no longer accessible to the processing machinery. Upon silencing of SND1, pre-miRs are not abducted by SND1 into stress granules but are still processed. This speculation needs further confirmation which would include the colocalization of SND1 and pre-miRs within stress granules as well as the stimulation with different stress stimuli.

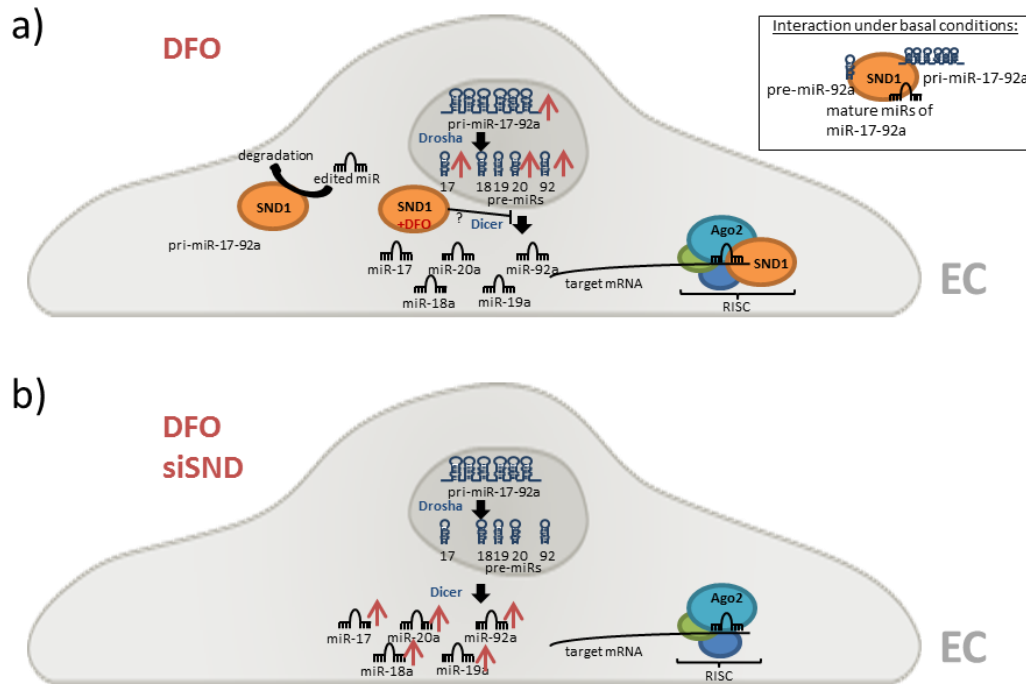


Figure 34: Summary of the effects of hypoxia mimicking conditions and silencing of SND1 on the miR-17-92a cluster. a) Hypoxia mimicking conditions caused an increase of pri-miR-17-92 and several pre-miRs of the miR-17-92a cluster, b) Silencing of SND1 under hypoxia mimicking conditions increases the processing of pre-miRs, thereby leading to an increase in mature miRs. EC: Endothelial cell, DFO: Deferoxamin, Ago2: Argonaute 2, RISC: RNA induced silencing complex.

In summary, in this study SND1 appears as an interesting new regulator of miR-17-92a processing. Silencing of SND1 under hypoxia mimicking conditions augments the maturation of miR-17-92a cluster members, which exhibit mostly antiangiogenic functions [96]. Therefore, it is conceivable that silencing of SND1 performs antiangiogenic functions in endothelial cells under hypoxia mimicking conditions. Therefore, the potential negative effect of SND1 on the maturation of miR-17-92a goes in line with the previous identification of SND1 as promoter of angiogenesis [151]. SND1 might be an important regulator of angiogenesis upstream of miRs of the miR-17-92a cluster. If SND1 is a negative regulator of angiogenesis, under conditions where an organism has to adapt to changes in the environment by angiogenesis, SND1 may repress antiangiogenic miRs as members of the miR-17-92a cluster. It would be interesting to investigate whether SND1 also affects other anti-angiogenic miRs, e.g. miR-21[156].

V.3. EIF4A2 – general RNA binding protein

EIF4A2, the eukaryotic translation initiation factor 4A2, also was highly enriched bound to pre-miR-92a and was not bound to the control sample of the first experiment. It is an RNA helicase of the DEAD box family [135] and able to unwind hairpin RNAs [136]. Interestingly, like the miR-17-92a cluster, eIF4A2 is deregulated in cancer [138]. More recently a central role of eIF4A2 in mediating the functionality of miRs has been described: EIF4A2 is essential for enabling the binding of miRs to the 3'UTR of target mRNAs [157]. EIF4A2 was bound to pre-miR-92a in the first RNA pulldown experiment and therefore was selected as a candidate for the regulation of the maturation of pre-miR-92a. While in the RIPs, eIF4A2 did not bind to pri-miR-17-92 or pre-miR-92a, an interaction with the mature miRs of miR-17-92a was observed. These findings confirm the correctness of the RIP, because eIF4A2 have been described to interact with mature miRs in order to mediate the binding of miRs to their target mRNAs [157]. However, it appears as if the mature miRs interacted with all tested proteins. It was not possible to identify a protein that is not bound by any miRs and represents a stable negative control. For example, Filamin A was also tested in the first round of RIP experiments. However, the binding to mature miRs to Filamin A was not reproducible. In contrast to Filamin A, the binding of mature miRs to eIF4A2, SND1 and Myoferlin was much more reliable.

V.3.1. Half-maximal inhibition of eIF4A2 does not affect the biogenesis of the miR-17-92a cluster

Although no interaction between eIF4A2 and pre-miR-92a could be observed in the RIP, we were still interested in elucidating the influence of eIF4A2 silencing on the expression of the miR-17-92a cluster members. Four different siRNAs directed against eIF4A2 were tested. While other siRNAs, for example against SND1, caused a down regulation of more than 90%, the tested siRNAs targeting eIF4A2 only reduced the expression of eIF4A2 mRNA to about 45% compared to the siControl treatment. This can be due to a lack of

affinity of the siRNA to the target mRNA but more likely, this is caused by a toxic effect of eIF4A2 silencing on the cells. This underlines the essential function of eIF4A2 in endothelial cells. For the results obtained with this siRNA, it can only be concluded that the half maximal inhibition of eIF4A2 does not affect the regulation of the biogenesis of the miR-17-92a cluster. Taken together, eIF4A2 is rather a general factor interacting with members of the miR-17-92a family than a specific regulator of individual cluster members.

V.4. Myoferlin – a versatile regulator of endothelial miRs

Myoferlin is a member of the Ferlin family that is highly conserved among eukaryotes. The family members (in humans: Otoferlin, Dysferlin, Myoferlin, Fer1L4, Fer1L5, and Fer1L6) share a structure of several C2 domains as well as a C-terminal transmembrane domain [158]. Ferlins have been described to regulated membrane fusion events in response to Ca^{2+} influx. Myoferlin is increased upon muscle damage [159] and mediates muscle regeneration [160]. It has been hypothesized that upon injury of the cell membrane Myoferlin senses the calcium influx and induces caveolae dependent endocytosis which leads to patching of the injured site [141]. Moreover, depletion of Myoferlin in human breast cancer cells induced the stabilization of phosphorylated epidermal growth factor receptor (EGFR), thereby impairing cell migration and epithelial-to-mesenchymal-transition [161]. It is a transmembrane protein that is highly expressed in skeletal and cardiac muscles [139]. In mice, the knockout of two Ferlins, Dysferlin and Myoferlin, at the same time induced muscular dystrophy as well as misaligned transverse tubules (T-Tubules) in skeletal muscle indicating a role for Dysferlin and Myoferlin in the biogenesis and remodeling of the sarcotubular system of the human muscle [159]. Interestingly, Myoferlin is of crucial importance for endothelial cell function. Myoferlin regulates angiogenic sprouting since it is essential for the expression of VEGFR2 [140]. Silencing of Myoferlin in mouse tissue reduced VEGFR2 expression and attenuated angiogenesis [141]. Since members of the miR-17-92a cluster can function as both pro- and antiangiogenic factors, it is conceivable that they are differentially regulated by a

factor that is also implicated in angiogenesis. Myoferlin could be specifically detected to be bound to pre-miR-92a in all four RNA pulldown experiments. The interaction of Myoferlin with pre-miR-92a could be confirmed via RIP. As Myoferlin is known to be critically involved in endothelial cell function, also other endothelial miRs, namely miR-92a, miR-126 and miR-145, were tested and could be identified to interact with Myoferlin in the RIPs. This is the first time an interaction of Myoferlin with miRs is described.

However, it is also possible that Myoferlin is binding to pre-miR-92a and the tested mature miRs in an indirect manner. EHD1 and EHD2, two endocytic recycling proteins, are already described interaction partners of Myoferlin [162]. Therefore, it is also conceivable that these proteins are mediating an indirect binding of Myoferlin to pre-miR-92a. In the mass spectrometry analysis of the RNA pulldown, EHD1 was detected in two of four experiments but it was bound to both the control sequence and pre-miR-92a. EHD2 was slightly enriched to pre-miR-92a in three of four experiments. The interaction of pre-miR-92a with EHD2 was further confirmed by RIP (data not shown). Although neither EHD2 nor Myoferlin have been described so far to bind miRs, it is still conceivable that both are potential interaction partners of miR-92a. Given that the influence of Myoferlin on the miR-17-92a cluster has been assessed and gave strong evidence for a role of Myoferlin in regulating endothelial miRs, in the course of this study EHD2 was not further investigated. To clarify whether Myoferlin directly interacts with pre-miR-92a, an electric mobility shift assay (EMSA) with recombinant Myoferlin and pre-miR-92a should be performed and compared to mobility of pre-miR-92a and EHD2.

V.4.1. Silencing of Myoferlin does not regulate the maturation of the members of the miR-17-92a cluster

Since the aim of this study was the identification of potential regulators of miR-92a biogenesis, that act on the level of pre-miR-92a, the implication of Myoferlin on the maturation miR-92a was assessed. It turned out that siRNA mediated silencing of Myoferlin did not affect the levels of mature miR-92a and the other tested members of the cluster (miR-17, miR-18a, miR-19a, and miR-20a). This shows that silencing of

Myoferlin does not accelerate or impair the turnover of pre-miR-92a to mature-miR-92a. Therefore, Myoferlin appears not to be a transcriptional regulator of pri-miR-17-92. When Myoferlin does not regulate the processing of miR-17-92a, it should be further investigated what else might be the biological consequence of Myoferlin binding to pre-miR-92a and mature miR-92a.

V.4.2. Silencing of Myoferlin alters the export of miR-92a mediated by microvesicles or exosomes, while miR-145 was not affected

V.4.2.1. Silencing of Myoferlin increases the relative number of exosomes

Based on the publications describing a role for Myoferlin in regulating the composition of the plasma membrane and the patching of injured sites by caveolae [141] as well as on the finding that Myoferlin is able to interact with the mature miR-92a, we wanted to investigate whether Myoferlin might also be involved in the formation of vesicles that are shed by endothelial cells. As recently described by Hergenreider et al. endothelial cells selectively shuttle miRs via vesicles to recipient cells. For example, miR-143 and miR-145 are expressed in endothelial cells under conditions of laminar flow and guided to SMCs where they induce the atheroprotective phenotype [65]. Nanoparticle tracking analysis revealed that silencing of Myoferlin did not change the total number of particles shed by endothelial cells. However, siMyof treated cells shed relatively fewer particles of a diameter of less than 100 nm than siCo treated cells, indicating that silencing of Myoferlin impairs the release of exosomes. This gives a hint toward a role for Myoferlin in mediating the release of exosomes. It is conceivable that Myoferlin either supports the function of Rab27a/b, two proteins described to mediate exosome release [163], or it can be speculated that Myoferlin itself has similar functions as Rab27a/b since both share structural features as the Calcium sensing domain as well as the transmembrane domain. It would be interesting to analyze whether silencing of Rab27a/b has similar effect as silencing of Myoferlin. To further discriminate which kind of vesicles are shed by the cells

in the presence or absence of Myoferlin, the cells could be treated with substances that are known to block the export of certain vesicle subclasses. Primaquine, e.g. inhibits the formation of transport vesicles by the Golgi apparatus [164].

V.4.2.2. MiR-92a levels in microvesicles or exosomes are increased after silencing of Myoferlin

MiRs can be secreted by cells via different mechanisms: First, miRs can be packed into exosomes, shedding vesicles or apoptotic bodies [165]. Second, miRs have been found to be bound to lipoproteins such as the high-density lipoprotein (HDL) [166]. Third, miRs are described to be extracellular bound to RNA binding proteins, such as Ago2 or NPM1 [3, 167]. Arroyo et al. showed that among other miRs, miR-92a is bound to Ago2 when exported into the circulation [3].

To elucidate whether Myoferlin plays a role in the selection of certain miRs for the export via microvesicles, the presence of miR-92a in the supernatant of endothelial cells was analyzed. In the absence of Myoferlin an increase of miR-92a in the supernatant was observed. Moreover, after silencing of Myoferlin, RNA was isolated from the pelleted microvesicles and exosomes and qRT-PCR analysis revealed that miR-92a levels were increased there as well. This indicates that the export of miR-92a in microvesicles or in exosomes is increased when Myoferlin is silenced. Since the extracellular levels of miR-150 were not altered in the absence of Myoferlin, and miR-145 was only slightly increased in the pelleted supernatant, the effect of Myoferlin on miR-92a levels appears to be sequence specific. To investigate to which degree miR-92a is bound to Ago2 or packed into microvesicles or exosomes, further studies regarding the origin of miR-92a in the supernatant should be assessed, including the digest of RNA and the lysis of vesicles by detergents. If miR-92a is protected by membrane enclosed particles, the RNA digest should not affect levels of miR-92a but the detergents should reduce the levels of extracellular miR-92a, because the membrane enclosed particles are destroyed and miR-92a is present in the supernatant without protection.

When silencing of Myoferlin increases the export of miR-92a one would expect a decrease of intracellular miR-92a levels. The fact that the cellular levels were not altered might be explained by a compensation of the loss of miR-92a after 72 hrs. Of note, it is important to be aware that extracellular levels cannot be directly compared to intracellular levels due to the different amounts of RNA that were used for the reverse transcription of RNA from cells and RNA from the supernatant or the pelleted microvesicles: While the RNA from the cells was diluted, the complete RNA isolated from 200 μ l supernatant or the complete pelleted supernatant was used for the reverse transcription.

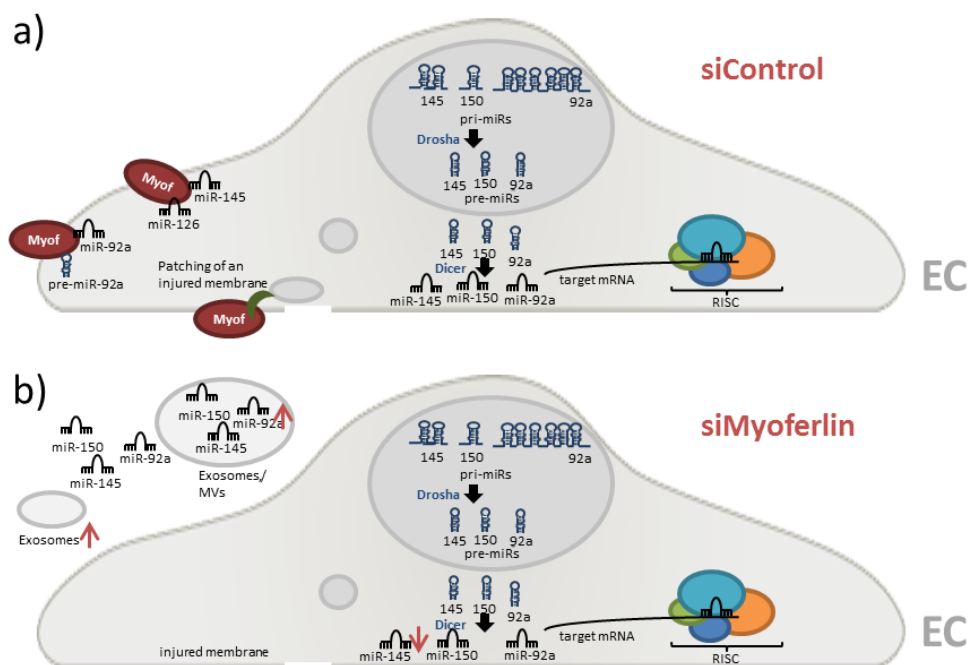


Figure 35: Schematic summary of the effects of silencing of Myoferlin on miR-92a, miR-145 and miR-150. a) Myoferlin mediates the patching of injured membrane sites and interacts with pre-miR-92a and the mature miRNAs miR-92a, miR-145 and miR-150, b) Silencing of Myoferlin decreased cellular levels of miR-145 and increases the number of miR-92a in the pelleted supernatant. Moreover, siMyof elevates the relative numbers of exosomes. EC= Endothelial cell, MV= microvesicles.

V.4.2.3. Myoferlin also interacts with mature miR-145

Hergenreider et al. recently showed that endothelial cells release miR-143/145 packed in vesicles in order to communicate with adjacent smooth muscle cells (SMCs) under conditions of atheroprotective laminar shear stress [65]. Thereby, miR-143/145 induces an atheroprotective phenotype in SMCs [65]. As previously discussed our data suggest an impact of Myoferlin on the generation of these miR-carrying vesicles. Therefore, it was also analyzed whether miR-145 is also bound by Myoferlin in RIP. Indeed, an interaction of miR-145 with Myoferlin could be detected to a similar extent as the interaction with mature miR-92a with Myoferlin while in endothelial cells, miR-145 is expressed at much lower levels than miR-92a but in the RIPs it was detected at similar levels like miR-92a. The levels of miR-145 in the supernatant or the pelleted microvesicles and exosomes were not affected by silencing of Myoferlin.

V.4.3. Silencing of Myoferlin alters the genesis and localization of miR-126

V.4.3.1. MiR-126 interacts with and its production is regulated by Myoferlin

The high levels of interaction of the endothelial enriched miR-126 with pre-miR-92a in the RIP together with the observed significant increase of mature miR-126 levels upon silencing of Myoferlin raised the question whether miR-126 maturation might be enhanced by silencing of Myoferlin. Indeed, in the absence of Myoferlin, both pri-miR-126 and pre-miR-126 levels were permanently and significantly decreased. Moreover, we could prove via RIP that Myoferlin also interacts with pri-miR-126. Based on these data, Myoferlin could function as a negative regulator of the processing of pri-miR-126 to pre-miR-126 and pre-miR-126 to mature miR-126 or as a positive effector of the transcription of pri-miR-126.

It would be interesting to investigate at which site Myoferlin interacts with the miRs. Therefore, a truncated version, lacking different domains of Myoferlin, should be tested regarding their ability to bind to the miRs, e.g. by EMSA. Maybe different sites are interacting with different miRs and therefore enable the differential effects of Myoferlin on endothelial miRs. Moreover, it would be interesting to elucidate how Myoferlin, as a transmembrane protein, is able to interact with nuclear located pri-miR-17-92 and pri-miR-126. It is not clear whether Myoferlin can translocate into the nucleus or whether pri-miR-17-92 and pri-miR-126 are able to leave the nucleus. Since the cytoplasmic factor SND1 also appeared to interact with pri-miR-17-92 in the RIPs and it has been described that upon virus infection pri-miRs can be processed in the cytoplasm [168], it is conceivable that the interaction between Myoferlin and the tested pri-miRs takes place in the cytoplasm.

V.4.3.2. Silencing of Myoferlin increases the levels of miR-126 in the supernatant of cells

Upon silencing of Myoferlin, in addition to the increase of miR-126 in the cells, also an increase in miR-126 levels in the supernatant, but not in the pelleted microvesicles and exosomes could be observed. This indicates that, in contrast to miR-92a, silencing of Myoferlin does not facilitate the export of miR-126 in microvesicles or exosomes but rather increases the protein bound miR-126 levels in the supernatant. Since the levels of miR-126 were not affected by silencing of Myoferlin in the pelleted supernatant, Myoferlin does not appear to regulate the loading of miR-126 into microvesicles. Both, extracellular miR-126 molecules that are bound by proteins and those that are protected by microvesicles have been described in literature. A recently published finding shows that miR-126 is exported from endothelial cells in a vesicle independent way and guided to SMCs while being bound to Ago2 [62]. In contrast to these observations, there are also publications indicating the presence of miR-126 in plasma microvesicles [169]. For example, it has been shown that in patients suffering from Diabetes Mellitus Type 2 miR-126 levels in the plasma are reduced, thereby making miR-126 a biomarker for Diabetes [169]. Since silencing of Myoferlin did not change the levels of miR-126 in microvesicles,

Myoferlin does not appear to account for the differential export of miR-126 into the circulation upon Diabetes. It could not be tested whether Myoferlin regulates the export of miR-126 in apoptotic bodies, since these particles are lost during the pre-clearing step (apoptotic bodies precipitate with 2,000 g, pre-clearing was performed with 4,000 x g) [170]. Interestingly, injured sites of a plasma membrane have been shown not to be efficiently patched in the absence of Myoferlin [141], thereby causing a leaky membrane that might account for the increase in extracellular miR levels. In this case, all tested miRs would be elevated extracellularly in the absence of Myoferlin. Since miR-150 is not elevated in the supernatant of cells after silencing of Myoferlin, inefficient patching of injured membrane sites does not appear to account for the effects observed with extracellular miRs. Based on the high levels of miR-92a and miR-126 bound to Myoferlin observed in the RIP, it is likely that Myoferlin normally binds these miRs and thereby impairs their export. In the absence of Myoferlin, miR-92a and miR-126 are free to enter export pathways: miR-92a molecules are increasingly loaded into microvesicles, while miR-126 levels are increasing only in the supernatant, not in the pelleted microvesicles, which indicates that miR-126 is exported in a microvesicle- and exosomes-independent manner. The versatile effects of silencing of Myoferlin on the tested miRs might also reflect secondary effects caused by a major restructuring of the membrane organization.

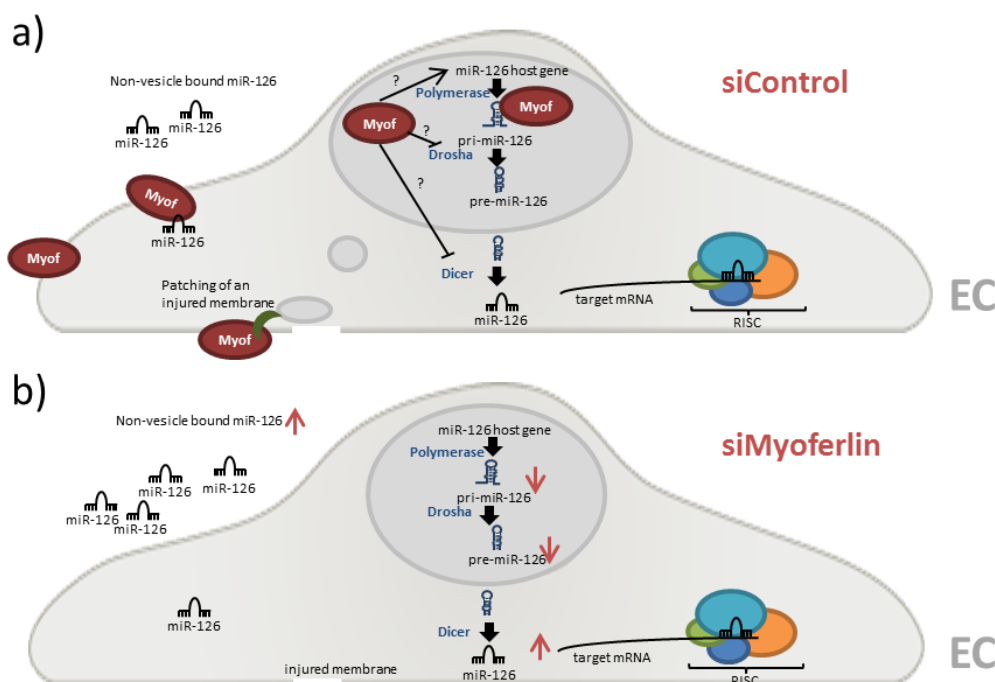


Figure 36: Schematic summary of the effects of silencing of Myoferlin on miR-126. a) Myoferlin mediates the patching of injured membrane sites and interacts with pri-miR-126 and mature miR-126, b) In the cells, silencing of Myoferlin decreased the levels of pri-miR-126 and pre-miR-126, while mature miR-126 levels were elevated. Extracellularly, an increase of miR-126 in the supernatant but not in the microvesicles or exosomes was observed. EC: endothelial cell, Myof: Myoferlin.

Taken together, Myoferlin, a known regulator of angiogenesis, also plays a role in regulating the endothelial miRs miR-92a and miR-126. On the one hand, Myoferlin is implicated in the export of these miRs: Silencing of Myoferlin elevated the extracellular levels of miR-92a in the microvesicles and exosomes as well as the extracellular levels of microvesicle- and exosome-independent miR-126. On the other hand, silencing of Myoferlin induces an increase in the maturation of miR-126 and therefore exhibits a possible new role as either a transcriptional or a posttranscriptional regulator of the biogenesis of miR-126.

VI. Conclusion

Previous studies have shown a differential regulation of the mature members of miR-17-92a and have been pointing towards a posttranscriptional regulation of this family. Pre-miR-92a interacting proteins that might potentially act as posttranscriptional regulators of miR-17-92a processing were identified by RNA pulldown and subsequent mass spectrometry. Three candidates were selected for further analysis:

SND1, a component of RISC and regulator of edited miRs was confirmed by RNA immunoprecipitation to be interacting with pre-miR-92a. Additionally an interaction with the mature members of the miR-17-92a cluster was observed. While under basal conditions siRNA mediated silencing of SND1 did not change the levels of pri-miR, pre-miRs or mature miRs of the miR-17-92a cluster, under hypoxia mimicking conditions the maturation of these miRs was significantly enhanced. Editing of miRs under hypoxia mimicking conditions and their degradation by SND1 did not account for this observation as it was shown by deep sequencing and ADAR1 silencing. Further investigation will elucidate whether SND1 functions for example by sorting miRs into stress granules upon a hypoxic stimulus, thereby preventing miR processing.

The second candidate, eIF4A2, an RNA helicase of the DEAD box family, could not be confirmed to interact with pre-miRs, but with the mature members of the miR-17-92a cluster. Silencing of eIF4A2 under basal conditions did not affect the maturation of the miR-17-92a family. Therefore, eIF4A2 does not appear to act as a regulator of the miR-17-92a cluster but is rather a general RNA binding protein.

Finally, a role of Myoferlin in regulating endothelial miRs has been described for the first time. Myoferlin is of known importance for angiogenesis as it regulates VEGFR2 and also appears to regulate endothelial miRs. Myoferlin is involved appears to be the export of miR-92a in microvesicles and the export of miR-126 in a vesicle-independent way. Additionally, Myoferlin was shown to regulate the generation of miR-126.

Together, these findings represent new aspects of the regulation of endothelial miRs, in particular of members of miR-17-92a and of miR-126. This contributes to the

understanding of processes that are involved in the fine tuning of pro- and anti-angiogenic factors.

VII. Zusammenfassung

MicroRNAs (miRs) sind kurze, einzelsträngige RNA Moleküle, die komplementär an den 3'UTR von Ziel-mRNAs binden und dadurch deren Translation hemmen oder die Degradierung der mRNA induzieren. Eine miR kann mehrere mRNAs anhand der Seed-Sequenz erkennen und daran binden. MiRs sind sehr wirksame Genregulatoren, die auch oftmals mehrere mRNAs von Proteinen mit ähnlicher Funktion binden können. Die miR-17-92a Familie umfasst sieben mature Mitglieder (miR-17-5p, miR-17-3p, miR-18a, miR-19a, miR-20a, miR-19b, miR-92a) und ist hoch exprimiert in Endothelzellen. Der miR-17-92a Cluster wurde zuerst im Kontext von Tumorentstehung beschrieben, doch inzwischen sind eine Vielzahl zusätzlicher Funktionen dieser miR Familie beschrieben worden. In Endothelzellen üben einige der Mitglieder des Clusters, z. B. miR-92a, eine antiangiogene Wirkung aus [96], indem sie an die mRNA von Angiogenese fördernden Faktoren binden. Es handelt sich bei miR-17-92a um einen polycistronischen Cluster, da alle Mitglieder unter der Kontrolle desselben Promoters stehen und als primäres Transkript (pri-miR) abgelesen werden. Dieses wird dann zuerst von der Endoribonuklease Drosha in die einzelnen Precursor-miRs (pre-miRs) geschnitten, woraus dann von Dicer, einer zweiten Endoribonuklease, die maturen einzelsträngigen miRs herausgeschnitten werden. Obwohl alle Mitglieder des miR-17-92a Clusters von einem Primärtranskript abstammen, wurde in vorangehenden Studien beobachtet, dass die individuellen maturen miRs differenziell exprimiert werden, so zum Beispiel während der endothelialen Differenzierung von murinen embryonalen Stammzellen oder nach Hinterlaufischämie in Mäusen. Zusammen mit der Veröffentlichung, dass hnRNP A1 an die Hairpin-Struktur von miR-18a innerhalb des Primärtranskripts bindet und damit die Maturierung von miR-18a erleichtert [38], deuten diese Beobachtungen darauf hin, dass die miR-17-92a Familie nicht nur auf Ebene der Transkription, sondern auch posttranskriptionell reguliert wird.

Identifizierung von pre-miR-92a bindenden Proteinen

Um Faktoren zu identifizieren, die an pre-miR-92a binden und somit möglicherweise posttranskriptionelle Regulatoren darstellen, wurde ein RNA pulldown mit in vitro transkribierten pre-miR-92a Molekülen etabliert. Als Negativkontrolle diente die Sequenz von pre-miR-92a in reverser Orientierung. Diese RNA Sequenzen wurden an Agarosebeads immobilisiert und mit nativen Proteinen aus Endothelzellen inkubiert. An pre-miR-92a gebundene Proteine wurden durch Zugabe von RNasen eluiert und anschließend mittels Massenspektrometrie analysiert. In vier Experimenten wurden insgesamt 962 Proteine identifiziert. Aus den 791 Proteinen, die an pre-miR-92a gebunden haben, aber nicht oder nur sehr schwach an die Kontrollsequenz, wurden drei Kandidaten zur weiteren Charakterisierung selektiert: SND1 (Staphylococcal nuclease domain containing protein 1) wurde ausgewählt, da es bereits beschrieben ist an RNA zu binden und außerdem im RISC nachgewiesen wurde [133]. Zudem vermittelt SND1 den Abbau von editierten Primärtranskripten und pre-miRs [134] und ist, ebenso wie die Mitglieder des miR-17-92a Clusters, an der Tumorentstehung beteiligt [149]. Bei dem zweiten Kandidaten, eIF4A2 (eukaryotischer Initiationsfaktor 4A2), handelt es sich um eine DEAD-Box Helikase, die unter anderem an der Entwindung von doppelsträngigen RNA Strukturen beteiligt ist [135]. Außerdem wurde Myoferlin, ein Transmembranprotein, das Angiogenese und Endozytose von Vesikeln reguliert [141], ausgewählt. Myoferlin wurde zuvor noch nicht als RNA bindendes Protein beschrieben, sodass wir erst durch statistische Auswertung aller vier RNA Pulldown Experimente Myoferlin ausgewählt haben. In allen vier Experimenten fand eine Interaktion von Myoferlin mit pre-miR-92a statt, während keine Interaktion von Myoferlin mit der Kontrollsequenz in drei von vier Experimenten gemessen wurde.

Die im RNA Pulldown detektierte Bindung dieser Proteine an pre-miR-92a sollte mittels RNA Immunopräzipitation (RIP) bestätigt werden. Während die Interaktion von pre-miR-92a mit SND1 und Myoferlin erfolgreich durch RIP bewiesen wurde, konnte keine Interaktion von pre-miR-92a mit eIF4A2 gemessen werden. Allerdings waren auch die Interaktionen mit SND1 und Myoferlin mit pre-miR-92a relativ gering, was einerseits am raschen Turnover der pre-miR-92a liegen kann, andererseits durch kompetitive Bindung anderer Faktoren, die eine Bindung an pre-miR-92a verhindert, erklärt werden kann.

Vergleichsweise hohe Werte wurden für die Bindung von maturen Mitgliedern der miR-17-92a Familie an SND1, eIF4A2 und Myoferlin bestimmt. Ago2 diene als Positivkontrolle für die RIP und wies, gemäß seiner Rolle als Bestandteil des RISC [133], ebenfalls hohe Werte von bindenden maturen miRs auf. Anschließend sollte der Einfluss von SND1, eIF4A2 und Myoferlin auf den miR-17-92a Cluster untersucht werden. Dafür wurde die Expression mit spezifischen siRNAs unterdrückt.

Die Hemmung der SND1 Expression verstärkt die Prozessierung des miR-17-92a Clusters unter hypoxischen Bedingungen

Transfektion von Endothelzellen mit siRNA gegen SND1 (siSND1) führte zu einer signifikanten Reduktion der Expression, die auch nach 96 Stunden noch stabil war. Um zu untersuchen, ob die Abwesenheit von SND1 die Biogenese der miR-17-92a Familie beeinflusst, wurden das Primärtranskript, die pre-miRs sowie die maturen Familienmitglieder mittels qRT-PCR bestimmt. Unter basalen Bedingungen hatte siSND1 keinen Effekt auf die pri-miR-17-92, sowie die pre-miRs und die maturen miRs. Da frühere Studien gezeigt haben, dass die Mitglieder des miR-17-92a Clusters vor allem unter Sauerstoffmangel differenziell reguliert werden, wie z.B. im Hinterlaufschämiemodell oder nach Myokardinfarkt [109], wurde der Effekt von siSND1 unter hypoxischen Bedingungen untersucht. Um die Effekte von Hypoxie auf die Zellen zu imitieren, wurden diese mit Deferoxamin (DFO) behandelt. Im Vergleich zu basalen Bedingungen, wurde nach DFO Behandlung ein Anstieg des Primärtranskripts, sowie eine signifikante Erhöhung von pre-miR-17, pre-miR-20a und pre-miR-92a gemessen, während die maturen Mitglieder nicht beeinflusst wurden. Wenn die Zellen zusätzlich zur DFO Behandlung noch mit siSND1 transfiziert wurden, wurde der Effekt von DFO teilweise wieder aufgehoben: Die Werte des Primärtranskripts sowie der pre-miRs fielen wieder ab, während die maturen miR-17-92a Mitglieder miR-17, miR-18a, miR-19a und miR-20a signifikant anstiegen. Dies deutet darauf hin, dass die Abwesenheit von SND1 unter hypoxischen Bedingungen zu einer erhöhten Prozessierungsrate von pre-miRs zu maturen miRs führt. Dies wird besonders deutlich, wenn man das Verhältnis von pre-miRs zu mature miRs betrachtet: Der errechnete Wert fällt für jedes miR-17-92a Mitglied deutlich auf unter 1 ab, was eine relative Erhöhung der maturen miRs und einen erhöhten turnover von pre-miR zu maturer miR anzeigt.

Pri-miR-17-92 und die pre-miRs des Clusters werden unter hypoxischen Bedingungen nicht verstärkt editiert

Da bereits gezeigt worden ist, dass SND1 editierte pri-miRs und pre-miRs degradiert [134], wurde als nächstes untersucht, ob die beobachteten Effekte darauf beruhen, dass die Abwesenheit von SND1 den Abbau solcher miRs verhindern, die eventuell unter hypoxischen Bedingungen editiert werden. Eine weitere Studie, die diese Hypothese untermauert, hat gezeigt, dass Hypoxie die Editierung von miRs erhöht [143]. Um zu überprüfen, ob nach DFO Behandlung in Abwesenheit von SND1 die pri-miR und die pre-miRs des miR-17-92a Clusters stärker editiert vorliegt als unter basalen Bedingungen in Anwesenheit von SND1, wurden das Primärtranskript und die pre-miRs mittels Deep Sequencing analysiert. Tatsächlich konnte kein Anstieg der Anzahl der Editierungs-Ereignisse unter hypoxischen Bedingungen in Abwesenheit von SND1 beobachtet werden. Auch die Herunterregulation des Adenosin-zu-Inosin-Editierungsenzyms ADAR1 mittels siRNA Transfektion unter hypoxischen Bedingungen konnte nicht die Effekte von siSND1 unter Hypoxie-imitierenden Bedingungen rekapitulieren. Es kann allerdings nicht ausgeschlossen werden, dass in ischämischem Gewebe die Editierungs-Ereignisse von pri-miR-17-92 und der pre-miRs ansteigen, oder auch, dass unter den beobachteten Bedingungen editierte miRs durch einen anderen Faktor als SND1 abgebaut werden.

Herunterregulation von eIF4A2 beeinflusst nicht die Biogenese der miR-17-92a Familie

Da eine Interaktion von eIF4A2 mit den maturen Mitgliedern des miR-17-92a Clusters detektiert wurde, untersuchten wir, ob Herunterregulation von eIF4A2 einen Einfluss auf diese miR Familie hat. Durch siRNA Transfektion gegen eIF4A2 konnte lediglich eine Reduktion der Expression um ca. 54% erzielt werden. Pri-miR-17-92, die pre-miRs, sowie die maturen miRs wurden dadurch nicht signifikant verändert.

Hemmung der Expression von Myoferlin reguliert die Entstehung von miR-126

Wir konnten zeigen, dass Myoferlin nicht nur an die pre-miR-92a und die mature miR-92a bindet, sondern zudem auch mit den endothelialen miRs miR-126 und miR-145 interagiert. Die Hemmung der Myoferlin Expression durch siRNA Transfektion hatte keinen Einfluss auf die Mitglieder des miR-17-92a Clusters, führte aber zu einem Anstieg von miR-126 und zu einem Abfall von miR-145. Deshalb wurde untersucht, ob Myoferlin

einen Einfluss auf die Biogenese von miR-126 hat. Tatsächlich konnte nach Transfektion mit siRNA gegen Myoferlin eine signifikante Herunterregulation von pri-miR-126 und pre-miR-126 gemessen werden. Außerdem konnte gezeigt werden, dass Myoferlin auch mit pri-miR-126 interagiert. Ob Myoferlin als Promoteraktivator von miR-126, während der Transkription oder erst posttranskriptionell Einfluss nimmt bleibt Gegenstand möglicher zukünftiger Studien.

Herunterregulation von Myoferlin verändert den Export von miR-92a und miR-126

Da Myoferlin zwar mit pre-miR-92a und der maturen miR-92a interagiert, aber keinen Einfluss auf die Entstehung von miR-92a zu haben scheint, wurden der Gehalt an miR-92a und anderer miRs im Überstand sowie im pelletierten Überstand gemessen. Dadurch sollte untersucht werden, ob Myoferlin noch eine andere biologische Funktion in Bezug auf miR-92a besitzt. Dies ergab, dass in Abwesenheit von Myoferlin miR-92a wahrscheinlich vermehrt in Microvesikeln exportiert wird, während miR-126 nur im Überstand und nicht in der Microvesikelfraktion angereichert war. Es scheint daher, dass Myoferlin nicht den Export von miR-126 in Vesikeln, sondern eher die extrazelluläre Lokalisation von proteingebundener miR-126 reguliert. Außerdem wurde gezeigt, dass sich in Abwesenheit von Myoferlin zwar nicht die absolute Anzahl der extrazellulären Vesikel verändert, aber die relative Anzahl von Exosomen (< 100 nm) zunimmt.

Zusammenfassend konnten mit dieser Arbeit pre-miR-92a bindende Proteine identifiziert werden und diese Bindung wurde für SND1 und Myoferlin erfolgreich bestätigt. Während eIF4A2 in der RIP ausschließlich an die maturen Mitglieder des miR-17-92a Clusters gebunden hat und keinen Einfluss auf die Biogenese dieser miRs zu haben scheint, konnten für SND1 und Myoferlin interessante neue Funktionen beschrieben werden. SND1 scheint hauptsächlich unter hypoxischen Bedingungen die Maturierung der miR-17-92a Familie zu beeinflussen. Myoferlin scheint aufgrund der Lokalisation in der Zellmembran vor allem am Export von miR-92a und miR-126 beteiligt zu sein und zusätzlich die Biogenese von miR-126 zu beeinflussen. Zusätzlich zu der beschriebenen Rolle von Myoferlin für die Angiogenese von Endothelzellen [140], konnte hiermit eine neue Funktion von Myoferlin als Regulator von Angiogenese regulierenden miRs gezeigt werden.

VIII. References

1. Elgar, G. and T. Vavouri, *Tuning in to the signals: noncoding sequence conservation in vertebrate genomes*. Trends Genet, 2008. **24**(7): p. 344-52.
2. Ohno, S., *So much "junk" DNA in our genome*. Brookhaven Symp Biol, 1972. **23**: p. 366-70.
3. Arroyo, J.D., et al., *Argonaute2 complexes carry a population of circulating microRNAs independent of vesicles in human plasma*. Proc Natl Acad Sci U S A, 2011. **108**(12): p. 5003-8.
4. Mariner, P.D., et al., *Human Alu RNA is a modular transacting repressor of mRNA transcription during heat shock*. Mol Cell, 2008. **29**(4): p. 499-509.
5. Beltran, M., et al., *A natural antisense transcript regulates Zeb2/Sip1 gene expression during Snail1-induced epithelial-mesenchymal transition*. Genes Dev, 2008. **22**(6): p. 756-69.
6. Peffault de Latour, R., et al., *Age-adjusted recipient pretransplantation telomere length and treatment-related mortality after hematopoietic stem cell transplantation*. Blood, 2012. **120**(16): p. 3353-9.
7. Batista, P.J., et al., *PRG-1 and 21U-RNAs interact to form the piRNA complex required for fertility in C. elegans*. Mol Cell, 2008. **31**(1): p. 67-78.
8. Aravin, A.A., et al., *Developmentally regulated piRNA clusters implicate MILI in transposon control*. Science, 2007. **316**(5825): p. 744-7.
9. Lee, R.C., R.L. Feinbaum, and V. Ambros, *The C. elegans heterochronic gene lin-4 encodes small RNAs with antisense complementarity to lin-14*. Cell, 1993. **75**(5): p. 843-54.
10. van Rooij, E., *The art of microRNA research*. Circ Res, 2011. **108**(2): p. 219-34.
11. Bartel, D.P., *MicroRNAs: genomics, biogenesis, mechanism, and function*. Cell, 2004. **116**(2): p. 281-97.
12. Wang, D., et al., *Quantitative functions of Argonaute proteins in mammalian development*. Genes Dev, 2012. **26**(7): p. 693-704.
13. Winter, J., et al., *Many roads to maturity: microRNA biogenesis pathways and their regulation*. Nat Cell Biol, 2009. **11**(3): p. 228-34.
14. Ruby, J.G., C.H. Jan, and D.P. Bartel, *Intronic microRNA precursors that bypass Drosha processing*. Nature, 2007. **448**(7149): p. 83-6.
15. Jan, C.H., et al., *Formation, regulation and evolution of Caenorhabditis elegans 3'UTRs*. Nature, 2011. **469**(7328): p. 97-101.
16. Ladewig, E., et al., *Discovery of hundreds of mirtrons in mouse and human small RNA data*. Genome Res, 2012. **22**(9): p. 1634-45.
17. Cheloufi, S., et al., *A dicer-independent miRNA biogenesis pathway that requires Ago catalysis*. Nature, 2010. **465**(7298): p. 584-9.
18. Fabian, M.R., N. Sonenberg, and W. Filipowicz, *Regulation of mRNA translation and stability by microRNAs*. Annu Rev Biochem, 2010. **79**: p. 351-79.
19. Bronkhorst, A.W., P. Miesen, and R.P. van Rij, *Small RNAs tackle large viruses: RNA interference-based antiviral defense against DNA viruses in insects*. Fly (Austin), 2013. **7**(4).

20. de Fougères, A., et al., *Interfering with disease: a progress report on siRNA-based therapeutics*. Nat Rev Drug Discov, 2007. **6**(6): p. 443-53.
21. Saj, A. and E.C. Lai, *Control of microRNA biogenesis and transcription by cell signaling pathways*. Curr Opin Genet Dev, 2011. **21**(4): p. 504-10.
22. Vrba, L., et al., *miRNA gene promoters are frequent targets of aberrant DNA methylation in human breast cancer*. PLoS One, 2013. **8**(1): p. e54398.
23. Krol, J., I. Loedige, and W. Filipowicz, *The widespread regulation of microRNA biogenesis, function and decay*. Nat Rev Genet, 2010. **11**(9): p. 597-610.
24. Fukuda, T., et al., *DEAD-box RNA helicase subunits of the Drosha complex are required for processing of rRNA and a subset of microRNAs*. Nat Cell Biol, 2007. **9**(5): p. 604-11.
25. Fuller-Pace, F.V., *DExD/H box RNA helicases: multifunctional proteins with important roles in transcriptional regulation*. Nucleic Acids Res, 2006. **34**(15): p. 4206-15.
26. Davis, B.N., et al., *SMAD proteins control DROSHA-mediated microRNA maturation*. Nature, 2008. **454**(7200): p. 56-61.
27. Kang, H., et al., *Bone morphogenetic protein 4 promotes vascular smooth muscle contractility by activating microRNA-21 (miR-21), which down-regulates expression of family of dedicator of cytokinesis (DOCK) proteins*. J Biol Chem, 2012. **287**(6): p. 3976-86.
28. Suzuki, H.I., et al., *Modulation of microRNA processing by p53*. Nature, 2009. **460**(7254): p. 529-33.
29. Venkitaraman, A.R., *Cancer susceptibility and the functions of BRCA1 and BRCA2*. Cell, 2002. **108**(2): p. 171-82.
30. Kawai, S. and A. Amano, *BRCA1 regulates microRNA biogenesis via the DROSHA microprocessor complex*. J Cell Biol, 2012. **197**(2): p. 201-8.
31. Dubrovskaya, A., et al., *TGFbeta1/Smad3 counteracts BRCA1-dependent repair of DNA damage*. Oncogene, 2005. **24**(14): p. 2289-97.
32. Zhang, H., et al., *BRCA1 physically associates with p53 and stimulates its transcriptional activity*. Oncogene, 1998. **16**(13): p. 1713-21.
33. Nicastro, G., et al., *Noncanonical G recognition mediates KSRP regulation of let-7 biogenesis*. Nat Struct Mol Biol, 2012. **19**(12): p. 1282-6.
34. Guil, S. and J.F. Caceres, *The multifunctional RNA-binding protein hnRNP A1 is required for processing of miR-18a*. Nat Struct Mol Biol, 2007. **14**(7): p. 591-6.
35. Michlewski, G., et al., *Posttranscriptional regulation of miRNAs harboring conserved terminal loops*. Mol Cell, 2008. **32**(3): p. 383-93.
36. Trabucchi, M., et al., *KSRP promotes the maturation of a group of miRNA precursors*. Adv Exp Med Biol, 2010. **700**: p. 36-42.
37. Trabucchi, M., et al., *The RNA-binding protein KSRP promotes the biogenesis of a subset of microRNAs*. Nature, 2009. **459**(7249): p. 1010-4.
38. Michlewski, G., S. Guil, and J.F. Caceres, *Stimulation of pri-miR-18a Processing by hnRNP A1*. Adv Exp Med Biol, 2010. **700**: p. 28-35.
39. Zisoulis, D.G., et al., *Autoregulation of microRNA biogenesis by let-7 and Argonaute*. Nature, 2012. **486**(7404): p. 541-4.
40. Lagier-Tourenne, C., M. Polymenidou, and D.W. Cleveland, *TDP-43 and FUS/TLS: emerging roles in RNA processing and neurodegeneration*. Hum Mol Genet, 2010. **19**(R1): p. R46-64.

41. Neumann, M., et al., *Ubiquitinated TDP-43 in frontotemporal lobar degeneration and amyotrophic lateral sclerosis*. *Science*, 2006. **314**(5796): p. 130-3.
42. Kawahara, Y. and A. Mieda-Sato, *TDP-43 promotes microRNA biogenesis as a component of the Drosha and Dicer complexes*. *Proc Natl Acad Sci U S A*, 2012. **109**(9): p. 3347-52.
43. Elston, R. and G.J. Inman, *Crosstalk between p53 and TGF-beta Signalling*. *J Signal Transduct*, 2012. **2012**: p. 294097.
44. Liu, Y. and Q. Liu, *ATM signals miRNA biogenesis through KSRP*. *Mol Cell*, 2011. **41**(4): p. 367-8.
45. Mullen, T.E. and W.F. Marzluff, *Degradation of histone mRNA requires oligouridylation followed by decapping and simultaneous degradation of the mRNA both 5' to 3' and 3' to 5'*. *Genes Dev*, 2008. **22**(1): p. 50-65.
46. Heo, I., et al., *TUT4 in concert with Lin28 suppresses microRNA biogenesis through pre-microRNA uridylation*. *Cell*, 2009. **138**(4): p. 696-708.
47. Yoshida, H., et al., *XBP1 is critical to protect cells from endoplasmic reticulum stress: evidence from Site-2 protease-deficient Chinese hamster ovary cells*. *Cell Struct Funct*, 2006. **31**(2): p. 117-25.
48. Upton, J.P., et al., *IRE1alpha cleaves select microRNAs during ER stress to derepress translation of proapoptotic Caspase-2*. *Science*, 2012. **338**(6108): p. 818-22.
49. Yang, W., et al., *Modulation of microRNA processing and expression through RNA editing by ADAR deaminases*. *Nat Struct Mol Biol*, 2006. **13**(1): p. 13-21.
50. Caudy, A.A., et al., *A micrococcal nuclease homologue in RNAi effector complexes*. *Nature*, 2003. **425**(6956): p. 411-4.
51. Yamagata, K., et al., *Maturation of microRNA is hormonally regulated by a nuclear receptor*. *Mol Cell*, 2009. **36**(2): p. 340-7.
52. O'Connell, M.A. and L.P. Keegan, *Drosha versus ADAR: wrangling over pri-miRNA*. *Nat Struct Mol Biol*, 2006. **13**(1): p. 3-4.
53. Fujiyama-Nakamura, S., K. Yamagata, and S. Kato, *Hormonal Repression of miRNA Biosynthesis Through a Nuclear Steroid Hormone Receptor*. *Adv Exp Med Biol*, 2011. **700**: p. 43-55.
54. Poliseno, L., et al., *A coding-independent function of gene and pseudogene mRNAs regulates tumour biology*. *Nature*, 2010. **465**(7301): p. 1033-8.
55. Hansen, T.B., et al., *Natural RNA circles function as efficient microRNA sponges*. *Nature*, 2013. **495**(7441): p. 384-8.
56. Kedde, M., et al., *RNA-binding protein Dnd1 inhibits microRNA access to target mRNA*. *Cell*, 2007. **131**(7): p. 1273-86.
57. Li, Z.F., et al., *Dynamic localisation of mature microRNAs in Human nucleoli is influenced by exogenous genetic materials*. *PLoS One*, 2013. **8**(8): p. e70869.
58. Bandiera, S., et al., *MitomiRs delineating the intracellular localization of microRNAs at mitochondria*. *Free Radic Biol Med*, 2013. **64**: p. 12-9.
59. Stalder, L., et al., *The rough endoplasmic reticulum is a central nucleation site of siRNA-mediated RNA silencing*. *EMBO J*, 2013. **32**(8): p. 1115-27.
60. Gibbings, D.J., et al., *Multivesicular bodies associate with components of miRNA effector complexes and modulate miRNA activity*. *Nat Cell Biol*, 2009. **11**(9): p. 1143-9.
61. Turchinovich, A., L. Weiz, and B. Burwinkel, *Extracellular miRNAs: the mystery of their origin and function*. *Trends Biochem Sci*, 2012. **37**(11): p. 460-5.

62. Zhou, J., et al., *Regulation of vascular smooth muscle cell turnover by endothelial cell-secreted microRNA-126: role of shear stress*. *Circ Res*, 2013. **113**(1): p. 40-51.
63. Zernecke, A., et al., *Delivery of microRNA-126 by apoptotic bodies induces CXCL12-dependent vascular protection*. *Sci Signal*, 2009. **2**(100): p. ra81.
64. Cocucci, E., G. Racchetti, and J. Meldolesi, *Shedding microvesicles: artefacts no more*. *Trends Cell Biol*, 2009. **19**(2): p. 43-51.
65. Hergenreider, E., et al., *Atheroprotective communication between endothelial cells and smooth muscle cells through miRNAs*. *Nat Cell Biol*, 2012. **14**(3): p. 249-56.
66. Battegay, E.J., *Angiogenesis: mechanistic insights, neovascular diseases, and therapeutic prospects*. *J Mol Med (Berl)*, 1995. **73**(7): p. 333-46.
67. Boettger, T., et al., *Acquisition of the contractile phenotype by murine arterial smooth muscle cells depends on the Mir143/145 gene cluster*. *J Clin Invest*, 2009. **119**(9): p. 2634-47.
68. Zhang, Y., et al., *miR-126 and miR-126* repress recruitment of mesenchymal stem cells and inflammatory monocytes to inhibit breast cancer metastasis*. *Nat Cell Biol*, 2013. **15**(3): p. 284-94.
69. Fish, J.E., et al., *miR-126 regulates angiogenic signaling and vascular integrity*. *Dev Cell*, 2008. **15**(2): p. 272-84.
70. Wang, S., et al., *The endothelial-specific microRNA miR-126 governs vascular integrity and angiogenesis*. *Dev Cell*, 2008. **15**(2): p. 261-71.
71. Kuhnert, F., et al., *Attribution of vascular phenotypes of the murine Eglf7 locus to the microRNA miR-126*. *Development*, 2008. **135**(24): p. 3989-93.
72. Sun, Y., et al., *miR-126 inhibits non-small cell lung cancer cells proliferation by targeting EGFL7*. *Biochem Biophys Res Commun*, 2010. **391**(3): p. 1483-9.
73. Tavazoie, S.F., et al., *Endogenous human microRNAs that suppress breast cancer metastasis*. *Nature*, 2008. **451**(7175): p. 147-52.
74. Li, X.M., et al., *Down-regulation of miR-126 expression in colorectal cancer and its clinical significance*. *Med Oncol*, 2011. **28**(4): p. 1054-7.
75. Feng, R., et al., *miR-126 functions as a tumour suppressor in human gastric cancer*. *Cancer Lett*, 2010. **298**(1): p. 50-63.
76. Saito, Y., et al., *Epigenetic therapy upregulates the tumor suppressor microRNA-126 and its host gene EGFL7 in human cancer cells*. *Biochem Biophys Res Commun*, 2009. **379**(3): p. 726-31.
77. Huang, T.H. and T.Y. Chu, *Repression of miR-126 and upregulation of adrenomedullin in the stromal endothelium by cancer-stromal cross talks confers angiogenesis of cervical cancer*. *Oncogene*, 2013.
78. Liu, B., et al., *MiR-126 restoration down-regulate VEGF and inhibit the growth of lung cancer cell lines in vitro and in vivo*. *Lung Cancer*, 2009. **66**(2): p. 169-75.
79. Sasahira, T., et al., *Downregulation of miR-126 induces angiogenesis and lymphangiogenesis by activation of VEGF-A in oral cancer*. *Br J Cancer*, 2012. **107**(4): p. 700-6.
80. Ota, A., et al., *Identification and characterization of a novel gene, C13orf25, as a target for 13q31-q32 amplification in malignant lymphoma*. *Cancer Res*, 2004. **64**(9): p. 3087-95.
81. He, L., et al., *A microRNA polycistron as a potential human oncogene*. *Nature*, 2005. **435**(7043): p. 828-33.
82. Dews, M., et al., *Augmentation of tumor angiogenesis by a Myc-activated microRNA cluster*. *Nat Genet*, 2006. **38**(9): p. 1060-5.

83. Uziel, T., et al., *The miR-17~92 cluster collaborates with the Sonic Hedgehog pathway in medulloblastoma*. Proc Natl Acad Sci U S A, 2009. **106**(8): p. 2812-7.
84. Yu, G., et al., *Prognostic values of the miR-17-92 cluster and its paralogs in colon cancer*. J Surg Oncol, 2012. **106**(3): p. 232-7.
85. Osada, H. and T. Takahashi, *let-7 and miR-17-92: small-sized major players in lung cancer development*. Cancer Sci, 2011. **102**(1): p. 9-17.
86. Hossain, A., M.T. Kuo, and G.F. Saunders, *Mir-17-5p regulates breast cancer cell proliferation by inhibiting translation of AIB1 mRNA*. Mol Cell Biol, 2006. **26**(21): p. 8191-201.
87. Lu, S., et al., *Increased expression of microRNA-17 predicts poor prognosis in human glioma*. J Biomed Biotechnol, 2012. **2012**: p. 970761.
88. Ventura, A., et al., *Targeted deletion reveals essential and overlapping functions of the miR-17 through 92 family of miRNA clusters*. Cell, 2008. **132**(5): p. 875-86.
89. Bonauer, A. and S. Dimmeler, *The microRNA-17-92 cluster: still a miRacle?* Cell Cycle, 2009. **8**(23): p. 3866-73.
90. Yu, Z., et al., *A cyclin D1/microRNA 17/20 regulatory feedback loop in control of breast cancer cell proliferation*. J Cell Biol, 2008. **182**(3): p. 509-17.
91. Trimarchi, J.M. and J.A. Lees, *Sibling rivalry in the E2F family*. Nat Rev Mol Cell Biol, 2002. **3**(1): p. 11-20.
92. Dyson, N., *The regulation of E2F by pRB-family proteins*. Genes Dev, 1998. **12**(15): p. 2245-62.
93. Olive, V., I. Jiang, and L. He, *mir-17-92, a cluster of miRNAs in the midst of the cancer network*. Int J Biochem Cell Biol, 2010. **42**(8): p. 1348-54.
94. Carraro, G., et al., *miR-17 family of microRNAs controls FGF10-mediated embryonic lung epithelial branching morphogenesis through MAPK14 and STAT3 regulation of E-Cadherin distribution*. Dev Biol, 2009. **333**(2): p. 238-50.
95. Pullamsetti, S.S., et al., *Inhibition of microRNA-17 improves lung and heart function in experimental pulmonary hypertension*. Am J Respir Crit Care Med, 2012. **185**(4): p. 409-19.
96. Doebele, C., et al., *Members of the microRNA-17-92 cluster exhibit a cell-intrinsic antiangiogenic function in endothelial cells*. Blood, 2010. **115**(23): p. 4944-50.
97. Shan, S.W., et al., *MicroRNA MiR-17 retards tissue growth and represses fibronectin expression*. Nat Cell Biol, 2009. **11**(8): p. 1031-8.
98. Li, S.H., et al., *miR-17 targets tissue inhibitor of metalloproteinase 1 and 2 to modulate cardiac matrix remodeling*. FASEB J, 2013. **27**(10): p. 4254-65.
99. Garg, N., et al., *microRNA-17-92 cluster is a direct Nanog target and controls neural stem cell through Trp53inp1*. EMBO J, 2013. **32**(21): p. 2819-32.
100. Trenkmann, M., et al., *Tumor necrosis factor alpha-induced microRNA-18a activates rheumatoid arthritis synovial fibroblasts through a feedback loop in NF-kappaB signaling*. Arthritis Rheum, 2013. **65**(4): p. 916-27.
101. Hirajima, S., et al., *Clinical impact of circulating miR-18a in plasma of patients with oesophageal squamous cell carcinoma*. Br J Cancer, 2013. **108**(9): p. 1822-9.
102. Vega, A.B., et al., *microRNA expression profile in stage III colorectal cancer: circulating miR-18a and miR-29a as promising biomarkers*. Oncol Rep, 2013. **30**(1): p. 320-6.
103. Xiao, C., et al., *Lymphoproliferative disease and autoimmunity in mice with increased miR-17-92 expression in lymphocytes*. Nat Immunol, 2008. **9**(4): p. 405-14.

104. Mavrakis, K.J., et al., *Genome-wide RNA-mediated interference screen identifies miR-19 targets in Notch-induced T-cell acute lymphoblastic leukaemia*. Nat Cell Biol, 2010. **12**(4): p. 372-9.
105. Chen, J., et al., *mir-17-92 cluster is required for and sufficient to induce cardiomyocyte proliferation in postnatal and adult hearts*. Circ Res, 2013. **112**(12): p. 1557-66.
106. Yang, J.T., H. Rayburn, and R.O. Hynes, *Embryonic mesodermal defects in alpha 5 integrin-deficient mice*. Development, 1993. **119**(4): p. 1093-105.
107. Francis, S.E., et al., *Central roles of alpha5beta1 integrin and fibronectin in vascular development in mouse embryos and embryoid bodies*. Arterioscler Thromb Vasc Biol, 2002. **22**(6): p. 927-33.
108. Urbich, C., et al., *Shear stress-induced endothelial cell migration involves integrin signaling via the fibronectin receptor subunits alpha(5) and beta(1)*. Arterioscler Thromb Vasc Biol, 2002. **22**(1): p. 69-75.
109. Bonauer, A., et al., *MicroRNA-92a controls angiogenesis and functional recovery of ischemic tissues in mice*. Science, 2009. **324**(5935): p. 1710-3.
110. Hinkel, R., et al., *Inhibition of MicroRNA-92a protects against ischemia/reperfusion injury in a large-animal model*. Circulation, 2013. **128**(10): p. 1066-75.
111. Loyer, X., et al., *Inhibition of microRNA-92a Prevents Endothelial Dysfunction and Atherosclerosis in Mice*. Circ Res, 2013.
112. Danielson, L.S., et al., *Cardiovascular dysregulation of miR-17-92 causes a lethal hypertrophic cardiomyopathy and arrhythmogenesis*. FASEB J, 2013. **27**(4): p. 1460-7.
113. Venturini, L., et al., *Expression of the miR-17-92 polycistron in chronic myeloid leukemia (CML) CD34+ cells*. Blood, 2007. **109**(10): p. 4399-405.
114. O'Donnell, K.A., et al., *c-Myc-regulated microRNAs modulate E2F1 expression*. Nature, 2005. **435**(7043): p. 839-43.
115. Fontana, L., et al., *Antagomir-17-5p abolishes the growth of therapy-resistant neuroblastoma through p21 and BIM*. PLoS One, 2008. **3**(5): p. e2236.
116. Northcott, P.A., et al., *The miR-17/92 polycistron is up-regulated in sonic hedgehog-driven medulloblastomas and induced by N-myc in sonic hedgehog-treated cerebellar neural precursors*. Cancer Res, 2009. **69**(8): p. 3249-55.
117. Schulte, J.H., et al., *MYCN regulates oncogenic MicroRNAs in neuroblastoma*. Int J Cancer, 2008. **122**(3): p. 699-704.
118. Sylvestre, Y., et al., *An E2F/miR-20a autoregulatory feedback loop*. J Biol Chem, 2007. **282**(4): p. 2135-43.
119. Woods, K., J.M. Thomson, and S.M. Hammond, *Direct regulation of an oncogenic micro-RNA cluster by E2F transcription factors*. J Biol Chem, 2007. **282**(4): p. 2130-4.
120. Fontana, L., et al., *MicroRNAs 17-5p-20a-106a control monocytopoiesis through AML1 targeting and M-CSF receptor upregulation*. Nat Cell Biol, 2007. **9**(7): p. 775-87.
121. Takakura, S., et al., *Oncogenic role of miR-17-92 cluster in anaplastic thyroid cancer cells*. Cancer Sci, 2008. **99**(6): p. 1147-54.
122. Heinrich, E.M., *Regulation and function of the miR-17-92 cluster in stem cell differentiation*, in *Faculty of Biosciences2010*, Ruprecht Karls University of Heidelberg

123. Viswanathan, S.R., G.Q. Daley, and R.I. Gregory, *Selective blockade of microRNA processing by Lin28*. *Science*, 2008. **320**(5872): p. 97-100.
124. Newman, M.A., J.M. Thomson, and S.M. Hammond, *Lin-28 interaction with the Let-7 precursor loop mediates regulated microRNA processing*. *RNA*, 2008. **14**(8): p. 1539-49.
125. Thomson, J.M., et al., *Extensive post-transcriptional regulation of microRNAs and its implications for cancer*. *Genes Dev*, 2006. **20**(16): p. 2202-7.
126. Chaulk, S.G., et al., *Role of pri-miRNA tertiary structure in miR-17~92 miRNA biogenesis*. *RNA Biol*, 2011. **8**(6): p. 1105-14.
127. Hervouet, E., et al., *HIF and reactive oxygen species regulate oxidative phosphorylation in cancer*. *Carcinogenesis*, 2008. **29**(8): p. 1528-37.
128. Steber, M., et al., *Mechanistic basis for RNA aptamer-based induction of TetR*. *Chembiochem*, 2011. **12**(17): p. 2608-14.
129. Caputi, M., et al., *hnRNP A/B proteins are required for inhibition of HIV-1 pre-mRNA splicing*. *EMBO J*, 1999. **18**(14): p. 4060-7.
130. Saul, V.V., et al., *HIPK2 kinase activity depends on cis-autophosphorylation of its activation loop*. *J Mol Cell Biol*, 2012.
131. Cox, J. and M. Mann, *MaxQuant enables high peptide identification rates, individualized p.p.b.-range mass accuracies and proteome-wide protein quantification*. *Nat Biotechnol*, 2008. **26**(12): p. 1367-72.
132. Ramaswami, G., et al., *Identifying RNA editing sites using RNA sequencing data alone*. *Nat Methods*, 2013. **10**(2): p. 128-32.
133. Buhler, D., et al., *Essential role for the tudor domain of SMN in spliceosomal U snRNP assembly: implications for spinal muscular atrophy*. *Hum Mol Genet*, 1999. **8**(13): p. 2351-7.
134. Scadden, A.D., *The RISC subunit Tudor-SN binds to hyper-edited double-stranded RNA and promotes its cleavage*. *Nat Struct Mol Biol*, 2005. **12**(6): p. 489-96.
135. Linder, P. and F.V. Fuller-Pace, *Looking back on the birth of DEAD-box RNA helicases*. *Biochim Biophys Acta*, 2013. **1829**(8): p. 750-5.
136. Ozes, A.R., et al., *Duplex unwinding and ATPase activities of the DEAD-box helicase eIF4A are coupled by eIF4G and eIF4B*. *J Mol Biol*, 2011. **412**(4): p. 674-87.
137. Linder, P. and P.P. Slonimski, *An essential yeast protein, encoded by duplicated genes TIF1 and TIF2 and homologous to the mammalian translation initiation factor eIF-4A, can suppress a mitochondrial missense mutation*. *Proc Natl Acad Sci U S A*, 1989. **86**(7): p. 2286-90.
138. Shaoyan, X., et al., *Downregulation of EIF4A2 in Non-Small-Cell Lung Cancer Associates with Poor Prognosis*. *Clin Lung Cancer*, 2013. **14**(6): p. 658-65.
139. Davis, D.B., et al., *Myoferlin, a candidate gene and potential modifier of muscular dystrophy*. *Hum Mol Genet*, 2000. **9**(2): p. 217-26.
140. Bernatchez, P.N., et al., *Myoferlin regulates vascular endothelial growth factor receptor-2 stability and function*. *J Biol Chem*, 2007. **282**(42): p. 30745-53.
141. Bernatchez, P.N., et al., *Myoferlin is critical for endocytosis in endothelial cells*. *Am J Physiol Cell Physiol*, 2009. **297**(3): p. C484-92.
142. Liu, J., et al., *Argonaute2 is the catalytic engine of mammalian RNAi*. *Science*, 2004. **305**(5689): p. 1437-41.
143. Nevo-Caspi, Y., et al., *A-to-I RNA editing is induced upon hypoxia*. *Shock*, 2011. **35**(6): p. 585-9.

144. Miettinen, M. and J.F. Fetsch, *Distribution of keratins in normal endothelial cells and a spectrum of vascular tumors: implications in tumor diagnosis*. Hum Pathol, 2000. **31**(9): p. 1062-7.
145. Evans, P.R., G.W. Farrants, and P.J. Hudson, *Phosphofructokinase: structure and control*. Philos Trans R Soc Lond B Biol Sci, 1981. **293**(1063): p. 53-62.
146. Park, Y.Y., et al., *Tat-activating regulatory DNA-binding protein regulates glycolysis in hepatocellular carcinoma by regulating the platelet isoform of phosphofructokinase through microRNA 520*. Hepatology, 2013. **58**(1): p. 182-91.
147. Mancini, M., et al., *MicroRNA-152 and -181a participate in human dermal fibroblasts senescence acting on cell adhesion and remodeling of the extra-cellular matrix*. Aging (Albany NY), 2012. **4**(11): p. 843-53.
148. Mann, M., *Functional and quantitative proteomics using SILAC*. Nat Rev Mol Cell Biol, 2006. **7**(12): p. 952-8.
149. Blanco, M.A., et al., *Identification of staphylococcal nuclease domain-containing 1 (SND1) as a Metadherin-interacting protein with metastasis-promoting functions*. J Biol Chem, 2011. **286**(22): p. 19982-92.
150. Notterman, D.A., et al., *Transcriptional gene expression profiles of colorectal adenoma, adenocarcinoma, and normal tissue examined by oligonucleotide arrays*. Cancer Res, 2001. **61**(7): p. 3124-30.
151. Santhekadur, P.K., et al., *Multifunction protein staphylococcal nuclease domain containing 1 (SND1) promotes tumor angiogenesis in human hepatocellular carcinoma through novel pathway that involves nuclear factor kappaB and miR-221*. J Biol Chem, 2012. **287**(17): p. 13952-8.
152. Keightley, M.C., et al., *In vivo mutation of pre-mRNA processing factor 8 (Prpf8) affects transcript splicing, cell survival and myeloid differentiation*. FEBS Lett, 2013. **587**(14): p. 2150-7.
153. Li, C.L., et al., *Structural and functional insights into human Tudor-SN, a key component linking RNA interference and editing*. Nucleic Acids Res, 2008. **36**(11): p. 3579-89.
154. Ho, J.J., et al., *Functional importance of Dicer protein in the adaptive cellular response to hypoxia*. J Biol Chem, 2012. **287**(34): p. 29003-20.
155. Weissbach, R. and A.D. Scadden, *Tudor-SN and ADAR1 are components of cytoplasmic stress granules*. RNA, 2012. **18**(3): p. 462-71.
156. Sabatel, C., et al., *MicroRNA-21 exhibits antiangiogenic function by targeting RhoB expression in endothelial cells*. PLoS One, 2011. **6**(2): p. e16979.
157. Meijer, H.A., et al., *Translational repression and eIF4A2 activity are critical for microRNA-mediated gene regulation*. Science, 2013. **340**(6128): p. 82-5.
158. Lek, A., et al., *Phylogenetic analysis of ferlin genes reveals ancient eukaryotic origins*. BMC Evol Biol, 2010. **10**: p. 231.
159. Demonbreun, A.R., et al., *Dysferlin and myoferlin regulate transverse tubule formation and glycerol sensitivity*. Am J Pathol, 2014. **184**(1): p. 248-59.
160. Demonbreun, A.R., et al., *Myoferlin regulation by NFAT in muscle injury, regeneration and repair*. J Cell Sci, 2010. **123**(Pt 14): p. 2413-22.
161. Turtoi, A., et al., *Myoferlin is a key regulator of EGFR activity in breast cancer*. Cancer Res, 2013. **73**(17): p. 5438-48.
162. Doherty, K.R., et al., *The endocytic recycling protein EHD2 interacts with myoferlin to regulate myoblast fusion*. J Biol Chem, 2008. **283**(29): p. 20252-60.

163. Fukuda, M., *Versatile role of Rab27 in membrane trafficking: focus on the Rab27 effector families*. J Biochem, 2005. **137**(1): p. 9-16.
164. Hiebsch, R.R., T.J. Raub, and B.W. Wattenberg, *Primaquine blocks transport by inhibiting the formation of functional transport vesicles. Studies in a cell-free assay of protein transport through the Golgi apparatus*. J Biol Chem, 1991. **266**(30): p. 20323-8.
165. Chen, X., et al., *Horizontal transfer of microRNAs: molecular mechanisms and clinical applications*. Protein Cell, 2012. **3**(1): p. 28-37.
166. Wagner, J., et al., *Characterization of levels and cellular transfer of circulating lipoprotein-bound microRNAs*. Arterioscler Thromb Vasc Biol, 2013. **33**(6): p. 1392-400.
167. Wang, K., et al., *Export of microRNAs and microRNA-protective protein by mammalian cells*. Nucleic Acids Res, 2010. **38**(20): p. 7248-59.
168. Shapiro, J.S., et al., *Evidence for a cytoplasmic microprocessor of pri-miRNAs*. RNA, 2012. **18**(7): p. 1338-46.
169. Willeit, P., et al., *Circulating microRNAs as novel biomarkers for platelet activation*. Circ Res, 2013. **112**(4): p. 595-600.
170. Crescitelli, R., et al., *Distinct RNA profiles in subpopulations of extracellular vesicles: apoptotic bodies, microvesicles and exosomes*. J Extracell Vesicles, 2013. **2**.

Eidesstattliche Erklärung

Hiermit versichere ich, dass ich die vorliegende Dissertation selbständig und nur unter zu Hilfenahme der hier angegebenen Quellen und Hilfsmitteln verfasst habe. Die Dissertation wurde bisher keiner anderen Fakultät vorgelegt. Ich erkläre, dass ich bisher kein Promotionsverfahren erfolglos beendet habe und dass keine Aberkennung eines bereits erworbenen Doktorgrades vorliegt.

Frankfurt, 23.12.2012

Curriculum Vitae

Eva-Marie Heinrich, Master of Science

Kleine Weissgasse 8

D-55116 Mainz

Tel.: +49 (0) 176 - 78 02 19 76

evamarie.heinrich@gmail.com

Born January 27th 1987, Mainz (Germany)

Education

- 09/2010-present **Dissertation**
“Posttranscriptional regulation of the microRNA-17-92a processing”
Institute for Cardiovascular Regeneration
(Prof. Dr. Stefanie Dimmeler), Goethe-University Frankfurt
- 09/2008-09/2010 **Molecular Life Sciences (Master)**
Ruprecht-Karls-University Heidelberg
Master Thesis “Regulation and function of the miR-17-92 cluster in stem cell differentiation”
Institute for Cardiovascular Regeneration
(Prof. Dr. Stefanie Dimmeler), Goethe-University Frankfurt
- 05/2005-05/2008 **Molecular Biology (Bachelor)**
Johannes-Gutenberg-University Mainz
Bachelor Thesis “Cloning and heterologous expression of zebra fish homologues of human polymerases”
Institute of Zoology
(Prof. Dr. Walter Stöcker), Johannes-Gutenberg-University Mainz
- 08/1997-03/2005 **Secondary School** (German high-school degree Abitur)
Maria-Ward-Schule Mainz
Skipped 9th grade in a program for gifted students

Professional experience

- 05/2008-07/2008 **Internship at Karolinska Institute**
Cloning and localization of a hypothalamus specific transcription factor in zebra fish brains via microinjection, Department of Molecular Biosciences (PD Giselbert Hauptmann), Karolinska Institute Stockholm

Courses

- 2010-present **Full day graduate school courses** at Goethe-University Frankfurt (graduate school “Biologicals”)
- Good laboratory practice (GLP) and good manufacturing practice (GMP) and Quality control
 - Regulatory Affairs
 - Patent law (2days)
 - Business plan, marketing and international trends in drug markets
 - Pharmacokinetics and Pharmacodynamics

Scholarship

- 2010-2013 Deutsche Forschungsgesellschaft (DFG) Graduate School “Biologicals“ GRK1172

Conferences with oral or poster presentation

- 04/2013 Annual Meeting of the German Society of Cardiology, Mannheim (Germany)
Posttranscriptional regulation of the miR-17-92a cluster (Poster)
- 09/2012 EMBO Meeting “Non coding RNAs”, Ascona (Switzerland)
Posttranscriptional regulation of the miR-17-92a cluster (Poster)
- 04/2012 International RNA symposium, Frankfurt (Germany)
Posttranscriptional regulation of microRNAs (Poster)
- 04/2012 Annual Meeting of the German Society of Cardiology, Mannheim (Germany)
Posttranscriptional regulation of microRNAs (Presentation)
- 12/2011 EMBO Molecular Medicine meeting, Heidelberg (Germany)
Posttranscriptional regulation of the miR-17-92a cluster (Poster)
- 02/2011 International Symposium “microRNAs” in Banff (Canada)
Regulation of the processing of the individual members of the miR-17-92a cluster (Poster)

Publications

Regulation of miR-17-92 cluster processing by the microRNA binding protein SND1.
Heinrich EM*, Wagner J*, Krüger M, John D, Uchida S, Weigand JE, Suess B, Dimmeler S
(*contributed equally), FEBS Letters, 2013, vol 587(15), pp 2405-11

Role of the microRNA-17-92 cluster in endothelial differentiation of stem cells. Tréguer K*, Heinrich EM*, Ohtani K, Bonauer A, Dimmeler S (*contributed equally), Journal of Vascular Research, 2012, vol 49(5), pp447-60

MicroRNAs and Stem cells: Control of Pluripotency, reprogramming and lineage commitment. Heinrich EM and Dimmeler S, Circulation Research, 2012, vol 110(7), pp 1014-22

Acknowledgements

I would like to express my gratitude to all of those who supported me to complete this thesis. Special thanks to...

... Professor Stefanie Dimmeler, for offering me the chance to write this thesis at her institute. I warmly appreciate all the advice and motivation and most importantly her optimism. I feel very much privileged for having been part of this team.

... Professor Beatrix Sues, for providing me with help in numerous discussions. Her RNA expertise had major impact on my work.

... GRK1172 for funding me and especially Dr. Brigitte Held for organizing excellent courses and career support for us.

... Dr. Angelika Bonauer for introducing this project to me and for all the support she offered me.

... Dr. Jasmin Wagner for her expertise in molecular biology and for being there for me whenever I needed advice.

... Ariane Fischer for cheering me up so many times. Thank you so much.

... all my colleagues for the good atmosphere in the lab. I want to thank especially Andrea for four years of answering my countless questions, as well as Annika, Anu, Dani, David K., David J., Cong, Ed, Karine, Kisho, Marion, Natalja, Nico, Reinier, Susanne, Timon, Tina, Tino and Yosif.

... my "Denkzellen"-Mates, for many days with lots of laughter in the lab. Thank you, Anne, Carmen, Jasmin, Katha, Patrick and Shemsi.

... Tillmann for his patient love and the unconditional support.

... my family. I am deeply grateful for the constant source of love, concern, support and strength all these years.

